



LUND UNIVERSITY

Reconstitution of Membrane-Bound Enzymes for Neutron Scattering Studies: A Case Study of Human Dihydroorotate Dehydrogenase

Orozco, Manuel

2022

Document Version:
Other version

[Link to publication](#)

Citation for published version (APA):

Orozco, M. (2022). *Reconstitution of Membrane-Bound Enzymes for Neutron Scattering Studies: A Case Study of Human Dihydroorotate Dehydrogenase*. [Doctoral Thesis (compilation), Department of Biology]. Lund University (Media-Tryck).

Total number of authors:
1

General rights

Unless other specific re-use rights are stated the following general rights apply:

Copyright and moral rights for the publications made accessible in the public portal are retained by the authors and/or other copyright owners and it is a condition of accessing publications that users recognise and abide by the legal requirements associated with these rights.

- Users may download and print one copy of any publication from the public portal for the purpose of private study or research.
- You may not further distribute the material or use it for any profit-making activity or commercial gain
- You may freely distribute the URL identifying the publication in the public portal

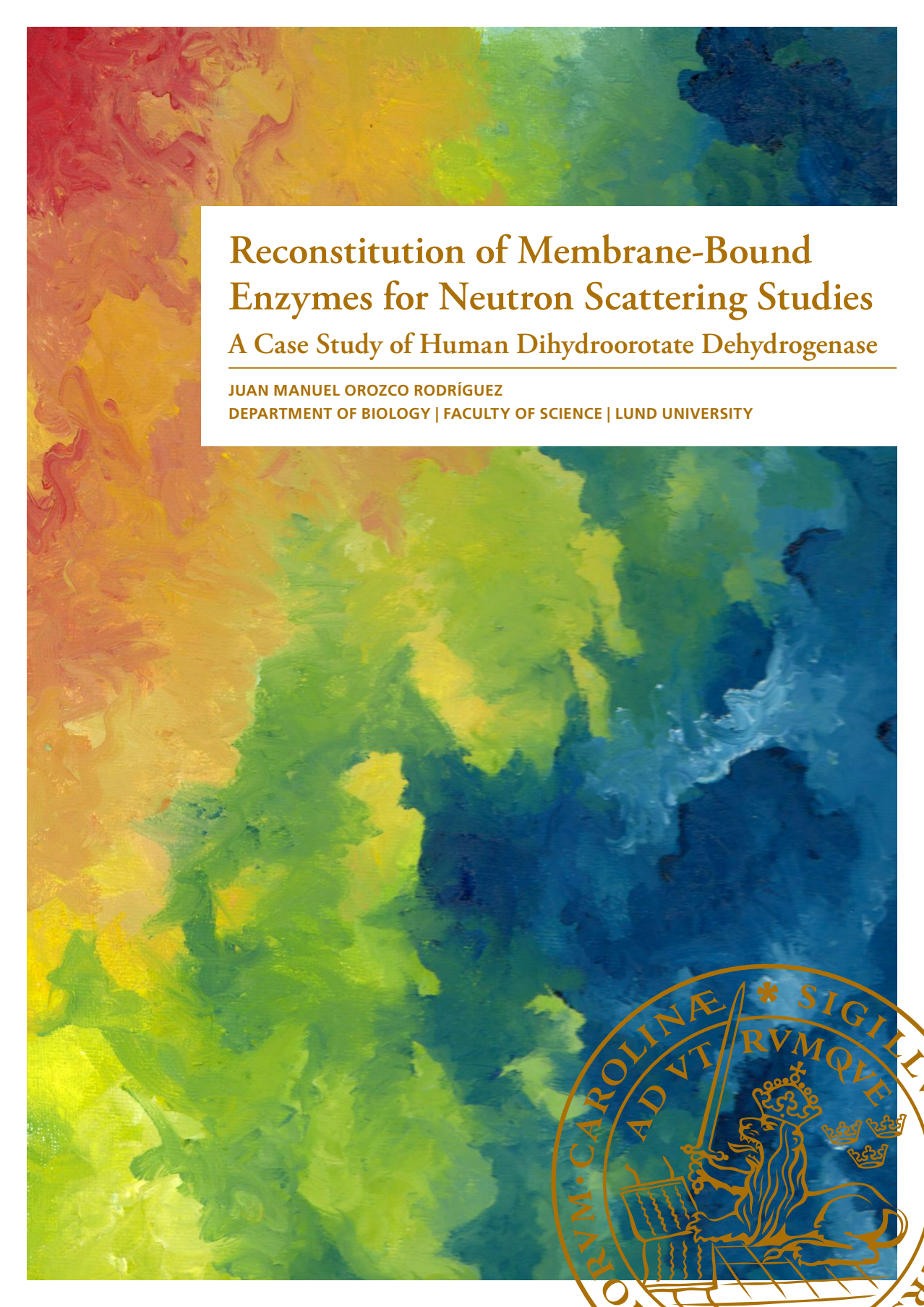
Read more about Creative commons licenses: <https://creativecommons.org/licenses/>

Take down policy

If you believe that this document breaches copyright please contact us providing details, and we will remove access to the work immediately and investigate your claim.

LUND UNIVERSITY

PO Box 117
221 00 Lund
+46 46-222 00 00



Reconstitution of Membrane-Bound Enzymes for Neutron Scattering Studies

A Case Study of Human Dihydroorotate Dehydrogenase

JUAN MANUEL OROZCO RODRÍGUEZ

DEPARTMENT OF BIOLOGY | FACULTY OF SCIENCE | LUND UNIVERSITY



Reconstitution of Membrane-Bound Enzymes for Neutron Scattering Studies: A Case
Study of Human Dihydroorotate Dehydrogenase

Reconstitution of Membrane-Bound Enzymes for Neutron Scattering Studies: A Case Study of Human Dihydroorotate Dehydrogenase

Juan Manuel Orozco Rodriguez



LUND
UNIVERSITY

DOCTORAL DISSERTATION

by due permission of the Faculty of Science, Lund University, Sweden.
To be defended at the Biology Lecture Hall at Biology Building A, Sölvegatan 35,
Lund, Sweden on June 3rd, 2022, at 9:00.

Faculty opponent

Prof. Jeremy H. Lakey, Ph.D.

Biosciences Institute, Newcastle University, United Kingdom.

Organization LUND UNIVERSITY Department of Biology, Sölvegatan 35, SE-223 62, Lund, Sweden Author Juan Manuel Orozco Rodriguez		Document name Doctoral dissertation Date of issue 03-June-2022 Sponsoring organization	
Title and subtitle Reconstitution of Membrane-Bound Enzymes for Neutron Scattering Studies: A Case Study of Human Dihydroorotate Dehydrogenase.			
Abstract <p>Membrane proteins are challenging to study due to the necessity to maintain a lipid-like environment to preserve their structure and function. Particularly difficult to study are membrane-bound enzymes that interact with lipophilic substrates. The aim of this doctoral thesis was to investigate the mechanism of action and inhibition of membrane-bound enzymes that interact with lipids and lipophilic substrates under non-crystalline, physiologically relevant conditions using neutron scattering methods. Neutron scattering techniques are suitable for the study of biological systems. Neutrons have no net charge and can therefore penetrate deeply into matter. Using neutrons, it is also possible to distinguish between isotopes of the same element, as is the case with the isotopes of hydrogen (protium and deuterium). Selective deuteration can be used to determine the structure and location of biological molecules in complex systems. Neutron reflectometry (NR) is a surface scattering technique capable of determining the structure and composition of thin films in the direction perpendicular to the surface. NR is therefore highly suitable for the study of membrane proteins and lipid bilayers</p> <p>A relevant example of this type of membrane proteins is human dihydroorotate dehydrogenase (<i>HsDHODH</i>). <i>HsDHODH</i> is an integral protein found in the inner mitochondrial membrane (IMM), where it catalyzes the oxidation of dihydroorotate to orotate with the concomitant reduction of ubiquinone Q₁₀ (coenzyme Q₁₀), thus linking pyrimidine biosynthesis and the respiratory chain. <i>HsDHODH</i> is the target of anti-inflammatory drugs and anti-proliferative compounds, and mutations in the <i>HsDHODH</i> gene have been identified as the cause of Miller syndrome, a rare genetic disorder characterized by malformations of the head, face, and limbs.</p> <p>Firstly, the production of the protein reagents needed for this thesis was established. A full biochemical characterization of <i>HsDHODH</i> and truncated <i>HsDHODH</i> as well as three variants associated with Miller syndrome (G19E, E52G, R135C) was performed. A particular focus was placed on their interaction with lipids including quartz crystal microbalance with dissipation (QCM-D) measurements of their binding to supported lipid bilayers (SLB). Miller syndrome mutants displayed lower activities compared to the wild-type enzymes, but showed also decreased stability, a probably impaired mitochondrial import, as well as differences in interactions with lipids (Papers I – III).</p> <p>As part of this thesis, the interactions between SLBs consisting of either synthetic lipids or a complex lipid mixture extracted from yeast with or without Q₁₀ and a soluble truncated form of <i>HsDHODH</i>, as well as the soluble bacterial analog from <i>E. coli</i> (<i>EcDHODH</i>), were investigated by NR. Q₁₀ was found to be located at the center of all the bilayers studied, between the lipid leaflets. Both enzymes were found to penetrate into the outer lipid leaflet of the bilayer upon interaction. The bacterial enzyme displayed a stronger binding and better retention than the human enzyme. Binding was also found to depend on the lipid composition of the bilayer as both enzymes displayed a stronger binding to complex bilayers consisting of several lipid species as opposed to those consisting of a few synthetic lipids. The interaction between both enzymes and ubiquinone was found to be mediated by protein penetration, as opposed to Q₁₀ migration (Paper IV).</p> <p>The reconstitution of <i>HsDHODH</i> into supported lipid bilayers was attempted using three different methodologies: adsorption of lipid-detergent micelles prepared with dodecyl D-maltoside (DDM), fusion of proteoliposomes, and hybrid approaches combining the adsorption of DDM-protein micelles and lipid vesicle fusion and characterized by NR. Micelle adsorption resulted in membranes with low lipid and protein coverage and with residual detergent. Proteoliposomes yielded a good lipid bilayer coverage but with a low protein content. The hybrid approaches resulted in good protein incorporation but also in the formation of an additional floating layer. The information obtained from these approaches can be used to guide and inform the reconstitution of proteins structurally similar to <i>HsDHODH</i> (Paper V).</p>			
Key words membrane proteins, dihydroorotate dehydrogenase, pyrimidine metabolism, neutron scattering, ubiquinone, QCM-D			
Classification system and/or index terms (if any)			
Supplementary bibliographical information		Language English	
ISSN and key title		ISBN (print) 978-91-8039-239-6 (pdf) 978-91-8039-240-2	
Recipient's notes	Number of pages 89		Price
	Security classification		

I, the undersigned, being the copyright owner of the abstract of the above-mentioned dissertation, hereby grant to all reference sources permission to publish and disseminate the abstract of the above-mentioned dissertation.

Signature



Date 2022-04-11

Reconstitution of Membrane-Bound Enzymes for Neutrons Scattering Studies: A Case Study of Human Dihydroorotate Dehydrogenase

Juan Manuel Orozco Rodriguez



LUND
UNIVERSITY

Cover picture by Juan Manuel Orozco Rodriguez ("*Contrast*", 2018, oil on canvas)

Copyright pp. 1–89 Juan Manuel Orozco Rodriguez

Paper I © Taylor & Francis Group, LLC

Paper II © Taylor & Francis Group, LLC

Paper III © Taylor & Francis Group, LLC

Paper IV © MDPI

Paper V © by the Authors (Manuscript unpublished)

Faculty of Science

Department of Biology

ISBN

(print) 978-91-8039-239-6

(PDF) 978-91-8039-240-2

Printed in Sweden by Media-Tryck, Lund University

Lund 2022



Media-Tryck is a Nordic Swan Ecolabel
certified provider of printed material.
Read more about our environmental
work at www.mediatryck.lu.se

MADE IN SWEDEN 

To my family (A mi familia)

Table of Contents

List of papers.....	10
Author contributions.....	11
Additional publications not included in this thesis	12
List of Symbols and Abbreviations.....	13
Aim	14
SECTION I: BACKGROUND.....	15
1. Proteins, lipids, and biological membranes.....	15
1.1. Biomolecules and biostructures.....	15
1.2. Surfactants and detergents	19
2. Membrane proteins: reconstitution and characterization.....	21
2.1. Expression and purification of membrane proteins.....	21
2.2. Methods for reconstituting membrane proteins	23
2.3. Methods for characterizing membrane proteins.....	25
2.4. Enzymatic activity assays and kinetics of membrane enzymes.....	33
3. Neutron scattering.....	36
3.1. Fundamentals of neutron scattering	36
3.2. Deuterium labelling	39
3.3. Neutron reflectometry.....	41
4. Dihydroorotate dehydrogenases.....	46
4.1. <i>De novo</i> pyrimidine biosynthesis and DHODHs	46
4.2. Class II dihydroorotate dehydrogenases.....	48
SECTION II: OUTCOME AND DISCUSSION OF THE STUDY.....	60
Paper I	60
Paper II.....	62
Paper III.....	64
Paper IV.....	66
Paper V	68
SECTION III: CONCLUSIONS AND FUTURE PERSPECTIVES.....	71
Popular science summary.....	73
Populär sammanfattning	74

Acknowledgements	75
References	77
Papers I-V.....	89

List of papers

This thesis is based on the following papers:

- I. **Orozco Rodriguez, J.M.**, Krupinska, E., Wacklin-Knecht, H.P., Knecht, W. (2020). Preparation of human dihydroorotate dehydrogenase for interaction studies with lipid bilayers. *Nucleosides, Nucleotides & Nucleic Acids*, 39(10–12), 1306–1319, DOI: 10.1080/15257770.2019.1708100.
- II. **Orozco Rodriguez, J.M.**, Krupinska, E., Wacklin-Knecht, H.P., Knecht, W. (2022). Protein production, kinetic and biophysical characterization of three human dihydroorotate dehydrogenase mutants associated with Miller syndrome. *Nucleosides, Nucleotides & Nucleic Acids*, DOI: 10.1080/15257770.2021.2023749. Epub ahead of print.
- III. **Orozco Rodriguez, J.M.**, Wacklin-Knecht, H.P., Knecht, W. (2022). Protein-lipid interactions of human dihydroorotate dehydrogenase and three mutants associated with Miller syndrome. *Nucleosides, Nucleotides & Nucleic Acids*, DOI: 10.1080/15257770.2022.2039393. Epub ahead of print.
- IV. **Orozco Rodriguez, J.M.**, Wacklin-Knecht, H.P., Clifton, L.A., Bogojevic, O., Leung, A., Fragneto, G., Knecht, W. (2022). New insights into the interaction of Class II dihydroorotate dehydrogenases with ubiquinone in lipid bilayers as a function of lipid composition. *International Journal of Molecular Sciences*, 23, 2437, DOI: 10.3390/ijms23052437.
- V. **Orozco Rodriguez, J.M.**, Wacklin-Knecht, H.P., Clifton, L.A., Bogojevic, O., Leung, A., Micciulla, S., Fragneto, G., Knecht, W. (2022). Reconstitution of human dihydroorotate dehydrogenase into supported lipid bilayers using detergent-lipid micelles and liposomes: A neutron scattering study. *Manuscript*.

Reprints were made with permission from the respective publisher.

Author contributions

My contributions to the here presented studies were as follows:

- I. I prepared the proteins used in this study and performed the biophysical assays. I also analyzed the data, contributed to their interpretation, wrote relevant parts of the manuscript, and edited the entire manuscript. I am one of the corresponding authors.
- II. I participated in the conception and design of the study. I prepared the proteins used in the study and performed the kinetic and biophysical assays. I also analyzed data, contributed to the interpretation of the data, wrote relevant parts of the manuscript, and edited the entire manuscript. I am one of the corresponding authors.
- III. I participated in the conception and design of the study. I prepared the proteins used in the study and performed the kinetic and biophysical assays. I also analyzed the data, contributed to the interpretation of the data, wrote relevant parts of the manuscript, and edited the entire manuscript. I am one of the corresponding authors.
- IV. I participated in the conception and design of the study and took part in the applications for beamtime. I prepared the proteins used in the study. I participated in the neutron reflectivity experiments and contributed to the analysis and interpretation of the data. I also wrote relevant parts of the manuscript and edited the entire manuscript.
- V. I participated in the conception and design of the study and took part in the applications for beamtime. I prepared the proteins used in the study. I participated in the neutron scattering experiments and contributed to the analysis and interpretation of the data. I wrote the initial draft of the manuscript and edited the entire manuscript.

Additional publications not included in this thesis

Wosniok, P.R., Knopf, C., Dreisigacker, S., Orozco Rodriguez, J.M., Hinkelmann, B., Müller, P.P., Brönstrup, M., Menche, D. (2020). SAR Studies of the Leupyrrins: Design and Total Synthesis of Highly Potent Simplified Leupylogs. *Chemistry – A European Journal*, 26(66), 15074–15078, DOI: 10.1002/chem.202002622.

Arisetti, N., Fuchs, H.L., Coetzee, J., Orozco Rodriguez, J.M., Ruppelt, D., Bauer, A., Heimann, D., Kuhnert, E., Bhamidimarri, S.P., Bafna, J.A., Hinkelmann, B., Eckel, K., Sieber, S.A., Müller, P.P., Herrmann, J., Müller, R., Winterhalter, M., Steinem, C., Brönstrup, M. (2021). Total synthesis and mechanism of action of the antibiotic armeniaspirol A. *Chemical Science*, 12(48): 16023–16034, DOI: 10.1039/D1SC04290D.

List of Symbols and Abbreviations

A	Area per molecule
b	Scattering length
CM4	Water contrast-matched to SLD = $4.0 \times 10^{-6} \text{ \AA}^{-2}$
CMSi	Water contrast-matched to Silicon (SLD = $2.07 \times 10^{-6} \text{ \AA}^{-2}$)
D ₂ O	Deuterium dioxide (heavy water)
DCIP	Dichlorophenolindophenol
DDM	n-dodecyl- β -D-maltoside
DHO	Dihydroorotic acid
DHODH	Dihydroorotate dehydrogenase
NR	Neutron reflectometry
POPC	Palmitoyl oleoyl phosphatidylcholine
POPE	Palmitoyl oleoyl phosphatidylethanolamine
POPG	Palmitoyl oleoyl phosphatidylglycerol
POPI	Palmitoyl oleoyl phosphatidylinositol
POPS	Palmitoyl oleoyl phosphatidylserine
Q	Scattering vector (momentum transfer vector)
Q ₀ , Bz	Benzoquinone
Q ₁₀	Ubiquinone Q ₁₀ (coenzyme Q ₁₀)
QCM-D	Quartz crystal microbalance with dissipation monitoring
Q _D	Decylubiquinone
R	Intensity of reflection
SEC	Size exclusion chromatography
TOCL	Tetraoleoyl cardiolipin
θ	Angle of incidence, measured to the surface normal
λ	Wavelength
ρ , SLD	Scattering length density
σ	Layer interfacial roughness
τ	Layer thickness
ϕ	Layer solvent content

Aim

The aim of this doctoral thesis project was to investigate the mechanism of action and inhibition of membrane-bound enzymes that interact with lipids and lipophilic substrates under non-crystalline, physiologically relevant conditions using neutron scattering methods.

A suitable and medically relevant example of this group of enzymes is human dihydroorotate dehydrogenase (*Hs*DHODH). *Hs*DHODH is the most researched member of the Class II DHODHs. It is a membrane-bound protein found in the inner mitochondrial membrane (IMM) where it catalyzes the oxidation of dihydroorotate to orotate with the concomitant reduction of ubiquinone Q₁₀ (coenzyme Q₁₀), thus acting as a link between pyrimidine metabolism and the mitochondrial respiratory chain. Another prominent member of Class II DHODHs is the DHODH from *E. coli* (*Ec*DHODH), which is found at the inner bacterial membrane. Both enzymes, which come from evolutionarily distinct hosts, have been investigated in order to characterise the common features of the interactions of Class II DHODHs with lipids and with the membrane-embedded substrate, ubiquinone.

A special subtopic of this thesis was the characterization of the effects of mutations found in *Hs*DHODH that cause a rare genetic disease known as Miller syndrome, which results from decreased *Hs*DHODH activity. Miller syndrome is an under-researched area of study and the defective enzymatic activity observed in the *Hs*DHODH mutants might, at least in part, be influenced by interactions between *Hs*DHODH and lipids of the IMM. The objective in this regard was to determine the biochemical basis for the interaction between *Hs*DHODH and lipids and how mutations associated with Miller syndrome affect these interactions.

SECTION I: BACKGROUND

1. Proteins, lipids, and biological membranes

1.1. Biomolecules and biostructures

The term *biomolecule* is used to refer to organic molecules found in living organisms that are essential for biological processes. Examples of biomolecules are proteins, carbohydrates, lipids, and nucleic acids.

Proteins are polymers of amino acids joined together by amide bonds known as peptide bonds. Proteins perform a vast array of functions in living beings: they catalyze chemical reactions, provide structure, transport molecules, and are involved in sensing and responding to stimuli. Proteins display four levels of structural organization. The *primary structure* of a protein refers to its amino acid sequence. Amino acids differ with respect to their side chains, which may be hydrophilic, hydrophobic, acidic, or basic. The *secondary structure* of a protein refers to structural motifs of amino acids stabilized by hydrogen bonds. The main types of secondary structures are α helices and β sheets (also called β strands). The *tertiary structure* of a protein refers to the three-dimensional structure of a single protein chain (a single polypeptide chain). A single chain may consist of one or more protein domains. The tertiary structure of a protein is made possible thanks to the interactions between both the side chains and the backbones of the amino acids that make up the protein. The *quaternary structure* refers to the overall three-dimensional structure that results from the interaction between two or more polypeptide chains. Each of these polypeptide chains is known as a subunit. The interactions that give rise to the tertiary and quaternary structures of proteins include hydrogen bonding, electrostatic interactions, and hydrophobic interactions.

The term *lipid* is used to describe any biomolecule consisting mostly of carbon and hydrogen, and that is largely insoluble in water but soluble in organic solvents such as chloroform, methanol, or acetone. The main categories of lipids found in biological systems are: glycerophospholipids, sphingolipids and sterols. Certain hydrophobic molecules such as the fat-soluble vitamins (A, D, E and K) are, however, not considered lipids.

Glycerophospholipids, often referred to as *phospholipids*, consist of two or more hydrophobic acyl chains or “tails” and a hydrophilic “head” composed of glycerol, phosphate, and an additional head group. Phospholipids are often classified based on

their head groups, which may be derived from amino acids (such as serine), carbohydrates (such as inositol), amines (such as choline and ethanolamine) or from glycerol itself.

Sterols are a class of lipid components derived from isoprene which are also found in biological membranes. The dominant sterol in animal membranes is cholesterol. Other sterols are present in the membranes of other eukaryotes: plants possess stigmasterol and sitosterol, whereas ergosterol is found in yeasts and fungi. Sterols are absent in bacterial membranes: bacteria possess triterpenoids known as hopanoids instead.

Biological membranes consist mostly of lipids, proteins and, to a lesser extent, carbohydrates (**Fig. 1.1**). They are essential to life as they provide compartmentalization: they separate the internal structures of cells from their surrounding environment. In eukaryotic cells, membranes also surround organelles such as the nucleus, mitochondria, chloroplasts, and lysosomes. Membranes are also essential for molecular transport, signal transduction and the formation of chemical and electric charge gradients necessary for energy generation.

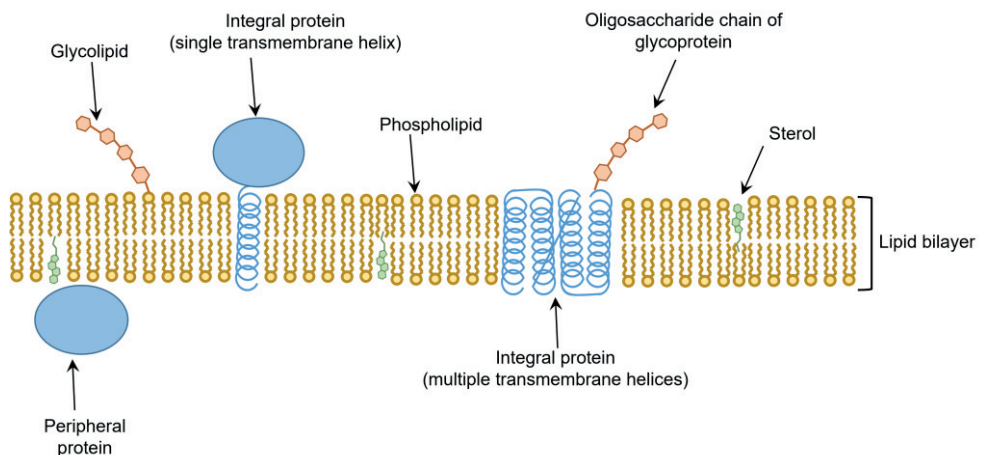


Fig. 1.1. Components of biological membranes. Modified from (Luckey, 2014).

Most biological membranes consist of a lipid bilayer with embedded or associated proteins. As its name indicates, a *lipid bilayer* consists of two layers of lipid molecules (often phospholipids). Lipid bilayers are arranged with the hydrophilic lipid headgroups oriented towards the aqueous bulk phase, thus shielding the hydrophobic lipid tails from the aqueous environment. Most living cells possess at least one lipid bilayer that separates their cytoplasm from the surrounding environment.

Most bacteria can be classified as either Gram positive or Gram negative. Gram positive bacteria possess a cytoplasmic or plasma membrane surrounded by a thick wall composed of peptides and sugars (the peptidoglycan layer). Gram negative bacteria such as *E. coli*, on the other hand, possess two membranes separated by a thin peptidoglycan layer: an inner membrane and an outer membrane.

Eukaryotic cells possess a single cytoplasmic membrane, but they also possess organelles such as mitochondria and chloroplasts. Mitochondria evolved from endosymbiotic bacteria and display both an inner mitochondrial membrane (IMM) and an outer mitochondrial membrane (OMM).

The main phospholipid classes (**Fig. 1.2**) found in biological membranes are phosphatidylcholines (PC), phosphatidylethanolamines (PE), phosphatidylglycerols (PG), phosphatidylserines (PS), phosphatidylinositols (PI), and cardiolipins (CL). The phospholipid tails are derived from fatty acids which range from 12 – 22 carbons in length and which may be saturated or unsaturated. However, most of the phospholipids found in biological membranes have chains composed of either 16 or 18 carbons. The structure of phospholipids is often denoted with the *sn* (stereospecifically numbered) notation. Usually, the *sn1* chain is saturated and the *sn2* is unsaturated.

Membrane proteins can be either integral membrane proteins (inserted into or surrounded by the lipid bilayer), peripheral membrane proteins (also called extrinsic), or lipid-anchored proteins. As is the case with phospholipids, membrane proteins are amphipathic, and this allows for the nonpolar portions of proteins and lipids to interact via hydrophobic interactions. Furthermore, the polar portions of proteins and lipids also interact often by means of hydrogen bonds and electrostatic interactions. It is estimated that about 30% of human proteins are either integral membrane proteins or membrane associated (Krogh *et al.*, 2001). Membrane proteins are also the targets of many drugs. For example, G protein coupled receptors (GPCRs) are the targets for 33% of the small molecule drugs approved by the FDA (Santos *et al.*, 2017).

The carbohydrates in biological membranes are most often found in the hydrophilic heads of phospholipids and sphingolipids and in the hydrophilic regions of membrane proteins. Lipids and proteins covalently bound to carbohydrates are known as glycolipids and glycoproteins, respectively.

The lipid composition and protein content of biological membranes varies depending on the organism. Within the same organism, the lipid composition of the membrane can also vary depending on the tissue and the organelle. The lipid compositions of several membranes have been reviewed elsewhere (Daum, 1985; Horvath & Daum, 2013).

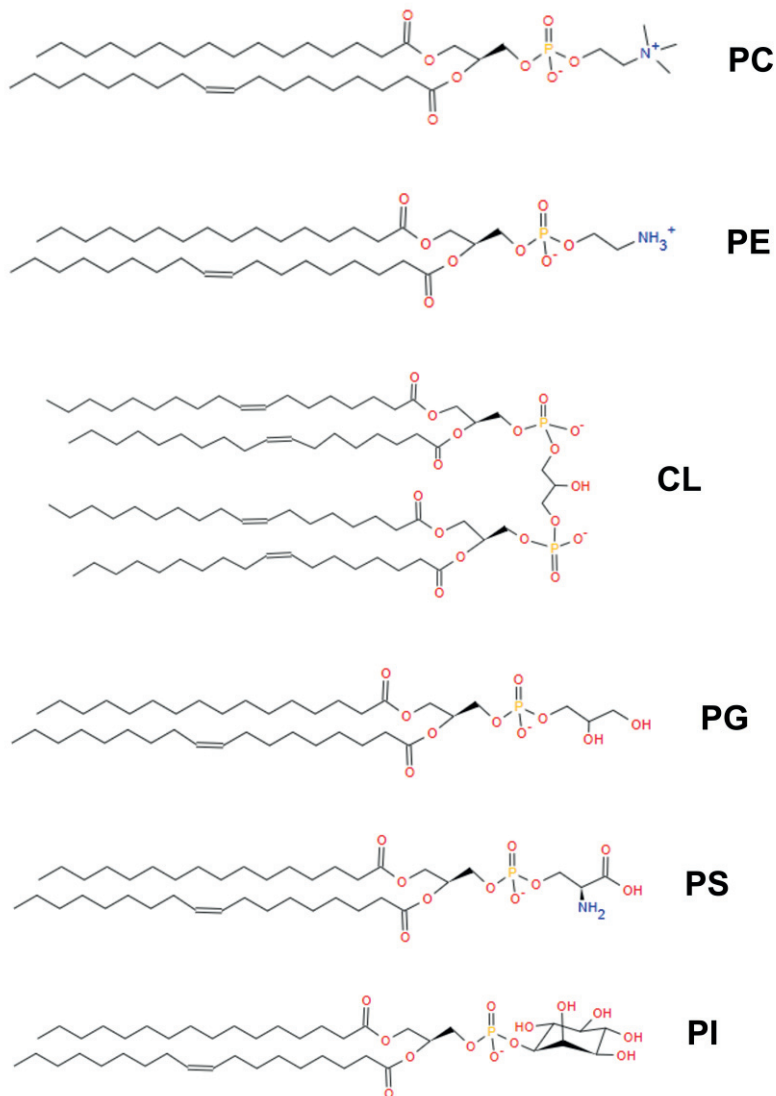


Fig. 1.2. The major phospholipid classes found in biological membranes.

In mammalian cells (rat liver), the plasma membrane consists mostly of PC (40 mol%) and PE (24 mol%), it contains very low amounts of CL (1 mol%) and has a phospholipid/protein ratio of 0.67 by weight. On the other hand, the mitochondria of rat liver cells consist mostly of PC and PE (44 mol% and 34 mol%, respectively), but

contain a much higher proportion of CL (14 mol%), as well as a lower phospholipid/protein ratio (0.17 by weight) (Daum & Vance, 1997). The IMM and OMM also differ in terms of lipid composition: in both membranes, PC and PE account for most of the phospholipids (40–50 mol% for PC and 29–34 mol% for PE), but CL is significantly enriched in the IMM, where it accounts for 18 mol%. Furthermore, the IMM contains a higher proportion of proteins compared to the OMM (Horvath & Daum, 2013). The sterol content in the IMM is very low (<0.05 mg sterol/mg phospholipid) compared to that of the cytoplasmic membrane (0.19 mg sterol/mg phospholipid) (Horvath & Daum, 2013).

In *E. coli*, the compositions of the inner and outer membranes also differ. When grown at 37 °C, the inner membrane consists of 82 mol% PE, 6 mol% PG and 12 mol% CL, whereas the outer membrane contains 91 mol% PE and 3 mol% PG, but has a significantly lower CL content (6 mol%) (Lugtenberg & Peters, 1976). *E. coli* cells lack phosphatidylcholine (which is zwitterionic and has a net neutral charge). The presence of negatively charged PG and CL give the bacterial membrane a net negative charge. The mammalian IMM also has a net negative charge due to the presence of negatively charged CL and PS.

1.2. Surfactants and detergents

A *surfactant* is a substance that can reduce the surface tension at the air-liquid interface. A *detergent* is a water-soluble surfactant. Detergents are amphiphilic (also called amphipathic) substances, meaning that they possess both hydrophilic and hydrophobic portions (Tanford & Reynolds, 1976).

Detergents are essential for the purification and characterization of membrane proteins. The isolation of membrane proteins typically begins by solubilizing the membrane with a suitable detergent. The detergent prevents the aggregation and precipitation of the target membrane protein after removal from its native lipid environment.

There are several types of detergents. They are often classified on the basis of their net charge and chemical identity. Anionic detergents such as sodium dodecyl sulfate (SDS) and sodium lauryl N-sarcosinate (Sarkosyl L) have a net negative. Cationic detergents such as cetyl trimethylammonium bromide (CTAB) have a net positive charge. Zwitterionic detergents have an equal number of positive and negative charges and therefore possess an overall neutral charge. Examples of zwitterionic detergents are alkyl amines (such as lauryldimethylamine oxide, LDAO) and sulphobetaines (such as CHAPS). Non-ionic detergents are uncharged. Examples of this category are alkyl glucosides (such as β -D-dodecyl D-maltoside (DDM) and β -D-octylglucoside (OG)),

polyoxyethylene octylphenols (such as Triton X-100), polyoxyethylene alcohols (such as the Brij series), and fatty acid esters of polyoxyethylene sorbitan (such as the Tween series).

The activity of most detergents involves their ability to form molecular assemblies known as *micelles*. Micelles are often spherical or elliptical in shape, but other configurations (such as wormlike micelles) are also observed for certain detergents (Zhao & Xie, 2012). In a micelle, the hydrophobic regions of the detergent are sequestered from the aqueous environment. An important property of detergents is the *critical micelle concentration* or CMC, which is defined as the concentration at which the detergent monomers self-associate to form micelles. Below the CMC, the detergent molecules exist as isolated monomers. Micelle formation is affected by factors such as the ionic strength of the solution and temperature. The size of the detergent micelles depends on the aggregation number, which is defined as the average number of detergent molecules per micelle. Examples of detergents commonly used for membrane protein purification and characterization are Triton X-100, DDM, OG, and LDAO.

Triton X-100 is an inexpensive detergent commonly used for extracting proteins from membranes. It has a CMC of 0.23 mM (equivalent to 0.14 mg/mL or 0.014 %w/v) and an aggregation number of 80–150, depending on the temperature of the solution (Paradies, 1980; Stubičar *et al.*, 1989). Triton X-100 is highly efficient at extracting proteins from their lipid environment, thus facilitating the isolation and purification of recombinantly expressed membrane proteins. A major disadvantage of Triton X-100, however, is the fact that it strongly absorbs at 280 nm, which corresponds to the wavelength at which most proteins absorb. The high extraction capability of Triton X-100 can also result in the removal of lipids and other hydrophobic molecules that are needed for protein function or stability. In addition, Triton X-100 cannot be removed by dialysis: a column chromatography step is necessary to achieve removal or exchange.

DDM is extensively used in protein purification, crystallization, and characterization. It is considered a mild detergent capable of preserving protein function. It has a CMC of 0.12–0.17 mM depending on the ionic strength of the solution (equivalent to 0.06–0.08 mg/mL) and aggregation numbers in the range of 98–149 (Vanaken *et al.*, 1986). Some disadvantages of DDM are its high price and its lower relative ability to extract proteins from membranes.

2. Membrane proteins: reconstitution and characterization

2.1. Expression and purification of membrane proteins

Membrane proteins are difficult to study for several reasons. The first challenge is obtaining the protein of interest in sufficient amount and with the purity required for analysis. Membrane proteins are usually present at low levels in their native membrane environment. It is therefore necessary to overexpress them in a suitable host.

In recent years, there has been significant progress in the methods for membrane protein expression and purification. Compared to soluble proteins, membrane proteins present additional challenges due to their hydrophobicity and due to the need to maintain a lipid-like environment to preserve activity. The production of recombinant membrane proteins involves the following steps: 1) selection of a suitable expression host; 2) selection of suitable expression conditions; and 3) selection and optimization of a purification protocol. **Figure 2.1** schematically represents the generic process for recombinant membrane protein expression, purification, and analysis.

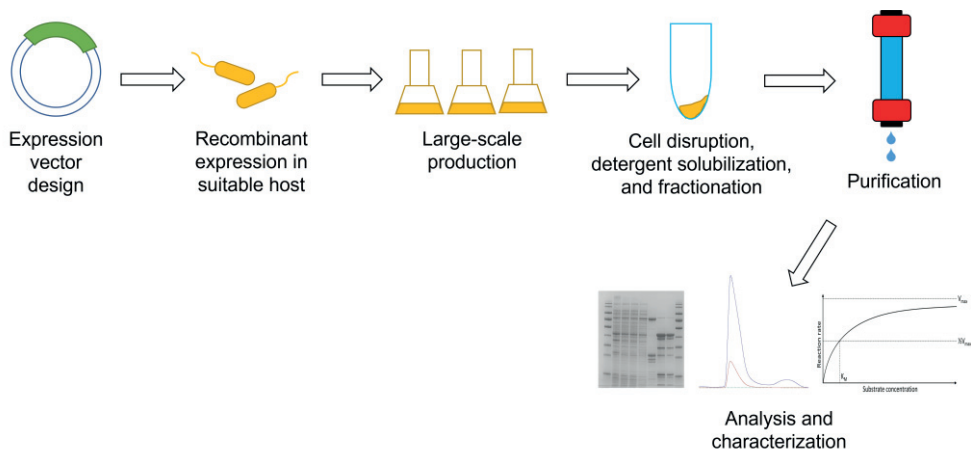


Fig. 2.1. Schematic representation of the protein expression, purification and analysis process.

There is a wide variety of expression hosts for recombinant membrane protein production (Pandey *et al.*, 2016). *Escherichia coli* is the most widely used system because it is easy to manipulate, does not require expensive growth media, and can yield large amounts of protein. *E. coli*, however, is unable to carry out many of the post-translational modifications (e.g., glycosylation) found in eukaryotic proteins.

Yeasts such as *Saccharomyces cerevisiae* and *Pichia pastoris* are also popular expression systems. Yeasts can grow to high cell densities, they can be genetically manipulated with ease and are able to perform several post-translational modifications (e.g., phosphorylation, glycosylation, acylation, etc.). Some disadvantages of using yeasts, however, are that glycosylation patterns vary between different strains and the yield of recombinant protein can vary dramatically depending on the strain used and on the protein being produced. With respect to the production of intracellular proteins, yeast cells are also very hard to disrupt due to their thick cell walls. An alternative consists of the expression of secreted (extracellular) proteins. Secreted proteins, however, are more susceptible to proteolytic degradation.

The Baculovirus Expression Vector System (BEVS) has gained popularity in recent years. The BEVS/insect cell system offers several advantages over microbial systems: proteins are typically properly folded, post-translational modifications are very similar to those found in higher eukaryotes, and multimeric proteins consisting of many subunits can be produced. Some disadvantages of the BEVS/insect cell system include the need for more complex and expensive growth media and cell densities that are lower compared to those of microorganisms. Expression in insect cells results in different glycosylation patterns compared to those obtained in mammalian cells, which is particularly relevant for secreted proteins.

Mammalian cell lines are often the system of choice if everything else fails to produce mammalian proteins for research purposes. Today, protein expression in mammalian cells is mainly performed using transient transfection. In transient transfection, the recombinant DNA material enters the cells but it does not integrate into the host genome. Mammalian cells can perform sophisticated post-translational modifications and can provide a suitable environment for the proper folding and activity of proteins of mammalian origin. Protein expression in mammalian cells however presents significant drawbacks: yields can be much lower compared to other expression systems (especially for intracellular proteins), the growth media are very complex and expensive, and the use of equipment with a constant CO₂ supply is required. Furthermore, transient transfection results in protein yields that can vary significantly, but the development of highly productive stable cell lines is a time consuming and expensive process.

Expression conditions often must be optimized depending on the expression host used. In the case of *E. coli*, the parameters that need to be optimized include media composition, temperature, duration of the protein production phase, and the concentration of the inducing agent. In the case of BEVS/insect cells, the parameters to optimize include the insect cell line to use (e.g. *Spodoptera frugiperda*, *Trichoplusia ni*, etc), the multiplicity of infection (MOI) to use (defined as the number of infectious

viral particles per insect cell), and the duration of the protein production phase (which is in the range of 24 – 72 h) (King, 2012).

For this study, both *E. coli* and BEVS/insect cells have been used as expression systems. *E. coli* was used due to its ease of use and ability to produce high protein yields for biophysical and neutron scattering studies. The BEVS/insect cell system was used to investigate protein expression and activity in a eukaryotic environment, as insect cells possess mitochondria. The choice of these systems was also done based on previous reports (Bader *et al.*, 1998; Knecht *et al.*, 1996).

The first step in the purification protocol is the extraction and solubilization of the protein of interest. In the case of membrane proteins, this step involves the use of a suitable detergent to extract the protein from the lipid environment. Modern protein purification protocols (Deutscher & Burgess, 2009) make use of some form of affinity chromatography for initial protein capture and size exclusion chromatography for the polishing step. Immobilized metal ion affinity chromatography (IMAC) is one of the most popular affinity chromatography methods. IMAC exploits the affinity of divalent metal ions (most often Ni^{2+} or Co^{2+}) towards short sequences (6 to 10 residues) of histidine amino acids in the expressed protein. Proteins can thus be expressed as His-tagged fusion proteins for this purpose. Size exclusion chromatography (SEC), also known as gel filtration, involves the use of porous beads to separate proteins based on their molecular size. Large molecules will be excluded from the pores of the beads and will elute earlier, while smaller molecules will have access to the pores and elute later. SEC is useful to produce a homogenous sample by removing protein aggregates and degradation products from the protein sample and it can be used to provide information on the oligomeric state of the protein of interest.

In the present study, to produce the DHODHs of interest, a purification protocol that combines two steps of IMAC and one step of SEC has been used and is described in detail in **Paper I** of this thesis (Orozco Rodriguez *et al.*, 2020).

2.2. Methods for reconstituting membrane proteins

Studying membrane protein structure and function is challenging due to the necessity of maintaining them in an environment that mimics their native membrane-bound state. This is because the function of membrane proteins is intrinsically linked to the membrane environment, and they need to be investigated under physiologically relevant conditions that mimic such an environment. Therefore, protein reconstitution protocols are needed. The term *reconstitution* refers to the reincorporation of a detergent-solubilized membrane protein into a natural or artificial membrane, which

can take different forms depending on the aim of the investigation and the techniques used.

As stated above, detergents are widely used for membrane protein purification. They enable the solubilization of membrane proteins to yield either spherical micelles, discoidal micelles (bicelles), or more complex assemblies (e.g., wormlike micelles). A wide variety of detergents is available and finding the best choice for a particular protein of interest is often not straightforward. Although micelles and bicelles provide a way to study membrane proteins in solution, a critical flaw with detergent approaches is the removal of the protein from the native lipid environment that is often required to maintain a functionally stable protein. In those cases, the use of lipid-based carriers such as liposomes and nanodiscs is advantageous.

Liposomes (Sessa & Weissmann, 1968) are colloidal particles consisting of one (unilamellar) or more (multilamellar) bilayers of amphiphilic lipids. They are usually spherical in shape and possess an aqueous interior known as the lumen. Proteoliposomes are liposomes in which membrane proteins have been embedded. The standard procedure for the reconstitution of membrane proteins into proteoliposomes (Rigaud *et al.*, 1995) requires the extraction of the proteins from the cell membranes using suitable detergents. The detergent-solubilized protein of interest is then purified by standard chromatographic methods. After purification, the solubilized protein is supplemented with an excess of lipids and detergent, which leads to the formation of mixed lipid-protein-detergent micelles and lipid-detergent micelles. Finally, the detergent is removed using various strategies: dialysis, gel filtration, dilution, or adsorption using hydrophobic resins. An important disadvantage of reconstituting proteins into proteoliposomes (as opposed to systems such as micelles or nanodiscs) is that the reconstituted protein will be randomly oriented. This is particularly problematic when the proteoliposome is fused to deposit a supported lipid bilayer on a planar surface, which may cause the protein to be inactive or yield inconsistent results.

Nanodiscs (Boldog *et al.*, 2007) consist of circular or elliptical fragments of phospholipid bilayers surrounded by a scaffold. The scaffold is often a membrane scaffold protein (MSP), usually derived from apolipoprotein A-1 (Bayburt *et al.*, 2002). The diameter of the discs ranges from 8 to 17 nm and can be modified by changing the number of amphipathic helices in the MSP amino acid sequence. In addition, nanodiscs stabilized by styrene maleic acid polymers (SMALPs) (Postis *et al.*, 2015) and peptides (Luchini *et al.*, 2020) have been used for membrane protein reconstitution. The incorporation of a membrane protein into nanodiscs involves the extraction of the protein from the membrane using suitable detergents; purification of the solubilized protein by standard chromatographic methods; incubation of the purified solubilized

protein with the MSP and the lipids of choice; and removal of the detergent by hydrophobic adsorption (using resins such as Bio-Beads™ or Amberlite™).

The term *supported lipid bilayer* (Sackmann, 1996) refers to lipid bilayers deposited on the surface of a solid substrate. Supported lipid bilayers (SLBs) are often separated from the surface by a very thin solvent layer (less than 10 Å thick). Floating lipid bilayers (Fragneto *et al.*, 2001), on the other hand, are lipid bilayers floating a few Å above either a bilayer or monolayer adsorbed on a smooth solid substrate. The reconstitution of proteins into SLBs and floating bilayers is often desirable as these systems provide a physiologically relevant environment for the immobilization of proteins under non-denaturing conditions. However, depositing a protein on a solid substrate presents several challenges. There is the possibility that the protein may bind the surface in the wrong orientation. Interaction with the surface may promote protein denaturation or aggregation and binding may effectively immobilize the protein rendering it unable to interact with substrates or lipids in the bilayer. Common methods of membrane assembly involve the use of some of the carriers mentioned above (e.g., micelles, nanodiscs, liposomes). Achieving sufficient surface coverage and proper protein orientation within the bilayer remain challenging. For the present thesis work, SLBs have been used to mimic the inner mitochondrial membrane and to study the interaction between the proteins of interest and lipids of the IMM and ubiquinone. SLBs provide a suitable system to study lipid bilayers and membrane proteins using a wide range of surface sensitive techniques, such as neutron and X-ray reflectometry, quartz crystal microbalance with dissipation monitoring (QCM-D), Fourier Transform Infrared (FTIR) spectroscopy, and atomic force microscopy (AFM). Because the membranes are oriented with respect to a planar surface, it is possible to study SLBs with higher resolution than what can be achieved with randomly oriented systems in solution.

2.3. Methods for characterizing membrane proteins

X-ray crystallography (Fankuchen, 1945) is so far the most used technique for providing atomic resolution protein structures. In 2021, there were about 9300 X-ray structures submitted to the Protein Data Bank (Berman *et al.*, 2000), compared to about 3000 structures solved by cryo electron microscopy (cryoEM) and 360 determined by NMR. Out of the nearly 185 000 protein structures currently in the PDB (as of April 2022), less than 10 000 correspond to integral or peripheral membrane proteins. Most of these membrane protein structures have been solved by X-ray diffraction (60%), but a significant proportion have been solved by cryoEM (31%). A major disadvantage of X-ray diffraction is that the proteins need to be crystallized, which requires both time and

effort. Membrane proteins are difficult to crystallize due to their inherent hydrophobicity. Methods for crystallizing membrane proteins involve their incorporation into detergent micelles (*in surfo* crystallization) or within a matrix of lipids with the ability to form a cubic phase (*in cubo* crystallization), such as monoolein. A third method involves the incorporation of membrane proteins into discoidal bicelles (Seddon *et al.*, 2004). Once diffracting crystals have been obtained, a beam of X-rays is directed at the sample and the intensities and angles of the reflected X-rays are recorded as the crystal is gradually rotated. This results in a series of diffraction patterns, which are computationally combined. The phases of the reflections can be determined using a variety of methods (deLaFortelle & Bricogne, 1997; Hendrickson, 1991; McCoy, 2007). The data is then refined to produce a model of the three-dimensional arrangement of the atoms in the sample.

Neutron protein crystallography (NPX) offers the additional advantage of being able to observe the position of the hydrogen atoms in the crystal structure, because neutrons interact with the atomic nuclei, not with the electrons. Contrary to X-ray crystallography, neutron crystallography allows for the protein crystals to be imaged at room temperature, without the need for cryocooling. The sample also receives less radiation damage than in the case of X-ray diffraction. However, the resolution obtained with NPX is usually lower than that of X-ray crystallography due to the limitations in the ability to access high momentum transfer values. The lower flux of neutron beams and the weaker interaction of neutrons with the sample require the need to grow very large protein crystals (sometimes in the mm³ range), which requires significant amounts of pure and stable protein as well as much longer measurement times compared to X-ray diffraction. Nonetheless, NPX can be used to investigate membrane proteins and the common practice is to perform joint X-ray and neutron diffraction data refinement. Approaches such as microdialysis and capillary counterdiffusion crystallization have been used to maximize crystal size (Hjorth-Jensen *et al.*, 2020).

Electron diffraction (Fujiiyoshi, 1998) is yet another method that has only recently been applied to the study of proteins. This technique can be used to determine the arrangement of atoms in proteins using a beam of electrons. The interaction between the accelerated electrons and the atoms of the sample is stronger than in the case of X-rays, making it possible to investigate small and thin crystals. As is the case with neutron crystallography, this method has the advantage of being able to locate the hydrogen atoms in the sample. There are, however, limitations in terms of sample preparation: the crystals need to have consistent thicknesses in the range of 100-500 nm (Clabbers & Abrahams, 2018; Palatinus *et al.*, 2017).

X-ray free-electron lasers (XFELs) and serial femtosecond crystallography (SFX) (Chapman *et al.*, 2006; Chapman *et al.*, 2011) are relatively new techniques that have also been applied to the study of membrane proteins. XFELs consist of X-ray pulses generated by bunches of electrons that are first accelerated to high energies (at nearly the speed of light) and then directed through periodic arrangements of magnets called undulators. As the electrons pass through the undulators, they emit extremely short and intense coherent X-ray flashes with properties similar to those of a laser. The pulses are typically 25 femtoseconds in duration and each pulse contains more than 10^{12} photons with a photon energy of 1.8 keV. XFELs make it possible to collect diffraction “snapshots” from a stream of nanocrystals or microcrystals. This technique is useful for the study of membrane proteins as they are difficult to crystallize, and their crystallization often yields small crystals. Radiation damage is minimized due to the short duration of the pulses and diffraction data can be collected at room temperature. In addition, mechanistic studies are also possible by mixing the crystals with substrates, inhibitors, etc. Major disadvantages of XFELs are the low number of facilities where these experiments can be conducted (there is only five as of 2022) and the fact that the sample still needs to be crystallized using conditions that are often not physiologically relevant.

All the crystallographic methods mentioned above have a major limitation: as the proteins are in a crystalline state, only part of the functional questions can be answered, since the activity of membrane proteins is intimately linked to their native membrane environment.

Nuclear magnetic resonance (NMR) spectroscopy (Wuthrich, 1990) is another tool with a long tradition, and is also capable of providing atomic resolution structures of macromolecules. NMR spectroscopy is based on the spin of atomic nuclei with an odd mass number (such as ^1H , ^{13}C , ^{15}N , ^{31}P). When placed in a static magnetic field, nuclei with a spin resonate with a characteristic frequency that depends on their local environment. The *chemical shift* is the resonant frequency of the nucleus relative to that of a standard compound in the magnetic field. NMR frequencies are also modified by couplings which depend on covalent bonding or internuclear distances. Using the information derived from these chemical shifts and couplings, NMR spectroscopy can be used to study proteins in solution, under non-crystalline conditions (Wuthrich, 1990). It is often a great advantage for the analysis of a protein by NMR to introduce the NMR active stable isotopes ^{13}C and ^{15}N . Furthermore, isotopic enrichment makes it possible to distinguish the molecule of interest from the unlabelled matrix. Multidimensional correlation ^{13}C , ^{15}N and ^1H NMR spectroscopy has been applied to many membrane proteins to elucidate their structure, dynamics, and mechanism of action. The major limitation of solution NMR lies in the difficulty of studying proteins

with molecular masses greater than 25-35 kDa, which require labelling with isotopes ^{13}C and ^{15}N . Solution NMR is limited to the study of proteins with molecular masses up to 50 kDa due to the extensive chemical shift overlap and degeneracy observed in the spectra (Cavanagh *et al.*, 1995; Sugiki *et al.*, 2017).

Solid-state NMR (Müller *et al.*, 2013; Reif *et al.*, 2021; Zhao, 2011) is a form of NMR spectroscopy that enables the study of complex biological systems that are difficult to study using solution NMR. Solution NMR spectroscopy requires fast moving molecules, which imposes a limitation on the molecular weight. Solid-state NMR imposes no restrictions on molecular size. This is accomplished by spinning the sample at a magic angle (54.7 degrees with respect to the magnetic field) to average out the anisotropic interactions of the sample and to avoid peak broadening in the spectra. This is known as magic-angle spinning (MAS) and makes it possible to study complex samples involving protein assemblies, proteins in lipid bilayers, protein-DNA complexes, and even viral particles, to gain information about the lipid-protein interactions, and to investigate the structure and dynamics of lipids. A disadvantage of MAS NMR is the requirement for the isotopic labelling of the biomolecule, which is time consuming and expensive.

High-resolution cryoEM (Dubochet *et al.*, 1988) is a relatively recent technique for determining the three-dimensional structures from projection images of macromolecules under cryogenic conditions and delivering structures at an atomic level that is sometimes comparable to what can be achieved by X-ray crystallography. However, in most cases the resolution achievable by cryoEM remains lower than that of X-ray diffraction and it does not provide information regarding the chemical identity of the sample. Although the resolution of cryoEM has improved significantly due to modern detectors and improved software for 3D reconstruction (Henderson, 2015; Murata & Wolf, 2018), there are challenges and limitations to the use of cryo-EM, even with the advantage that samples can be imaged under native, non-crystalline conditions. These include the complicated analysis of multiple conformations of molecules in their native environment, electron beam-induced movement during exposure, radiation damage of the sample, and low signal-to-noise ratio. CryoEM has molecular weight limitations, making it less suitable for the study of smaller monomeric proteins (<100 kDa in size). In that aspect, cryoEM still lags behind conventional methods such as X-ray crystallography and NMR.

A variety of fluorescence based methods (Lindon *et al.*, 2016) can be used to investigate membrane proteins. *Fluorescence polarization* (FP) measurements provide information on the molecular orientation and mobility of molecules. This technique requires the presence of an excitable fluorophore, which can be either an exogenous dye or an intrinsic fluorophore such as tryptophan. The degree of polarization is determined from

measurements of fluorescence intensities parallel and perpendicular with respect to the plane of linearly polarized excitation light. *Fluorescence resonance energy transfer* (FRET) relies on the distance-dependent interaction between the electronic excited states of two fluorescent molecules in which excitation is transferred from a donor molecule to an acceptor molecule without emission of a photon. FRET has been used to investigate protein-protein interactions, protein-DNA interactions, enzyme-substrate interactions, and protein conformational changes (Zadran *et al.*, 2012). The efficiency of FRET is inversely proportional to the distance between the two molecules. *Fluorescence correlation spectroscopy* (FCS) (Haustein & Schwille, 2007) records the fluorescence fluctuations of single labelled molecules in a given volume. FCS can be used to determine local concentrations, mobility coefficients or characteristic rate constants of inter- or intramolecular reactions of fluorescently labelled biomolecules in nanomolar concentrations. *Stimulated emission depletion* (STED) microscopy (Blom & Widengren, 2017; Eggeling *et al.*, 2009) creates high resolution images via the selective deactivation of fluorophores, minimizing the area of illumination at the focal point and enhancing the achievable resolution well below the optical diffraction limit. In classical fluorescence microscopy, the resolution is limited by the so-called diffraction limit (Rayleigh, 1903) that refers to the inability to resolve two elements which are closer than about half the wavelength of the light used, which is typically 250 nm. The resolution of STED microscopy however is well below 200 nm and down to 20 nm in biological samples (Blom & Widengren, 2017). It should be noted that fluorescence methods cannot provide structural information from within the thickness of a single lipid bilayer, and often require the use of fluorescent labels which may alter the behaviour of then native biomolecules.

Certain light scattering methods can be used to gather information about membrane proteins that have been either solubilized with detergents or reconstituted into liposomes, nanodiscs or bicelles. Light consists of particles known as photons. What is known as “visible light” consists of electromagnetic radiation having wavelengths in the range between 400 and 700 nm that can be detected by the human eye. Matter can interact with light in several ways: the photons can be absorbed, transmitted, or scattered, depending on the properties of the sample. These interactions can be used to derive information about the size and composition of the particles in the sample. It should be noted, however, that due to the higher wavelengths of visible light, the resolution of light scattering methods is far below that of X-ray and neutron scattering techniques. Light scattering is therefore suitable for the study of larger structures, ranging from several nm to a few micrometers.

Dynamic light scattering (DLS) (Lindon *et al.*, 2016) measures the self-correlation function or motion of the particles in a liquid due to the random collision with the

molecules of the liquid that surrounds the particles (Brownian motion) and relates this to the size of the particles. This is accomplished by illuminating the particles with a laser and analysing the intensity fluctuations in the scattered light as a function of time. The Stokes-Einstein equation is then used to relate the size of the particle to its diffusion speed due to Brownian motion. Large particles move slowly, while small ones move faster. DLS can be used to determine the size of particles in the range from 1 nm to 10 μm (in terms of radius), as well as the distribution of sizes in the sample. DLS is therefore useful for the analysis of proteins, micelles, nanoparticles, etc.

Another light scattering-based technique based on static light scattering is *multiangle light scattering* (MALS) (Lindon *et al.*, 2016; Wyatt, 1997), which consists of measuring the light scattered by the particles in a sample as a function of angle. MALS is used for determining both the absolute molar mass and the average size of the particles in a solution by detecting how they scatter light. MALS can be used to determine the molecular weight of particles in the range between 200 Da and 10^9 Da, and it can be used to determine the size of particles with a radius of gyration (R_g) in the range between 10 nm and 500 nm. Common applications of MALS include the study of proteins, micelles, polysaccharides, and nanoparticles.

Both DLS and MALS are non-destructive techniques that enable the study of samples in solution. The difference between DLS and MALS is that DLS is based on the analysis of the fluctuations of scattered light as a function of time, whereas MALS is a type of static light scattering based on the analysis of the absolute mean intensity of light scattering. MALS measures the amplitude of the scattering regardless of its fluctuations. One major limitation of these techniques is their inability to provide detailed information about the composition of the particles (whether they consist of proteins, lipids, detergents, or mixtures thereof). This is a consequence of the lack of contrast among the light refractive indexes of the molecules involved.

Infrared (IR) and Raman spectroscopy (Schrader, 2008) are techniques based on the interaction of infrared radiation with matter. IR is the wavelength region between 700 nm and 1000 μm , which is equivalent to a wavenumber range of $14\,000\text{ cm}^{-1}$ to 10 cm^{-1} . These techniques allow for the observation of the vibrational spectra of molecules. Certain bonds in chemical groups of atoms have characteristic vibrations defined by specific ranges of frequencies and intensities in the spectra. For example, it is possible to distinguish the protein amide bond vibrations from those of the lipid hydrocarbon bonds.

Attenuated total reflection IR spectroscopy (ATR-FTIR) is a non-invasive and non-destructive technique that uses the property of total internal reflection. In ATR-FTIR, a beam of infrared light is passed through a crystal (often made of silicon, germanium,

or zinc selenide) in such a way that the light is reflected at least once off the internal surface in contact with the sample. This results in enhanced surface sensitivity compared to solution FTIR, and it is therefore possible to investigate surface phenomena such as protein binding to supported lipid bilayers, protein adsorption, lipid vesicle fusion, etc (Glassford *et al.*, 2013).

Circular dichroism (CD) (Lindon *et al.*, 2016) relies on the difference in absorption between left and right-circularly polarized light of a chiral molecule. CD is used to determine the presence of secondary structure elements commonly found in proteins (α helices and β sheets) and the local tertiary structure of the aromatic amino acids and can also be applied to membrane-embedded proteins or peptides to detect conformational changes. CD is advantageous in the sense that it allows for measurements to be performed in solution and requires no extrinsic labels.

Atomic force microscopy (AFM) (Lal & John, 1994) is a surface-sensitive technique that consists of a molecular needle or tip attached to a cantilevered spring that moves over the surface of the sample and is deflected by the interaction forces between the atoms of the tip and the atoms of the sample. This interaction results in the generation of a pseudo three-dimensional map of the sample surface. In addition to being used for imaging, AFM can also quantify the interaction between the tip and a region of the sample, being capable of detecting forces in the piconewton range. AFM has been used to image lipid membranes, nucleic acids, proteins, and even whole cells (Santos & Castanho, 2004).

Optical tweezers (Zhang *et al.*, 2013), also called optical traps, are instruments that use a highly focused laser beam to hold and move microscopic beads which can be attached to and used to manipulate single molecules, including nucleic acids and proteins. It is possible to probe the mechanical properties of the biological molecule by measuring the optical force under controlled displacement of the trapped particle. Examples of mechanical signals from the attached molecules include the extension changes due to folding/unfolding transitions or translocations which result in displacements of the beads from the centre of the trap. Optical tweezers have been used to investigate the elastic properties of DNA molecules, to investigate protein-DNA interactions, and to perform protein folding studies and studies with molecular motors such as RNA polymerase (Bustamante *et al.*, 2021).

The phenomenon known as *surface plasmon resonance* (SPR) (Nguyen *et al.*, 2015) occurs when an incident photon hits a metal surface (typically gold) at an angle of incidence in which a portion of the light energy couples with the electrons on the metal surface layer. These electrons then become excited and propagate in the direction parallel to the surface. Such movement is called a *plasmon*. When the light source

wavelength and the metal surface properties are kept constant, the SPR angle at which resonance occurs can be correlated to the mass bound to the surface. SPR can be used to determine the binding constants and the binding affinities between two molecules. In commercial SPR sensors, probe molecules are first immobilized onto the metal surface. Then, a solution of target molecules is injected. Binding between the probe and the target causes a change in mass that can be detected. The binding kinetics can be quantified by tracking the resonance angle shifts. One limitation of SPR is that the probe needs to be immobilized on the metal surface, which can result in denaturation or in inactive configurations, and the target molecule must be soluble. Another limitation is that anything which alters the refractive index at the sensor surface will interfere with the analysis.

Ellipsometry (Azzam & Bashara, 1977) is another surface scattering technique which can be used to determine the refractive index and surface coverage of thin films by detecting changes in the intensity and phase of polarized light upon reflection or transmission. It can be used to monitor protein or lipid adsorption as a function of time. One important limitation, however, is that it cannot resolve the composition of the film due to the lack of contrast between the molecules under study in terms of their light refractive indexes.

Quartz crystal microbalance with dissipation monitoring (Marx, 2003), known as QCM-D, is an acoustic surface technique that can provide information about the mass and viscoelastic properties of the substances adsorbed on the surface of the quartz crystal. When subjected to an alternating electric field, the quartz crystal oscillates at a fundamental frequency (usually 5 MHz), with several overtones or harmonics (3rd, 5th, 7th, 9th, 11th, 13th). When additional mass is deposited on the crystal, the oscillation frequency decreases proportionally. Variations in mass in the nanogram range can be detected using this technique. QCM-D can provide information regarding the mass or mass density adsorbed on the surface of the quartz crystal, but it does not provide information about the composition and chemical identity of the materials adsorbed. To gain information regarding the latter, techniques such as neutron reflectometry (NR) need to be used. However, QCM-D can use chemically similar crystal surfaces as those used in NR (e.g., SiO₂), and it is therefore often used for preliminary studies in preparation for NR experiments as exemplified in **Paper I** (Orozco Rodriguez *et al.*, 2020) and **Paper III** (Orozco Rodriguez *et al.*, 2022b) of this thesis. In such pre-studies the goal is to determine the conditions that lead to an interaction between two partners, such as a supported lipid bilayer and a protein.

Small-angle scattering (SAS) is a technique that can provide structural information on a scale ranging from nanometers to micrometers regarding the shape, size, relative orientation, and interactions of macromolecules in solution. SAS is based on the

scattering of radiation, either in the form of X-rays (SAXS) or neutron beams (SANS), at small angles (typically ranging from 0.1° to 10°) after it interacts with structures that are much larger than the wavelength of the radiation (Jacques & Trewhella, 2010). SANS has been used to study a wide variety of biological systems (Mahieu & Gabel, 2018; Svergun & Koch, 2003), including protein solutions, liposomes (Komura *et al.*, 1982), proteins in nanodiscs (Skar-Gislinge *et al.*, 2010), proteins in micelles (Osborne *et al.*, 1978) and viral particles (Cusack *et al.*, 1985). Selective deuteration and contrast matching can be used to increase the natural contrast between chemically different molecules, or to create an artificial contrast between chemically similar molecules. In this way, it is possible to separate the signal from the protonated and the deuterated partners in a complex, and to focus on the structural signal from either of them separately.

2.4. Enzymatic activity assays and kinetics of membrane enzymes

A commonly used model for enzymatic reactions is the Michaelis-Menten equation (Johnson & Goody, 2011; Michaelis & Menten, 1913), which describes the initial rate of the reaction (v) as a function of substrate concentration:

$$v = \frac{V_{\max} [S]}{K_m + [S]} \quad (\text{Eq. 2.1})$$

Figure 2.2 depicts the initial reaction rate as a function of substrate concentration.

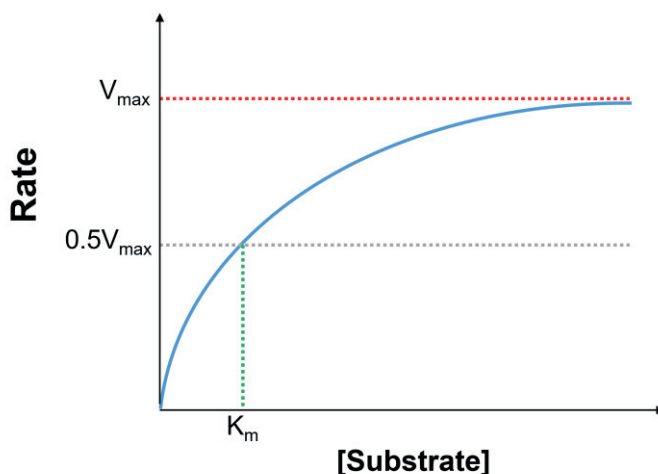


Fig. 2.2. Initial reaction rate as a function of substrate concentration as given by the Michaelis Menten equation.

The catalytic behaviour of many enzymes can be approximated using this equation. The kinetic characterization of an enzyme consists of the determination of its kinetic parameters with respect to one or more substrates. Examples of such parameters are the maximum reaction velocity (V_{\max}), the Michaelis-Menten constant (K_m) and the turnover number (k_{cat}). For the Michaelis-Menten equation to be valid, however, certain conditions must be met: the enzyme concentration should be much lower than the substrate concentration and the formation of the enzyme-substrate complex (ES complex) must be much faster than the formation of product. Furthermore, the ES complex is assumed to reach a *steady state*, where its concentration is assumed to be constant throughout the measured portion of the reaction. The Michaelis-Menten equation is not valid when there is substrate inhibition or activation due to the binding of a second substrate. Many enzymes with two or more substrates obey the Michaelis-Menten equation with respect to one substrate when the other substrates are kept constant at concentrations well above the K_m (10–20 times higher) (Copeland, 2000; Cornish-Bowden, 2013).

As its name indicates, the maximum reaction velocity is the maximum reaction rate that can be achieved under saturating substrate conditions ($[S] \gg K_m$). V_{\max} is often expressed in μmol of substrate converted (or product formed) per unit time under specific conditions of temperature, ionic strength, and pH.

The Michaelis-Menten constant (K_m) is defined as the substrate concentration that corresponds to a reaction velocity equal to half of V_{\max} . An alternative definition for K_m is the substrate concentration at which half of the enzyme active sites are saturated with substrate. For a single substrate, the value of K_m can vary widely from one enzyme to another. For a single enzyme, the K_m can also vary considerably from one substrate to another.

The *turnover number* (k_{cat}) is the maximum number of substrate molecules that can be converted into products per unit time per enzyme molecule (or per active site). It is calculated by dividing the V_{\max} value by the total number of enzyme molecules. If an enzyme only contains one active site, k_{cat} is often referred to as the *catalytic constant*. For a given enzyme and a given substrate, it is common to report the *catalytic efficiency* of an enzyme, which is given by the ratio k_{cat}/K_m . This ratio is also informative about substrate utilization for a particular enzyme that can use different substrates (e.g., deoxyribonucleoside kinases) (Cornish-Bowden, 2013).

To determine the kinetic parameters of an enzyme in the presence of a given substrate, the initial velocity is measured over a wide range of substrate concentrations. It is therefore necessary to be able to monitor either the depletion of substrate or the generation of product as a function of time. Detection can be performed by a wide

variety of methods, often by means of spectroscopy (absorbance, fluorescence), radioactivity, immunodetection, or by separating the products by chromatographic (thin layer or liquid chromatography) or electrophoretic means. The isolated products can be further detected by means of mass spectroscopy or nuclear magnetic resonance.

It is often not possible or practical to directly monitor either the substrate or the product. In such cases, it is necessary to couple product generation to an additional reaction. An example is the use of the redox sensitive dye, dichlorophenolindophenol (DCIP), to detect DHODH activity (Hines *et al.*, 1986; Miller *et al.*, 1968). Another example is the pyruvate kinase/lactate dehydrogenase coupled assay (Roskoski, 1983) used to determine the activities of kinases or ATPases. Pyruvate kinase uses the ADP produced by the target enzyme to convert phosphoenolpyruvate to pyruvate. Pyruvate is then used by lactate dehydrogenase to oxidize NADH to NAD⁺ which is measured by the decrease of absorbance at 340 nm.

DHODH is an interesting case as its enzymatic activity can be determined by direct methods (monitoring orotate formation), indirect methods (monitoring DCIP reduction) and using coupled assays involving the monitoring of O₂ consumption in isolated mitochondria (Löffler *et al.*, 1997).

As previously mentioned, membrane-bound enzymes are challenging to study due to the need to maintain a membrane-like environment to preserve their stability and activity. Membrane preparations are often turbid and tend to aggregate and precipitate, making spectroscopic measurements difficult or impossible. In addition, membrane extracts may contain several enzyme activities that interfere with the measurement of the activity of the target enzyme. Furthermore, membrane-bound enzymes that interact with membrane-bound or lipophilic substrates and co-substrates present yet another challenge in terms of kinetic characterization as the reaction system involves two-dimensional objects rather than only an isotropic three-dimensional solution. Under these conditions, the conventional Michaelis-Menten equation is not necessarily valid. The membrane-partitioning effects of both the protein and the (co)substrates must therefore be considered. Approaches such as interfacial membrane kinetics (Deems, 2000; Gelb *et al.*, 2000) take into consideration the partitioning of both the substrates and the enzyme between the membrane and the aqueous phases. This phenomenon is addressed in **Paper III** of this thesis (Orozco Rodriguez *et al.*, 2022b). It is often necessary to use detergents to solubilize the membrane protein of interest and to isolate it from other non-target enzymes present in the membrane. Solubilization may result in changes in protein stability and in modified kinetic properties. It is therefore necessary to screen a panel of different classes of detergents to select one which results in good protein stability, purity and which preserves enzymatic activity. It should be noted however, that removing a membrane protein from its native environment is likely

to result in the loss of other protein and lipid components that might naturally associated with the enzyme of interest. It is therefore useful to perform enzyme assays in the presence of relevant lipids and other membrane components suspected or known to be associated with the enzyme. Furthermore, membrane protein solubilization results in a transition from a planar lipid bilayer environment into the spherical or elliptical environment of a detergent micelle. Such a transition can influence substrate specificity and availability, as substrate molecules might have a limited access to the active site of the enzyme.

3. Neutron scattering

3.1. Fundamentals of neutron scattering

Neutrons are subatomic particles with no net electric charge. They possess mass and a magnetic moment. Their existence was predicted by Ernest Rutherford in 1920 and confirmed by James Chadwick in 1932. Neutrons can interact with matter via both nuclear and magnetic interactions. Due to their neutral charge, neutrons interact weakly with the atoms in the sample and can penetrate deep into the sample in a non-destructive manner. The energies associated with X-rays used in scattering techniques are in the keV (kiloelectron volt) range, whereas those of neutrons of similar wavelengths are in the meV (millielectron volt) range. Neutrons can be generated by either nuclear fission or by spallation (Fernandez-Alonso & Price, 2013). The latter is a process in which high energy proton beams excite atomic nuclei which emit neutrons upon relaxation back to their ground state without nuclear fission or a chain reaction.

Both X-ray and neutron scattering techniques (Sivia, 2011) can be used to probe the structure of matter in a length scale ranging from 10^{-10} to 10^{-3} meters (Ångströms to millimeters). X-rays are scattered by the electrons surrounding the nucleus of an atom, whereas neutrons are scattered by the atomic nuclei.

The use of neutrons as a probe to study biological materials (Fernandez-Alonso & Price, 2013) offers several advantages over X-rays. Neutrons are non-destructive. Neutrons are also highly penetrating due to their neutral charge. And finally, neutrons interact differently with different isotopes of certain elements, most notably with two of the isotopes of hydrogen: protium (^1H) and deuterium (^2H or D).

In physics, *scattering* refers to a process in which moving particles (e.g., a beam of neutrons) or radiation are forced to change their direction of motion after interacting with another particle or group of particles. Neutron scattering processes can be elastic

or inelastic. In *elastic scattering*, there is no change in the energy of the incident neutron beam. In *inelastic scattering*, the interaction also results in a change in the kinetic energy of the incident neutron beam.

Neutron scattering can be coherent or incoherent. In *coherent* scattering, the incident neutrons interact with the nuclei in a sample in a coordinated manner and the scattered waves display well-defined relative phases. Thus, the scattered waves from different nuclei interfere with each other. Coherent scattering provides information about the arrangement of atoms in the sample. On the other hand, in *incoherent* scattering, the neutron wave interacts with each nucleus in an independent manner and the scattered waves display random relative phases and do not interfere with each other. Incoherent scattering provides information about the motion of atoms in the sample, but it contains no structural information.

Every nucleus has a characteristic *neutron scattering length* (b_i), which is a measure of the strength of the interaction between a given nucleus and a neutron. **Table 3.1** displays the coherent neutron scattering lengths of the elements most commonly found in biological systems. The coherent nuclear scattering length varies randomly across the periodic table of elements. In contrast, the X-ray scattering lengths depend only on the number of electrons in the element. It should be noted that protium (^1H) has a rather large incoherent neutron scattering length ($25.3 \times 10^{-5} \text{ \AA}^{-1}$). This gives rise to background that does not contain information about the structure of the atoms in the sample and is particularly problematic for techniques such as neutron crystallography.

Table 3.1. Coherent neutron scattering lengths of common nuclei (Sears, 1992). If no isotope has been specified, the value of b has been calculated based on natural abundance.

Nucleus	b_i (10^{-5} \AA^{-1})
^1H	-3.741
^2H	6.671
C	6.646
N	9.36
O	5.803
Na	3.63
Si	4.149
P	5.13
S	2.847
Cl	9.577
Ca	4.70
F	5.654

The scattering length density ρ (also referred to as SLD) of a material, as given in **Equation 3.1**, is the sum of the coherent nuclear scattering lengths b_j of its constituent atoms and the number of atoms per unit volume, n_j (Fragneto-Cusani, 2001):

$$\rho = \sum_j b_j n_j \quad (\text{Eq. 3.1})$$

The different neutron scattering properties of protium (^1H , $b_j = -3.741$ fm) and deuterium (^2H or D, $b_j = 6.671$ fm) give rise to very different scattering length densities for H_2O ($-0.562 \times 10^{10} \text{ cm}^{-2}$) and D_2O ($6.404 \times 10^{10} \text{ cm}^{-2}$). By mixing different proportions of H_2O and deuterium oxide (D_2O), solvents with specific SLDs in this range can be made. **Table 3.2** lists the neutron scattering length densities of different materials and solvents.

Table 3.2. Neutron scattering length densities of some bulk materials (Sears, 1992).

Compound	ρ (10^{-6} \AA^{-2})
H_2O	-0.57
D_2O	6.35
CMSi (Si-matched water)	2.07
Si	2.07
SiO_2	3.41

In a scattering experiment (**Fig. 3.1**), an incident beam of neutrons characterized by an energy E_i and wave vector k_i is directed at the sample. Because neutrons interact weakly with matter, most of them are transmitted without interacting with the sample. Nonetheless, some neutrons will be scattered and will be measured by a detector placed at an angle θ , which is designated as the scattering angle.

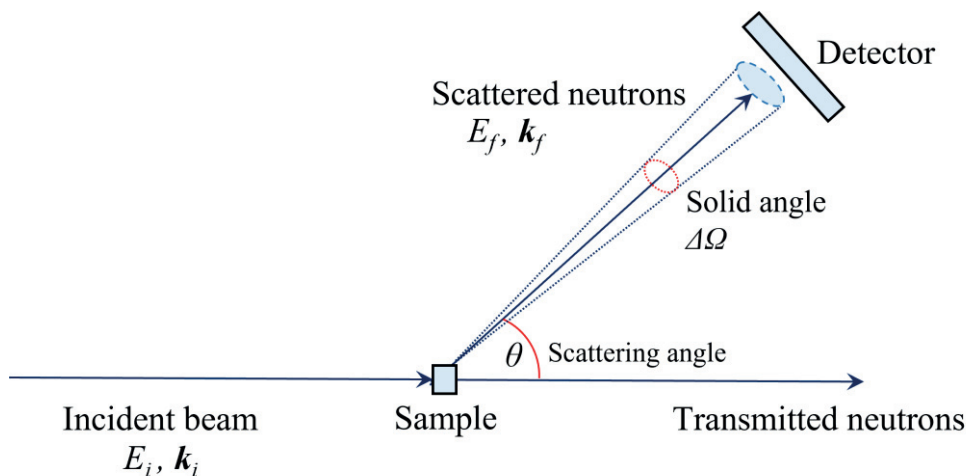


Figure 3.1. Schematic diagram of a generic arrangement for neutron-scattering experiments. Modified from (Sivia, 2011).

3.2. Deuterium labelling

In neutron scattering, *contrast* is defined as the difference between the average scattering length density of a material, molecule or group of molecules and that of the surrounding medium, e.g. solvent (Stuhrmann, 2012). Contrast variation refers to the use of chemically identical systems with different isotopic compositions, and therefore different scattering length density profiles, to collect datasets that are co-analyzed.

In neutron scattering, different structures with different scattering length density profiles can give rise to the same scattering pattern. Contrast variation is therefore essential as it makes it possible to find a unique solution to the structure of the system by simultaneously fitting the scattering patterns derived from systems with different isotopic compositions to a common physical system. Biological samples often consist of multiple components (proteins, lipids, nucleic acids, small molecules, etc.) and selective deuteration allows for the identification of specific components in the sample.

Figure 3.2 displays the scattering length densities of the four major macromolecules present in biological systems (proteins, phospholipids, DNA, and RNA) as a function of the concentration of D₂O in the solvent. The SLD of proteins tends to increase as a function of the D₂O concentration in the solvent due to the presence of exchangeable protons in the amino acid side chains. On the other hand, the SLD of phospholipids is less sensitive to changes in D₂O content due to presence of non-exchangeable protons in their acyl chain regions. The *match point* of a biomolecule corresponds to the intersection of the solvent SLD with that of the biomolecule. By changing the SLD of

the solvent to match specific parts of the biomolecule being studied, each part of the complex can be individually ‘matched out’ and rendered invisible. Contrast matching therefore makes it possible to distinguish different components (proteins, lipids) based on their SLD values.

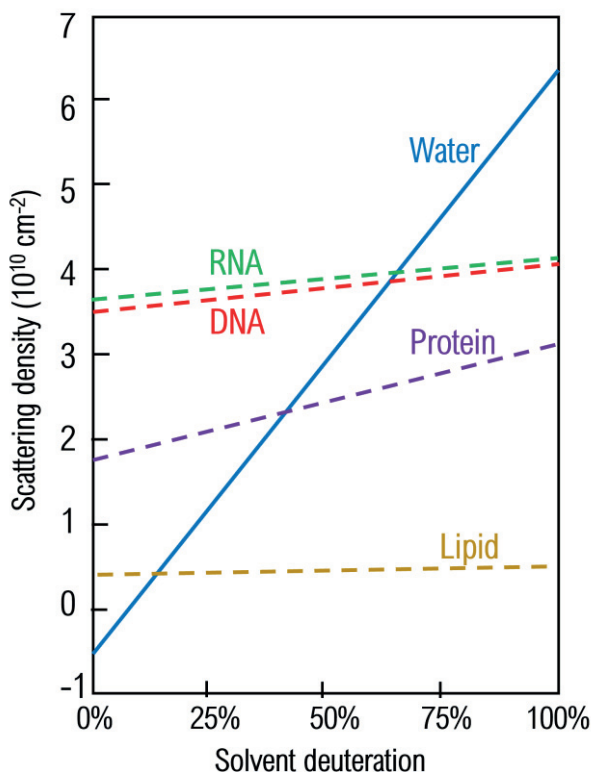


Figure 3.2. Scattering length densities of biomolecules as a function of solvent deuteration. Modified from (Dunne *et al.*, 2017).

Deuteration is defined as the partial or total replacement of protium (^1H) for deuterium (^2H , also designated as D) in a sample. The term *perdeuteration* refers to full deuteration (99% D incorporation). Since hydrogen and deuterium have dramatically different values of b , it is possible to alter the scattering length of hydrogenous materials.

Deuterium labelling is highly advantageous for neutron scattering techniques used in structural biology, such as neutron protein crystallography, neutron reflectometry and small angle neutron scattering. As previously mentioned, neutron protein crystallography offers several advantages compared to X-ray crystallography, including

low radiation damage to the crystal and the ability to discriminate between two isotopes of hydrogen: protium and deuterium due to the differences in their scattering lengths. This makes it possible to observe the position of the hydrogen atoms in the crystal structure. However, the negative scattering length and large incoherent scattering of protium lead to a low signal-to-noise ratio. As a result, neutron protein crystallography often requires partial or total deuteration of the sample, which is labour intensive and expensive. In addition, due to the weak interaction between neutrons and the sample under study, much larger crystals are required compared to those intended for X-ray diffraction.

3.3. Neutron reflectometry

Neutron reflectometry (NR) (Penfold & Thomas, 1990) is a neutron scattering technique used to determine the structure and composition of adsorbed thin films in the direction perpendicular to the interface and is applicable to liquid-solid, liquid-liquid, solid-gas, and liquid-gas interfaces. These interfaces have to satisfy three essential criteria. To begin with, the thickness of the film should ideally not exceed 1 μm as it is difficult to characterize thick films because the oscillations in the momentum transfer vector Q (known as “Kiessig fringes”) that correspond to the thicker layers are too closely spaced to be experimentally resolved in the low- Q reflectivity region. Second of all, there have to be differences in the neutron refractive indexes (that is, differences in neutron SLDs) of the materials on either side of the interface, and/or a film at the interface. Finally, the surrounding materials need to be transparent to neutrons (i.e., capable of transmitting neutrons) in order for the neutron beam to be able to reach the interface and for the reflection to be observable. This is the reason why the samples are often deposited on silicon or sapphire crystals, and it is also the reason why the neutron beam enters and exits the sample through air or solids such as silicon, and not through liquids. In addition to these essential criteria, the sample area must be large enough (typically 50×80 mm) to ensure that enough neutrons will be reflected as neutrons interact weakly with matter. The interface must be very flat (i.e., not curved or bent) and the roughness of the interface should be low (<20 Å rms, ideally less than 5 Å).

NR has been used to investigate a wide variety of biological systems, including lipid bilayers and monolayers (Fragneto *et al.*, 2001; Kučerka *et al.*, 2008; Wacklin, 2010) and membrane-protein interactions, interactions between membranes and small molecules (Benedetto *et al.*, 2014; de Ghellinck *et al.*, 2015), protein denaturation (Brouette *et al.*, 2013), biosurfactants, biosensors (Le Brun *et al.*, 2011), and whole cell adhesion to interfaces (Smith *et al.*, 2010).

The sensitivity of NR measurements depends to a large extent on the scattering contrast between different layers and between different components of each single layer. An adsorbed film has a characteristic SLD profile $\rho(z)$ which is a function of its nuclear composition and nuclear density.

When a beam of neutrons impinges on a planar interface between two media with different SLDs (ρ_1 and ρ_2) (**Fig. 3.3**), the following phenomena may take place: the neutrons can be reflected (either by specular or off-specular reflection), the neutrons can be transmitted, or they can be scattered incoherently. The transmitted neutron beam is said to be refracted if it changes direction due to differences in SLD between the layers. Absorption and multiple scattering are negligible in thin films due to the neutrons being weakly interacting particles.

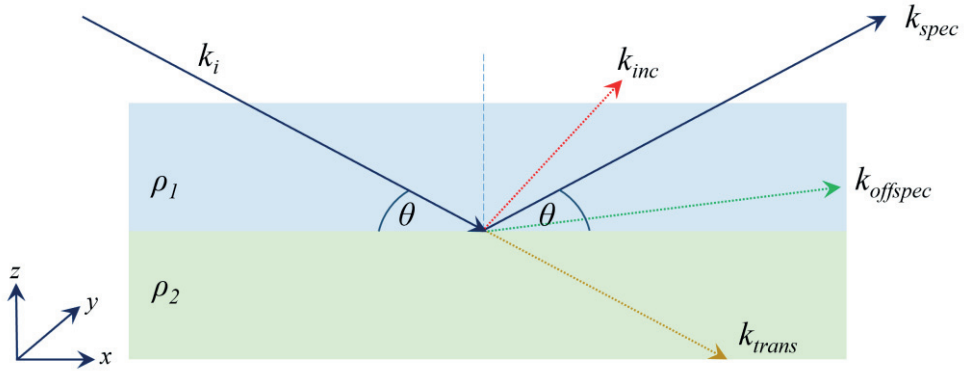


Figure 3.3. Neutron scattering events at an interface

Specular (mirror-like) neutron reflection occurs when the angle between the incident beam and the interface is equal to the angle between the reflected beam and the interface. In *off-specular* reflection, the angles are not the same. Off-specular reflection typically arises from the roughness of the interface. To describe specular neutron reflection, it is convenient to think in terms of momentum transfer perpendicular to the interface, in the z direction. The total momentum transfer in the z direction, Q_z , is thus given by **Equation 3.2**:

$$Q_z = 2k_i = \frac{4\pi \sin \theta}{\lambda} \quad (\text{Eq. 3.2})$$

where λ is the wavelength of the incoming neutron beam and θ is the angle of the beam with the interface. **Figure 3.4** illustrates the phenomenon of specular neutron reflectivity.

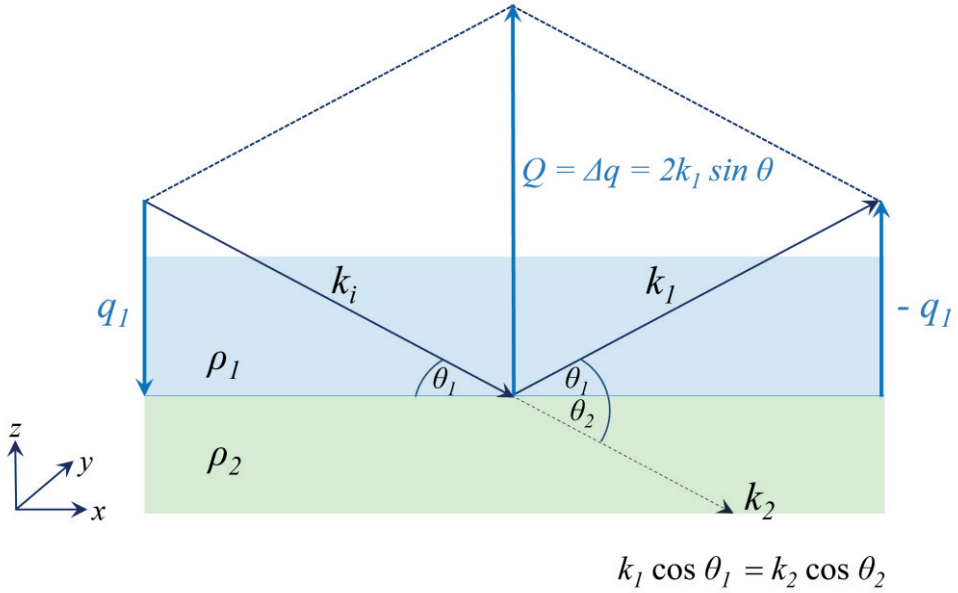


Figure 3.4. Geometry of specular reflection and transmission

Total internal reflection occurs when $\theta_2 = 0$. Under this condition, a *critical angle*, θ_c , can be defined. The total momentum transfer in the z direction at the critical angle (Q_c) is given by **Equation 3.3**:

$$Q_c = 2k_i = \frac{4\pi \sin \theta_c}{\lambda} \quad (\text{Eq. 3.3})$$

As the critical angle is a function of the SLDs on both sides of the interface, the critical momentum transfer is unique to each pair of materials. The $\text{SiO}_2\text{-D}_2\text{O}$ interface has a critical momentum transfer value of 0.0147 \AA^{-1} .

Reflectivity (R) is defined as the ratio between the number of reflected neutrons and the number of transmitted neutrons. In a NR experiment, reflectivity is recorded as a function of momentum transfer (Q).

In a thin adsorbed film consisting of several layers (**Fig 3.5**), reflection and transmission are given by the Fresnel coefficients r_{ij} and t_{ij} at each interface. The Fresnel reflection coefficients can be calculated using the optical matrix method as described by Born and

Wolf for *s*-polarised light (Born & Wolf, 2013). In the optical matrix method, adsorbed layers are modelled as smooth, homogeneous slabs with characteristic SLDs. A matrix describing the reflection and transmission of neutrons can be defined for each layer. The Motofit software package (Nelson, 2006) makes use of the Abelès optical matrix method (Abelès, 1950) to accomplish this task.

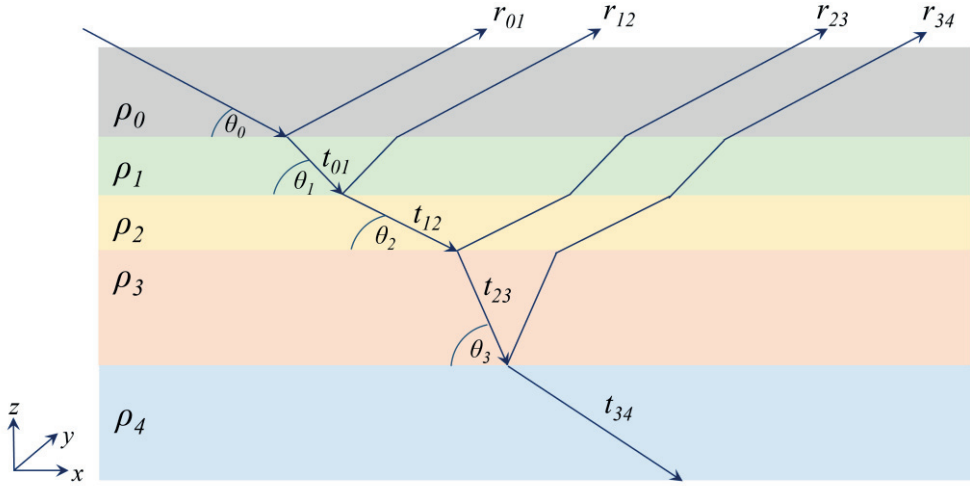


Figure 3.5. Reflection from a film consisting of multiple layers

NR, like all other scattering techniques, suffers from the limitations imposed by the phase problem. Due to this, different scattering length density profiles can give rise to the same reflectivity profile. The most common way to circumvent this limitation is by using the principle of contrast variation. In this case, the reflectivity profiles of chemically identical systems with different isotopic composition (and therefore different scattering length densities) are analyzed together and fitted to a common physical system.

There are several neutron reflectometers available. A recent listing and description of their capabilities can be found in (Fisher *et al.*, 2017). As part of this thesis work NR experiments have been performed on the D17 and INTER reflectometers, which are shortly described below.

The D17 reflectometer (Cubitt & Fragneto, 2002) (**Fig. 3.6**) is located at the Institut Laue-Langevin (ILL) in Grenoble, France. The ILL fission reactor operates with a power output of 58 MW. The useful cold neutron wavelength range is 2 – 20 Å. The incoming neutron beam is cut into pulses by a chopper and collimated by two sets of slits to provide a beam area of 10 × 70 mm. D17 has an area detector placed in a housing

filled with ^{10}B -enriched BF_3 gas to capture neutrons. Two incident angles (0.7° and 3.0°) were used to obtain the full reflectivity profiles covering the range between $0.01 < Q < 0.25 \text{ \AA}^{-1}$ with a 7% wavelength resolution. The scattering geometry in D17 is horizontal, and therefore the reflectivity cells are mounted vertically in the neutron beam.

The INTER reflectometer (Webster *et al.*, 2006) (**Fig. 3.7**) is located at the ISIS Neutron and Muon Source in Didcot, UK. At ISIS the neutron beam is produced by a spallation process from a tantalum metal target bombarded by protons. In the case of the INTER reflectometer, the incidence angles used were 0.7° and 2.3° and reflectivity profiles were recorded using neutron wavelengths in the range from 1 to 15 \AA , covering a Q range from 0.009 to 0.3 \AA^{-1} and a momentum transfer resolution of 4%. Contrary to D17, the scattering geometry in INTER is vertical, and therefore the reflectivity cells are mounted horizontally in the neutron beam.

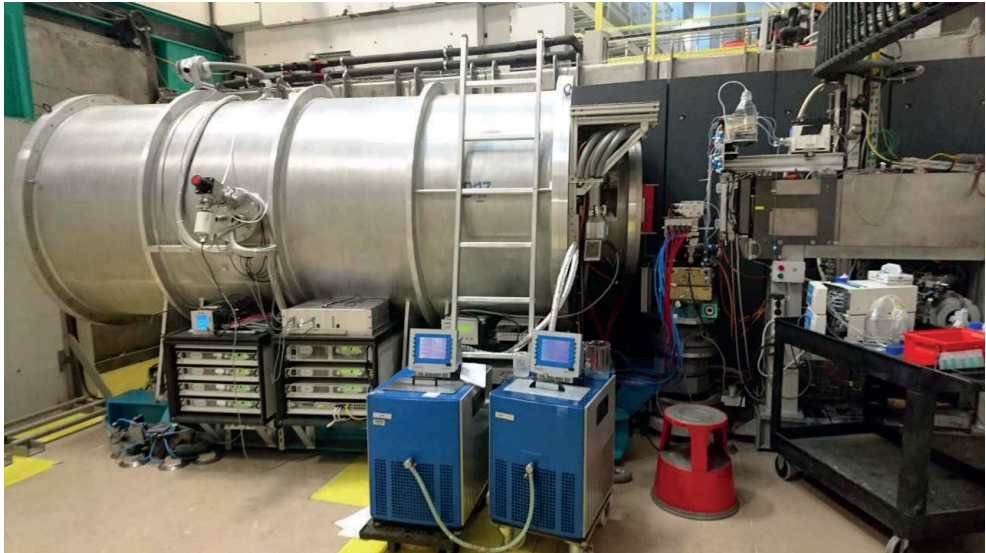


Figure 3.6. The D17 reflectometer (Cubitt & Fragneto, 2002) at the ILL.



Figure 3.7. The INTER reflectometer at ISIS (Webster *et al.*, 2006) and the author of this report during an experiment presented in **Paper IV** (Orozco Rodriguez *et al.*, 2022c) of this report.

4. Dihydroorotate dehydrogenases

4.1. *De novo* pyrimidine biosynthesis and DHODHs

The supply of the different cellular pyrimidine pools can occur by *de novo* synthesis or by salvage of degraded pyrimidine nucleosides. The *de novo* pyrimidine biosynthesis pathway is nearly universal to all organisms and consists of six steps (**Fig. 4.1**). The final product of the pathway, uridine monophosphate (UMP), is the starting point to deliver dNTP precursors for DNA synthesis, as well as NTP precursors for RNA synthesis (Denis-Duphil, 1989; Evans & Guy, 2004; Hermansen *et al.*, 2015; Löffler *et al.*, 2005). UMP also acts as a precursor for several molecules: UDP-glucose, which is involved in the synthesis of proteoglycans; UDP N-acetylglucosamine (UDP-GlcNAc), which plays a role in protein glycosylation; and CDP-choline, which participates in phosphatidylcholine synthesis (Wang *et al.*, 2021).

The fourth enzymatic reaction of the *de novo* pyrimidine biosynthesis pathway, the oxidation of dihydroorotate to orotate, is catalyzed by flavoenzymes known as *dihydroorotate dehydrogenases* (DHODHs). DHODHs have been reviewed extensively elsewhere (Löffler *et al.*, 2020; Munier-Lehmann *et al.*, 2013; Reis *et al.*, 2017).

On the other hand, the pyrimidine salvage pathway uses the nucleoside breakdown products of DNA and RNA as starting material to form nucleoside monophosphates. Pyrimidine salvage involves the phosphorylation of uridine, cytidine, deoxycytidine and deoxythymidine by a variety of cytosolic and mitochondrial nucleoside and deoxynucleoside kinases (Christiansen *et al.*, 2015; Löffler *et al.*, 2005; van Kuilenburg & Meinsma, 2016; Wang, 2016).

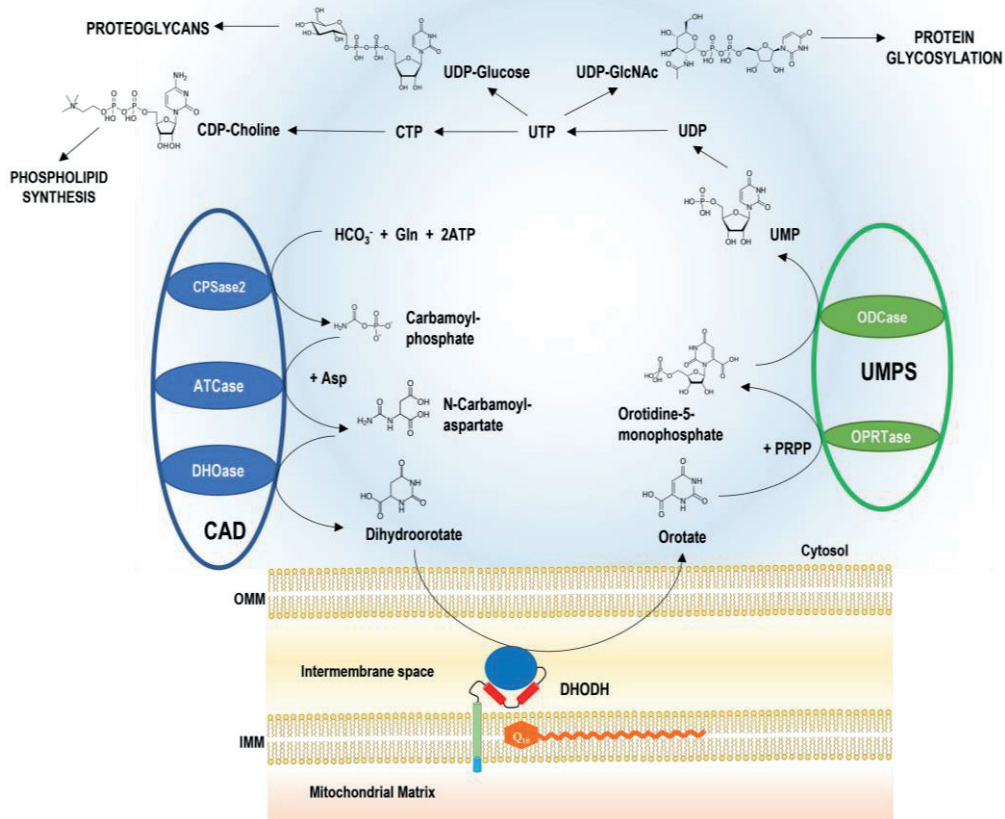


Figure 4.1. *De novo* pyrimidine biosynthesis in humans. CAD: carbamoyl-phosphate synthetase 2, aspartate transcarbamylase, and dihydroorotase. UMPS: uridine monophosphate synthetase. CPSase2: carbamoyl phosphate synthetase 2. ATCase: aspartate transcarbamylase. DHOase: dihydroorotase. DHODH: dihydroorotate dehydrogenase. OPRTase: orotate phosphoribosyl transferase. ODCase: Orotidine 5'-phosphate decarboxylase. Q₁₀: coenzyme Q₁₀. OMM: outer mitochondrial membrane. IMM: inner mitochondrial membrane. Asp: aspartate. PRPP: phosphoribosyl pyrophosphate. UMP: Uridine monophosphate. UDP: Uridine diphosphate. UTP: Uridine triphosphate. CTP: Cytidine triphosphate. UDP-GlcNAc: UDP-N-acetyl glucosamine. Modified from (Orozco Rodriguez *et al.*, 2022a) and (Wang *et al.*, 2021).

The DHODHs discovered so far can be divided into two major families or classes based on sequence similarity, quaternary structure, subcellular localization, and preference for electron acceptors (Björnberg *et al.*, 1997; Nørager *et al.*, 2002). Class I DHODHs are cytosolic proteins and are either homodimeric (Class IA) or heterotetrameric (Class IB). In contrast to Class I enzymes, Class II DHODHs are monomeric, membrane-bound proteins that use ubiquinones as electron acceptors.

4.2. Class II dihydroorotate dehydrogenases

The DHODH from *E. coli* (*Ec*DHODH) is regarded as the prototype for Class II DHODHs (Björnberg *et al.*, 1999; Björnberg *et al.*, 1997). The overall fold of dihydroorotate dehydrogenases is that of an α/β barrel consisting of a central barrel of parallel β -strands surrounded by α -helices. The flavin mononucleotide (FMN) prosthetic group is located between the barrel and additional antiparallel β -strands. In Class II DHODHs, there is a distinct N-terminal domain that typically consists of two α -helices linked by a short loop. This helical domain forms a tunnel leading to the active site. The α/β barrel corresponds to the catalytic domain. In higher eukaryotes, additional residues (20–50) are present at the N-terminus and play a role in targeting and subcellular localization (Reis *et al.*, 2017) as first shown for the human DHODH (Rawls *et al.*, 2000). The N-terminus also plays a role in stability (Löffler *et al.*, 2002; Orozco Rodriguez *et al.*, 2022a), and substrate specificity and usage (Orozco Rodriguez *et al.*, 2022a).

The overall catalytic cycle of DHODHs (Fig. 4.2) consists of two reactions. In the first reaction, dihydroorotate (DHO) is oxidized to orotate (ORO) with the simultaneous reduction of the FMN prosthetic group. The catalytic base (either serine in Class II DHODHs or cysteine in Class I DHODHs) is responsible for deprotonating DHO. In the second reaction, FMN is oxidized by an electron acceptor, which is a quinone in the case of Class II DHODHs.

A recent analysis (Sousa *et al.*, 2021) of 6394 genomes corresponding to 4135 different species found 1514 genes encoding quinone-dependent dihydroorotate dehydrogenases (Class II DHODHs). These genes were found in species from all domains of life (Archaea, Bacteria, Eukarya).

This dogma of Class II DHODHs dependence on quinones has recently been challenged. Class II DHODHs have been identified in certain yeasts (*Dekkera*, *Schizosaccharomyces*) and fungi (*Anaeromyces*) which do not require ubiquinones and use other molecules such as free FAD, FMN, and fumarate as electron acceptors, thus

enabling these organisms to support anaerobic pyrimidine biosynthesis (Bouwknegt *et al.*, 2021).

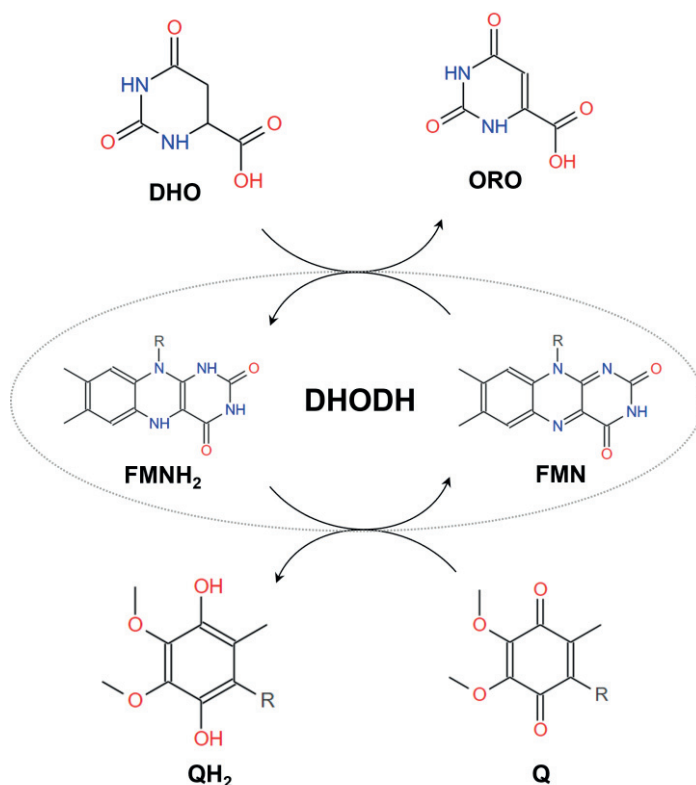


Fig 4.2. Overall catalytic cycle for Class II DHODHs.

4.2.1. Activity assays for Class II DHODHs

Several assays have been developed to determine the enzymatic activity and inhibition of dihydroorotate dehydrogenases. These assays can be classified as spectrophotometric, fluorometric and radiometric.

Spectrophotometric assays can be either direct or indirect. DHODH activity can be determined by directly monitoring the formation of the product, orotate, at 300 nm in the presence of the substrate (dihydroorotate) and the co-substrate (ubiquinone or some other electron acceptor or oxidizing agent) both with isolated enzyme or DHODH activity measured in mitochondria (Feliciano *et al.*, 2006; Knecht *et al.*, 1996). A reaction buffer is often supplemented with the detergent Triton X-100 to aid in the

solubilization of the enzyme. One major disadvantage of the direct measurement of orotate is that Triton X-100 strongly absorbs in the near UV region, making it impossible to detect orotate formation in the presence of this detergent. In these situations, it is necessary to use indirect assays to detect enzymatic activity. The most widely used indirect assay consists of using 2,6-dichlorophenolindophenol (DCIP) (Miller *et al.*, 1968). DCIP is a redox sensitive dye that acts as the electron acceptor in the assay. DCIP displays an intense blue colour when oxidized and becomes colourless when reduced. Enzymatic activity can therefore be indirectly determined by monitoring the colour change spectrophotometrically at 600-610 nm. Electrons are transferred from dihydroorotate to the FMN cofactor, from FMN to ubiquinone, and finally from ubiquinone to DCIP. The reduction of DCIP is assumed to be stoichiometrically equivalent to the oxidation of dihydroorotate. It should be noted, however, that DCIP has been reported to act as an alternative substrate to ubiquinone (Hines *et al.*, 1986). It has been estimated that 10-30% of the detected enzymatic activity can be due to the direct reduction of DCIP by DHODH (McLean *et al.*, 2001).

Fluorimetric assays make use of fluorogenic agents to determine enzyme activity. A fluorescent assay based on resazurin was recently developed to assess the activity of the DHODH from *Plasmodium falciparum* (Caballero *et al.*, 2016). Resazurin is a redox-sensitive fluorescent dye which is blue in colour non-fluorescent when oxidized and becomes resofurin upon reduction, which is pink and fluorescent. This transition is monitored at 590 nm (Caballero *et al.*, 2016). Another fluorimetric assay uses the fluorogenic agent 4-trifluoromethylbenzamidoxime (4-TFMBAO) (Yin *et al.*, 2017). This agent displays strong fluorescence when it reacts with orotic acid in the presence of $K_3[Fe(CN)_6]$, and K_2CO_3 in an aqueous solution at 80 °C. This assay has been used to determine DHODH activity in complex biological samples, such as tissues and cultured mammalian cells (Yin *et al.*, 2017).

Radiometric assays to determine DHODH activity make use of substrates labelled with radioactive isotopes. One such assay consists of the conversion of L-[carboxy- ^{14}C] dihydroorotate to [carboxy- ^{14}C]orotic acid by DHODH. The reaction mixture also contains the enzymes orotate phosphoribosyltransferase (OPRTase) and orotidylate decarboxylase (ODCase), which produce labelled $^{14}CO_2$ as the final product (Smithers *et al.*, 1978). Another radiometric assay is based on the conversion of DL-[4- ^{14}C]DHO to [4- ^{14}C]orotic acid, followed by product isolation by electrophoresis or chromatography (Dileepan & Kennedy, 1983).

DHODH activity can be indirectly determined by monitoring oxygen consumption in isolated mitochondria in the presence of dihydroorotate (Löffler *et al.*, 1997). This is an example of an *in vivo* coupled enzyme assay, as electrons flow from the substrate to

DHODH and to the respiratory complexes III and IV in the inner mitochondrial membrane.

DHODH activity has also been determined via catalytic histochemistry in mammalian tissues (Löffler *et al.*, 1996), monitoring the reduction of the dye nitroblue tetrazolium (NBT). The *in situ* determination of hydrogen peroxide enzymatically generated by DHODH using electron microscopy and cerium capture in the mitochondria of rat heart and kidney with the purpose of localizing DHODH activity has also been reported (Angermüller & Löffler, 1995). Mitochondria have been shown to generate reactive oxygen species from multiple sites under certain conditions of substrate supply and inhibition of the electron transport chain. Reactive oxygen species are produced at the ubiquinone binding site of DHODH (D_Q site) upon DHODH inhibition (Goncalves *et al.*, 2020).

4.2.2. Human dihydroorotate dehydrogenase

Human DHODH (*HsDHODH*) is a Class II DHODH located in the inner mitochondrial membrane and uses ubiquinone Q_{10} as the electron acceptor. Therefore, *HsDHODH* serves as a link between pyrimidine biosynthesis and the respiratory chain (Knecht *et al.*, 1996; Löffler *et al.*, 2005; Rawls *et al.*, 2000). The structure and orientation of *HsDHODH* in the IMM is illustrated in **Fig. 4.3**, which also shows the proposed location of ubiquinone within the membrane. The N-terminus of *HsDHODH* contains a bipartite signal, consisting of mitochondrial signal (MS) and a transmembrane segment (TM), that determines its import and correct insertion into the IMM (Rawls *et al.*, 2000). The N-terminal parts of Class II DHODHs are connected to the catalytic domain via a microdomain containing two amphipathic alpha helices ($\alpha 1$ and $\alpha 2$). Nearly all literature suggests that human DHODH is a stand-alone enzyme and not part or even loosely associated with any respiratory supercomplexes (Boukalova *et al.*, 2020).

There are several mitochondrial enzymes that use ubiquinone Q_{10} apart from DHODH and the complexes of the respiratory chain. Examples of these Q_{10} -dependent enzymes include choline dehydrogenase (CHDH), electron-transferring flavoprotein dehydrogenase (ETF_{FDH}), mitochondrial glycerol-3-phosphate dehydrogenase (GPD2), proline dehydrogenases 1 and 2 (PRODH1 and PRODH2), and sulfide:quinone oxidoreductase (SQOR) (Banerjee *et al.*, 2021)

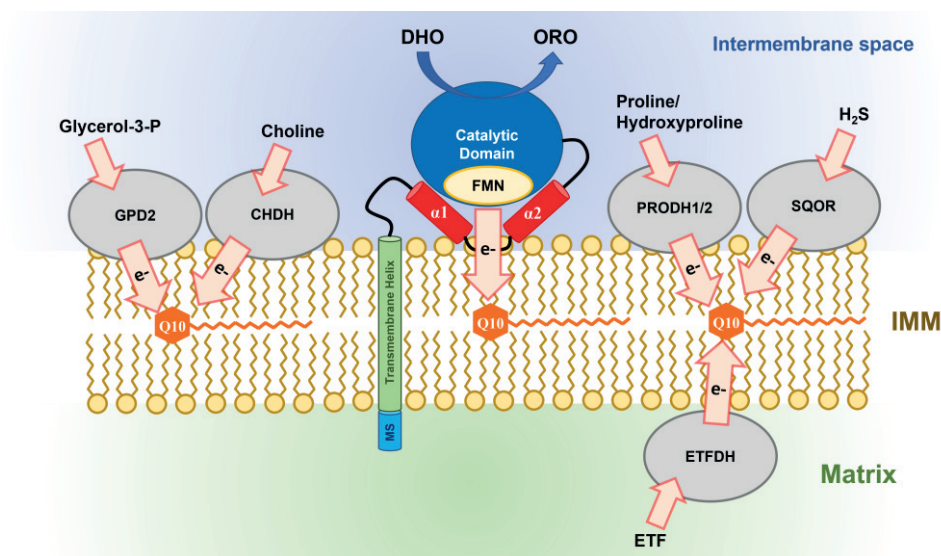


Figure 4.3. Proposed location and orientation of human DHODH and coenzyme Q₁₀ in the inner mitochondrial membrane (IMM) and ubiquinone-dependent mitochondrial enzymes. MS: mitochondrial signal peptide. FMN: flavin mononucleotide prosthetic group. Q₁₀: coenzyme Q₁₀. e⁻: electron flow. DHO: dihydroorotate. ORO: orotate. GPD2: mitochondrial glycerol-3-phosphate dehydrogenase. CHDH: choline dehydrogenase. PRODH1/2: proline/hydroxyproline dehydrogenase 1 and 2. SQOR: sulfide:quinone dehydrogenase. ETF: electron-transferring flavoprotein. ETFDH: ETF dehydrogenase. Modified from **Paper I** (Orozco Rodriguez *et al.*, 2020) and (Banerjee *et al.*, 2021).

Medical relevance of HsDHODH

Inhibition of pyrimidine biosynthesis has been explored as a strategy for treating autoimmune and inflammatory disorders, infectious diseases, and certain types of cancer. *HsDHODH* has therefore been the target of extensive efforts directed at finding and developing inhibitors. *HsDHODH* is currently the target for the anti-inflammatory drugs leflunomide (ARAVA®), approved for the treatment of rheumatoid arthritis and its active metabolite, teriflunomide (AUBAGIO®), approved for multiple sclerosis.

DHODH activity is believed to be linked to certain cancers because abnormal cell proliferation is correlated with an aberrant pyrimidine metabolism. Due to their excessive growth rate, cancer cells extensively utilize *de novo* pathways for nucleotide biosynthesis (Robinson *et al.*, 2020). The inhibition of DHODH with small organic molecules is being evaluated as a strategy for cancer treatment and recent advances regarding the current development and future perspectives of these inhibitors have recently been reviewed (Zhang *et al.*, 2022).

Proliferating cancer cells need to adapt to harsh conditions such as hypoxia and nutritional deficiency. Under hypoxia, cancer cells depend on glutamine as a carbon source, which leads to excretion of excess nitrogen in the form of dihydroorotate. The inhibition of the CAD (carbamoyl-phosphate synthetase 2/aspartate transcarbamylase/dihydroorotase) and DHODH by short-hairpin RNA (shRNA), which are indispensable for pyrimidine biosynthesis, led to a suppressive effect on the proliferation of HeLa cells. Furthermore, knockdown of CAD and DHODH also repressed *in vivo* tumour growth in a mouse model (Wang *et al.*, 2019).

HsDHODH was recently validated as a target for the treatment of acute myeloid leukemia (AML) (Sykes *et al.*, 2016), as its inhibition overcomes the myeloid cell differentiation blockade. It was recently demonstrated that it is possible to block the proliferation of activated T-cells by inhibiting *HsDHODH* with Brequinar in a dose-dependent manner and that this cytostatic effect is due to decreased intracellular levels of deoxypyrimidines and not linked to the downstream impairment of oxidative phosphorylation (Peeters *et al.*, 2021).

Only very recently, *HsDHODH* was identified as the mitochondrial gatekeeper of cell death by ferroptosis (a programmed cell death characterized by the accumulation of lipid peroxides) because DHODH deletion promotes ferroptosis, even in the presence of uridine (Mao *et al.*, 2021). This new functionality of DHODH is coupled to its substrate, ubiquinone Q₁₀, because the reduced form of Q₁₀, ubiquinol, has antioxidant properties and can repair lipid peroxides. These new findings revealed that DHODH protects mitochondrial lipids from damage by reducing Q₁₀.

Inhibition of *HsDHODH* has also been investigated as a therapy against the SARS-CoV-2 virus. The *HsDHODH* inhibitor PTC299 was recently found to display a robust, dose-dependent inhibition of viral replication in human and primate cell lines (Luban *et al.*, 2021).

Miller syndrome

Miller syndrome (Donnai *et al.*, 1987; Genée, 1969; Miller *et al.*, 1979; Trainor & Andrews, 2013; Wiedemann, 1973), also known as Genée-Wiedemann and Wildervanck-Smith syndrome or Postaxial Acrofacial Dysostosis: POADS (OMIM #263750) is a rare autosomal Mendelian disorder. At least 30 cases have been reported and it is estimated to affect fewer than 1 in 1 million new-borns. It presents itself as a recognizable acrofacial dysostosis syndrome with a combination of craniofacial and limb anomalies.

Miller Syndrome was found to be caused by mutations in the human dihydroorotate dehydrogenase gene and became the first Mendelian disorder whose molecular basis

was revealed by whole-exome sequencing (Ng *et al.*, 2010). All patients were found to be compound heterozygotes, and each parent was found to be a carrier. To this date, 15 missense mutations have been identified (<https://omim.org/entry/126064>, accessed 2022-01-31), as well as one non-sense mutations (R326) and two frameshift mutations (at H55 and L204) (Al Kaissi *et al.*, 2011; Duley *et al.*, 2016; Kinoshita *et al.*, 2011; Ng *et al.*, 2010; Rainger *et al.*, 2012). Three of the non-sense mutations are of particular interest to us due to their location: G19E, located in the transmembrane domain; E52G, located in the alpha helical microdomain; and R135C, located in the putative ubiquinone binding region. **Figure 4.4** displays a schematic representation of human DHODH with the mutations of interest highlighted in yellow. Amino acid numbering is given above, the structural elements MS, TM, $\alpha 1$, $\alpha 2$ and catalytic domain are aligned approximately. **Paper II** of this thesis (Orozco Rodriguez *et al.*, 2022a) contains the latest comprehensive review of Miller syndrome.

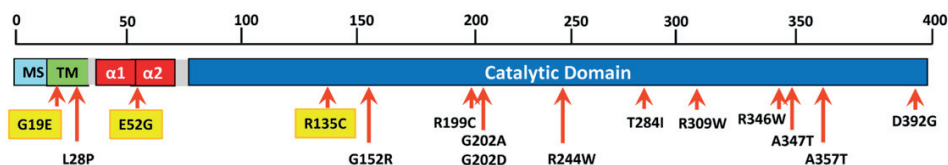


Fig. 4.4. Schematic representation of human DHODH, missense mutations associated with Miller syndrome. Adapted from **Paper II** (Orozco Rodriguez *et al.*, 2022a).

Structural and membrane studies of HsDHODH

The crystallization of a truncated variant of HsDHODH (lacking the mitochondrial signal peptide and transmembrane domain) was first reported in 2000 (Liu *et al.*, 2000). Many crystal structures of the soluble catalytic domain of HsDHODH in complex with inhibitors have been reported ever since (Reis *et al.*, 2017) but there is virtually no experimental structural data of the enzyme in a membrane-bound state.

So far, spectroscopic measurements indicate that the $\alpha 1$ - $\alpha 2$ microdomain assumes a different conformation in detergent micelles and phospholipid vesicles (Vicente *et al.*, 2015), indicating that the nature of the membrane environment may play a role in the structure adopted. Studies combining circular dichroism, NMR spectroscopy and electron spin resonance (Vicente *et al.*, 2017) have also shown that a peptide corresponding to the N-terminal $\alpha 1$ - $\alpha 2$ microdomain is disordered in buffer solution but acquires an α -helical conformation in membrane mimics and that the lipid composition influences the conformation of the microdomain, as it preferentially interacts with cardiolipin-containing membranes.

It has been reported that the addition of phospholipids such as phosphatidylcholine (PC), phosphatidylethanolamine (PE) and cardiolipin increases the reaction rate (V_{\max}) of *Hs*DHODH (Costeira-Paulo *et al.*, 2018). It should be noted, however, that the enzyme used in those studies contained an N-terminal polyhistidine tag. A thorough kinetic characterization of several variants of *Hs*DHODH (including wild-type, truncated and Miller syndrome mutants) was recently performed and no increase in enzymatic activity upon phospholipid addition was observed as shown in **Paper III** (Orozco Rodriguez *et al.*, 2022b).

Non-denaturing mass spectrometry studies have shown that cardiolipin exhibits the most stable association with *Hs*DHODH compared to PC and PE (Costeira-Paulo *et al.*, 2018).

Another interesting question is how the enzyme interacts with the ubiquinone, which has been shown to be located in the hydrophobic center of lipid membranes (Hauß *et al.*, 2005), but also needs to access the DHODH membrane-targeting microdomain (Walse *et al.*, 2008). Recently, it has been proposed that inhibitor binding to DHODH is influenced by interactions with lipids in the IMM (Cao *et al.*, 2019). This is supported by previous findings showing differences in the inhibition of *Hs*DHODH by Brequinar depending on whether the TM is present or not (Ullrich *et al.*, 2001).

4.2.3. *E. coli* dihydroorotate dehydrogenase: structural and membrane studies

The dihydroorotate dehydrogenase from *E. coli* (*Ec*DHODH) is a Class II DHODH associated with the cytosolic membrane. In contrast to human DHODH, *Ec*DHODH is not an integral membrane protein, but rather membrane-associated (Karibian, 1978; Taylor & Taylor, 1964). It was initially reported to remain in the insoluble fraction of lysed *E. coli* cells (Taylor & Taylor, 1964). *Ec*DHODH is encoded by the *pyrD* gene, has a mass of 37 kDa and contains one FMN molecule (Larsen & Jensen, 1985). *Ec*DHODH uses ubiquinones as electron acceptors during aerobic growth but must be able to use alternative electron receptors (menaquinone, demethylmenaquinone) during anaerobic growth (Nitzschke & Bettenbrock, 2018).

The crystal structure of *Ec*DHODH was first determined by Nørager *et al.* (Nørager *et al.*, 2002). *Ec*DHODH is a monomer and consists of 11 α -helices, four 3_{10} helices, and 13 beta strands. Its overall fold is that of an α/β barrel, as is the case for *Hs*DHODH and other Class II DHODHs. The N-terminal domain of *Ec*DHODH consists of two α -helices and a short 3_{10} helix; it is essential for stability and activity, and is connected to the catalytic domain by a long flexible loop (Nørager *et al.*, 2002).

The interaction of *Ec*DHODH with mixed dioleoyl phosphatidylcholine (DOPC)/Triton X-100 vesicles has been investigated by electronic spin resonance

(Couto *et al.*, 2008). Addition of *Ec*DHODH to the DOPC vesicles resulted in the formation of a spacer effect in the hydrophobic region of the membrane, indicating that the enzyme is being docked on the surface of the vesicles.

The binding of *E. coli* DHODH and N-terminally truncated *Hs*DHODH to supported lipid bilayers (SLB) of palmitoyl-oleoyl phosphatidylcholine (POPC), tetraoleoyl cardiolipin (TOCL) and ubiquinone Q₁₀ has been characterized in **Papers I** and **IV** (Orozco Rodriguez *et al.*, 2020; Orozco Rodriguez *et al.*, 2022c). The results indicated that *Ec*DHODH displayed a stronger binding and better retention towards bilayers consisting of synthetic lipids (POPC, TOCL, Q₁₀) compared to truncated *Hs*DHODH. The lipid composition also played a major role as the interaction between *Ec*DHODH and lipid bilayers mimicking the composition of the inner bacterial membrane (POPC, POPE, POPG, TOCL) was stronger and more stable than that between *Ec*DHODH and membranes lacking POPG and POPE.

4.2.4. Other Class II DHODHs

As previously mentioned, a recent bioinformatic analysis (Sousa *et al.*, 2021) identified 1514 Class II DHODH coding genes by sequence analysis. To this date, 14 Class II DHODHs have been successfully isolated and biochemically characterized. These include with most data available the DHODHs from model organisms and some pathogens like *Arabidopsis thaliana*, *Drosophila melanogaster*, *Candida albicans*, *Rattus norvegicus*, *Mus musculus*, and *Plasmodium falciparum* (in addition to *Hs*DHODH and *Ec*DHODH) and are therefore described below.

Plasmodium falciparum is the major malarial parasite in humans. However, *P. falciparum* lacks pyrimidine salvage pathways and is completely dependent on *de novo* pyrimidine biosynthesis (Cassera *et al.*, 2011). Therefore, the DHODH from *P. falciparum* (*Pf*DHODH) has been evaluated as a drug target to combat malaria (Singh *et al.*, 2017). The drug Malarone™, which is a combination of atovaquone (an analogue of ubiquinone) and proguanil, is a medication used to treat and prevent malaria that targets the malarial respiratory chain. In *Plasmodium* species, the site of action of atovaquone appears to be the cytochrome *bc1* complex (Complex III) and that of proguanil is dihydrofolate reductase (McKeage & Scott, 2003).

*Pf*DHODH is less inhibited by A771726 and Brequinar analogues than human DHODH (Baldwin *et al.*, 2002). On the other hand, *Pf*DHODH is selectively inhibited by triazolopyrimidines including DSM265, which is an antimalarial agent targeting *Pf*DHODH, it has proven to be effective against *Pf*DHODH in blood and liver stages (Phillips *et al.*, 2015) and is currently being evaluated in clinical trials (Bélard & Ramharter, 2018). The X-ray structure of N-terminally truncated (lacking

the first 158 amino acid residues) *Pf*DHODH bound to teriflunomide was first determined by Hurt *et al.* (Hurt *et al.*, 2006). It should be noted that the N-terminus in *Pf*DHODH is much longer compared to other DHODHs, and its function remains largely unknown. *Pf*DHODH consists of 565 amino acid residues and displays an overall α/β barrel fold similar to that of other Class II DHODHs. The catalytic domain consists of 8 parallel β -strands surrounded by 8 α -helices. *Pf*DHODH contains a 44-residue insertion (376–419) in the core domain. The N-terminal domain also consists of two α -helices. The putative quinone binding tunnel in *Pf*DHODH is much smaller than that of *Hs*DHODH and may explain why inhibitors larger than A771726 are less effective (Hurt *et al.*, 2006). The binding of N-terminally truncated *Pf*DHODH to phosphatidylcholine (PC) and phosphatidylethanolamine (PE) liposomes was demonstrated by means of size exclusion chromatography (Malmquist *et al.*, 2007).

The DHODH from *Candida albicans* (*Ca*DHODH), the most prevalent yeast pathogen in humans, has previously been investigated as well (Zameitat *et al.*, 2006). Similar to human DHODH, full-length *Ca*DHODH also possesses a mitochondrial signal peptide and transmembrane domains. It also contains the N-terminal α -helical microdomain characteristic of Class II DHODHs and a C-terminal catalytic domain. *Ca*DHODH has been shown to be sensitive to inhibition by brequinar and redoxal. The enzymatic activity of *Ca*DHODH with respect to a variety of electron acceptors was also investigated. Ubiquinone Q_6 resulted in higher reaction rates compared to other ubiquinone acceptors (Q_D , Q_0 , Q_{10}) (Zameitat *et al.*, 2006). Truncation of the N-terminal mitochondrial signal peptide and transmembrane domains resulted in modified enzymatic parameters with respect to co-substrates such as Q_6 and Q_{10} . The enzymatic activity of the truncated enzyme (Δ N*Ca*DHODH) was significantly lower than that of the full-length protein, suggesting that, as is the case for *Hs*DHODH, the N-terminal segments are not only structural elements, but have an effect on enzymatic activity. Interestingly, *Ca*DHODH was not inhibited by teriflunomide and Δ N*Ca*DHODH was only mildly inhibited (Zameitat *et al.*, 2006).

The isolation, kinetic characterization, and inhibition of the DHODH from rat (*Rat*DHODH) has been described previously (Bader *et al.*, 1998; Knecht *et al.*, 1997; Knecht & Löffler, 1998). Full-length *Rat*DHODH is 43 kDa in size and has an 88% sequence similarity to *Hs*DHODH. *Rat*DHODH has been isolated both from the rat liver mitochondria and from the mitochondria insect cells. Both the native and recombinant forms of the enzyme have the ability to use Q_{10} and Q_D as electron acceptors (Knecht *et al.*, 1997).

The DHODH from *Mus musculus* (*Mm*DHODH) (Ullrich *et al.*, 2001) was shown to display elevated kinetic parameters with respect to DHO and Q_D compared to those of

the human and rat enzymes. N-terminally truncated *Mm*DHODH was found to be more sensitive to Teriflunomide than the human analogue, but far less sensitive to Brequinar.

The DHODH from *Arabidopsis thaliana* (*At*DHODH) differs significantly from animal DHODHs in terms of substrate specificity and inhibition (Ullrich *et al.*, 2002). *At*DHODH is a 48.5 kDa protein with a 54.9% sequence identity with respect to human DHODH. The N-terminus of *At*DHODH also contains a mitochondrial signal peptide and a transmembrane domain. However, the mitochondrial signal peptide in *At*DHODH is considerably longer (57 amino acids) than that of human DHODH and its function remains unknown. *At*DHODH displays K_m values with respect to Q_D and DHO that are considerably higher than those of mammalian DHODHs. Truncation of the N-terminal segments of *At*DHODH results in significant changes in the catalytic efficiencies with respect to Q_D and DHO compared to the full-length *At*DHODH. Truncated *At*DHODH displayed a lower relative specific activity with respect to short-chain ubiquinone analogues (Q_0) compared to the full-length enzyme, indicating that the N-terminal segments play a role in kinetics and are not merely structural elements. *At*DHODH was found to be only marginally inhibited by teriflunomide, but no significant inhibition was observed in the presence of Brequinar.

The DHODH from *Drosophila melanogaster* (*Dm*DHODH) (Rawls *et al.*, 1993) has been shown to exhibit similar properties and sequence compared to other mammalian DHODHs. The biochemical characterization of full-length and three N-terminal truncated derivatives of *Dm*DHODH (Löffler *et al.*, 2002) revealed that the N-terminus of the enzyme does not influence the catalytic activity or inhibition. However, the truncated derivatives were unable to support normal pyrimidine metabolism during fly development, most likely due to decreased stability. *Dm*DHODH was found to be very similar to mammalian DHODHs with respect to its catalytic kinetic properties. Furthermore, *Dm*DHODH is inhibited by Teriflunomide, but Brequinar was found to be a much weaker inhibitor than in the case of human DHODH.

It is evident that Class II DHODHs have been studied extensively and there are currently several crystal structures available, most of them correspond to N-terminal truncated *Hs*DHODH in complex with inhibitors. However, there is virtually no information regarding how Class II DHODHs interact with ubiquinone Q_{10} in a membrane-bound state. There are no structural studies of full-length *Hs*DHODH reconstituted in lipid bilayers or *in-situ* interaction studies between lipid membranes and truncated *Hs*DHODH or *Ec*DHODH. As a consequence, much is still completely unknown regarding the structure and arrangement of these enzymes within a lipid bilayer and the function of their N-terminus. The native lipid environments of

*Hs*DHODH and *Ec*DHODH are quite different as the lipid compositions of the IMM and the bacterial inner membrane differ significantly. There are no studies addressing how the differences between *Hs*DHODH and *Ec*DHODH are coupled to their native environments.

For these reasons, this thesis provides new knowledge about the interaction of *Hs*DHODH (as well as *Ec*DHODH) and ubiquinone in supported lipid bilayers mimicking the structure and composition of the IMM under non-crystalline, physiologically relevant conditions. As previously mentioned, NR allows for the *in-situ* study of the structure and composition of thin films. QCM-D was used as a validation method in order to determine the best conditions needed to perform the NR experiments.

SECTION II: OUTCOME AND DISCUSSION OF THE STUDY

Paper I

Orozco Rodriguez, J.M., Krupinska, E., Wacklin-Knecht, H.P., Knecht, W. (2020). Preparation of human dihydroorotate dehydrogenase for interaction studies with lipid bilayers. *Nucleosides, Nucleotides & Nucleic Acids*, 39(10–12), 1306–1319, DOI: 10.1080/15257770.2019.1708100.

The aim of this doctoral thesis project was to investigate the mechanism of action and inhibition of membrane-bound enzymes that interact with lipids and lipophilic substrates under non-crystalline, physiologically relevant conditions using neutron scattering methods with *Hs*DHODH as the case example.

In this paper, methods for the preparation and characterization of proteins necessary for subsequent NR and other studies are presented. The recombinant expression and purification of human DHODH as well as an N-terminally truncated variant lacking the mitochondrial signal peptide and transmembrane domain (*Hs*Δ29DHODH) are described. Protein purification was accomplished using two steps of IMAC, followed by SEC. IMAC was used because the recombinant enzymes were expressed as His-tagged proteins. Most of the non-target contaminant proteins were removed after the second IMAC step and removal of the His-tag. SEC was used to remove high molecular weight aggregates and low molecular weight degradation products and to exchange the protein into the final buffer for storage. Previous reports had shown that it is possible to obtain pure and active human and bacterial DHODHs using *E. coli* as the expression system and using a purification procedure combining affinity chromatography and size exclusion chromatography (Bader *et al.*, 1998; Björnberg *et al.*, 1999; Ullrich *et al.*, 2001).

The ability to produce the necessary bioreagents in high quality for all subsequent work in this PhD project was demonstrated. The same protocols established in this paper for *Hs*DHODH were also used to produce selected DHODH mutants found in patients diagnosed with Miller syndrome. **Paper I** therefore forms the basis for all the subsequent work presented and the future work to come.

In addition, the interaction of *Hs*Δ29DHODH with lipid bilayers of varying lipid composition using QCM-D was characterized and compared to that of the DHODH from *E. coli*, a protein that naturally lacks an MS and TM. QCM-D is a surface technique that can provide information about the mass and viscoelastic properties of substances adsorbed on the surface of a quartz crystal that resonates with a frequency inversely proportional to the mass deposited. This study describes for the first time the interactions between Class II DHODHs and supported lipid bilayers using QCM-D.

Mixtures containing POPC and TOCL were used to mimic the inner mitochondrial membrane of mammalian cells. TOCL was included in the mixture as it is a lipid that is enriched in the IMM, where it accounts for 10-20 mol% (Horvath & Daum, 2013). The protein-lipid interaction was studied using bilayers of four different compositions: 100 mol% POPC, POPC + 10 mol% Q₁₀, POPC + 10 mol% TOCL, and POPC + 10 mol% Q₁₀ + 10 mol% TOCL.

The results obtained indicated that the presence of TOCL significantly enhanced the binding between the lipid bilayers and *Hs*Δ29DHODH compared to bilayers consisting only of POPC. TOCL also promoted the binding between the bilayer and bacterial *Ec*DHODH. The enhanced affinity between bilayers containing TOCL and *Hs*Δ29DHODH and *Ec*DHODH could be explained by electrostatic interactions between the negatively charged phosphate groups in TOCL and positively charged residues found in the α-helical microdomains of both enzymes. Addition of Q₁₀ did not have a detectable effect when compared to bilayers consisting only of POPC. Previous neutron diffraction studies have shown that Q₁₀ mostly localizes to the hydrophobic center of the lipid bilayer (Hauß *et al.*, 2005)..

The interaction between the lipids and *Hs*Δ29DHODH was mostly transient, as rinsing removed most of the initially bound protein. This suggests that the N-terminal segments (MS and TM) may be required for a stable interaction and for securing the enzyme on the outer surface of the IMM. On the other hand, the lipid interaction of the naturally soluble *Ec*DHODH was more stable, as less of the initially bound protein was removed by rinsing. The α-helical microdomain in *Ec*DHODH contains more cationic amino acid residues than that of *Hs*Δ29DHODH (Nørager *et al.*, 2002), which could be the reason why the binding between the lipid bilayers containing TOCL and the bacterial enzyme are more stable.

In conclusion, both *Hs*Δ29DHODH and *Ec*DHODH displayed low affinities for bilayers consisting only of POPC and POPC/Q₁₀. The presence of TOCL increased the affinity between the lipid bilayers and both enzymes. Since *Ec*DHODH naturally lacks a TM domain, it is likely to depend on the affinity between the α-helical microdomain and the membrane lipids to a greater extent than the human enzyme.

This study also delivered important input into further studies, in particular the NR study (**Paper IV**), to determine what lipid bilayer compositions and enzyme concentrations to use, as neutron beamtime is limited and only a few selected conditions can be tested.

Paper II

Orozco Rodriguez, J.M., Krupinska, E., Wacklin-Knecht, H.P., Knecht, W. (2022). Protein production, kinetic and biophysical characterization of three human dihydroorotate dehydrogenase mutants associated with Miller syndrome. *Nucleosides, Nucleotides & Nucleic Acids*, DOI: 10.1080/15257770.2021.2023749. Epub ahead of print.

In this publication, a review of the state of knowledge of Miller Syndrome was presented and the recombinant expression, purification, and kinetic and biophysical characterization of three mutant versions of human dihydroorotate dehydrogenase associated with this disease (G19E, E52G, R135C) were described, building on the results from **Paper I**.

As previously stated, the overall aim of this thesis was to investigate the mechanisms by which human DHODH interacts with lipids of the inner mitochondrial membrane and ubiquinone Q₁₀. In this context, it was also relevant to understand how mutations associated with Miller syndrome affect such interactions. The focus was placed on selected mutations which occur in regions of the enzyme that are expected to interact with lipids and ubiquinone. These mutations are: G19E, located in the transmembrane domain; E52G, located in the α -helical microdomain; and R135C, located in the tunnel postulated to allow ubiquinone access to the catalytic site.

To achieve these goals, two approaches were followed. In the first approach, all the proteins of interest were expressed and purified in *E. coli* (wild-type and Miller syndrome mutants, both full-length and truncated). A full biochemical characterization of the purified proteins was then performed. The kinetic constants (K_m , V_{max} , k_{cat}/K_m) with respect to the substrate (dihydroorotate, DHO), the natural co-substrate (ubiquinone Q₁₀), and the ubiquinone analogue decylubiquinone (Q_D) were determined using the standard chromogen reduction assay. The half-maximal inhibitory concentration values (IC₅₀) for two common DHODH inhibitors, Brequinar and Teriflunomide, were also determined. In addition, the melting temperatures (T_m) for all the enzymes of interest was determined by differential scanning fluorimetry. The kinetic characterization with respect to DHO, Q_D and Q₁₀

revealed that the V_{\max} for the mutants decreased compared to the wild type. The K_m values decreased in some cases and increased in others. For the full-length enzymes, the specific activity and catalytic efficiency was lowest for the R135C variant. The decrease was less pronounced for E52G and even milder for G19E. For all enzymes, the V_{\max} , K_m and k_{cat}/K_m were significantly lower for Q₁₀ than for Q_D. For the truncated enzymes, the V_{\max} values were lower for the mutants compared to the wild type. When comparing the full-length versus the truncated wild type enzyme, significant decreases in the catalytic efficiencies for DHO and Q₁₀ for the truncated enzyme were observed. In terms of inhibition only the R135C mutants (both truncated and full length) displayed significant increases in IC₅₀ values with respect to Brequinar and Teriflunomide. In terms of thermal stability, the E52G mutants stood out by their greatly decreased T_m values. Furthermore, all proteins could be stabilized by high concentrations (well above the IC₅₀) of Brequinar and Teriflunomide.

In the second approach, DHODH and the corresponding Miller syndrome mutants were recombinantly expressed in insect cells using the BEVS system to investigate the activity and expression levels of the different proteins in a eukaryotic cellular environment. The specific activities in the whole cell extracts of infected insect cells were lower for all the mutants compared to the wild type. The E52G and R135C displayed the lowest activities. The decrease was less pronounced for G19E. Western blotting and immunodetection revealed that the wild-type enzyme and the R135C mutant are found at the same level. The lowest protein level was observed for E52G. The G19E variant was also found at a lower level.

The activity of the enzymes in insect cell extracts was also evaluated in the absence of any exogenous detergents or quinones. The mutants displayed lower specific activities than the wild type. It should be noted, however, that the differences in activity among the mutant variants were less pronounced than in the presence of exogenous detergent and ubiquinone. Despite the quite drastic differences in stability, potential mitochondrial import disruption and reduced activity observed in *in vitro* assays, the residual activities for all three mutants in cell lysates, using the endogenous electron acceptor as substrate, were at surprisingly similar levels.

Taken together, these results suggest that the effects of the mutations characterized differ widely. The G19E mutation decreases enzymatic activity and results in a decrease in expression level. This might be indicative of problems with correct mitochondrial import or location of the transmembrane domain. The E52G mutation severely reduces the thermostability of the protein and results in significantly lower protein levels. The residues in the alpha helical microdomain are not highly conserved in Class II DHODHs, except for E52 (Sousa *et al.*, 2021). The results would suggest this to be a generally important residue for stability of Class II DHODHs. The R135C mutation

resulted in a dramatic loss of enzyme activity but did not lead to decreased protein levels or thermal instability. Previous studies (Sousa *et al.*, 2021) have suggested that both the R135 and E52 residues may be important for quinone binding and orientation based on their proximity to the location where the aromatic head group of ubiquinone is expected to bind. Furthermore, the N-terminal segments in DHODH are not only structural elements necessary for the correct import into mitochondria and anchoring into the IMM. These segments have an effect on the kinetic parameters of the enzyme and, to a lesser extent, on its thermal stability and inhibition by Brequinar and Teriflunomide. The G19E, E52G, and R135C mutants have been described in previous studies (Fang *et al.*, 2012; Rainger *et al.*, 2012). Overall, the findings of this paper are in agreement with these authors but add additional findings.

Paper III

Orozco Rodriguez, J.M., Wacklin-Knecht, H.P., Knecht, W. (2022). Protein-lipid interactions of human dihydroorotate dehydrogenase and three mutants associated with Miller syndrome. *Nucleosides, Nucleotides & Nucleic Acids*, DOI: 10.1080/15257770.2022.2039393. Epub ahead of print.

In this paper, the interaction between lipids and the enzymes described in Paper II (DHODH and the G19E, E52G and R135C Miller syndrome mutants) was investigated by means of enzymatic assays, thermal stability assays, and QCM-D experiments.

The enzyme activity was measured in the presence of lipids representative of the inner mitochondrial membrane (POPC, POPE, and TOCL). Three ubiquinone variants were evaluated: the natural ubiquinone Q₁₀, decylubiquinone (Q_D) and an analogue consisting only of the ubiquinone headgroup (benzoquinone, Bz). Furthermore, the thermal stability of the different proteins was determined by means of differential scanning fluorimetry in the presence of lipids (POPC, POPE, TOCL), substrates (DHO, Q₁₀, Bz, Q_D) and detergents (DDM).

For the QCM-D assays, supported lipid bilayers (the same as used in **Paper I**) of various compositions (POPC, POPC/Q₁₀, POPC/TOCL and POPC/Q₁₀/TOCL) were prepared by vesicle fusion and solutions of two truncated mutant enzymes (E52G and R135C) were injected onto the bilayers, followed by rinsing with buffer.

Almost all enzymatic activities with either Bz or Q₁₀ were lower than those observed with Q_D, except for the truncated R135C mutant. The different ubiquinone analogues display differences in solubility and partitioning between detergent micelles and the

bulk aqueous solution: Bz is highly water soluble and assumed to be less accessible to the enzymes in the detergent micelles, Q_D can freely exchange between the micelles and the aqueous phase, Q_{10} is highly hydrophobic and found exclusively in detergent micelles.

In most cases, and contrary to what has been published previously with an N-terminal His-tagged *Hs* $\Delta 30$ DHODH (Costeira-Paulo *et al.*, 2018), supplementation with lipids resulted in a reduction in the measured enzymatic activity. This might be explained by a strengthening effect of the lipids on the enzyme-micelle binding, thus limiting the ability of the enzyme to access the co-substrates in the aqueous phase or in other micelles. It should also be noted that Costeira-Paulo *et al.* did not remove the polyhistidine tag from their protein construct, and therefore it cannot be ruled out that the effects observed are influenced by the tag itself.

QCM-D analysis indicated that the R135C variant displayed a stronger affinity towards bilayers consisting only of POPC and POPC/ Q_{10} compared to the wild-type enzyme. R135C displayed a stronger affinity to bilayers that lack TOCL compared to those that do contain TOCL. The E52G variant displayed a strong affinity to bilayers that contain TOCL. E52G also displayed a stronger affinity to bilayers consisting only of POPC or POPC/ Q_{10} compared to the wild-type enzyme and a better retention as indicated by a lower amount of protein removed by rinsing. Both mutants differed significantly in their interactions with SLBs compared to the wild type, which suggests that there were changes in the regions of the enzymes that interact with the bilayer. The replacement of the negative charge in the E52G mutant is likely to have facilitated binding to negatively charged phospholipids such as TOCL. The R135C mutation resulted in the loss of a positive charge, which could explain why this variant displayed increased affinity towards the zwitterionic POPC compared to the other two enzymes.

In terms of thermal stability, supplementation with TOCL resulted in an increase in the T_m value, whereas POPC had a slight destabilizing effect and POPE had no significant effect. This is in line with previous findings indicating that TOCL promoted *Hs* $\Delta 29$ DHODH binding to a large extent to SLB containing this lipid in contrast to those with only POPC (**Paper I**). Furthermore, DHO had a stabilizing effect whereas Q_{10} had a slight destabilizing effect on the enzymes.

In conclusion, the results indicated that the N-terminal segments of human DHODH are not only structural elements required for proper mitochondrial import and anchoring to the inner mitochondrial membrane, but also influence enzymatic activity and utilization of ubiquinone Q_{10} and ubiquinone analogues in *in vitro* assays by influencing the location of the enzymes. The results also supported the role of cardiolipin as a lipid that interacts with DHODH. The QCM-D assays showed that

the interactions between the Miller syndrome mutants and the supported lipid bilayers studied differ from those of wild-type DHODH. This was the first investigation of the protein-lipid interactions of DHODH variants associated with Miller syndrome. The partition of molecules between the bulk solution and the hydrophobic environment in lipid micelles also has important consequences for DHODH inhibitors and their development: for example, Brequinar (LogP = 5.6) and Teriflunomide (LogP = 3.3) are hydrophobic molecules that would be expected to preferentially partition to the lipid phase.

Studies of the protein-lipid interactions of DHODHs would need to be extended to more complex, physiologically relevant lipid mixtures in combination with varying substrate concentrations and techniques such as solid-state NMR that allow either residue specific or spatial resolution of the observed events, such as the neutron reflectivity studies presented in **Paper IV**.

Paper IV

Orozco Rodriguez, J.M., Wacklin-Knecht, H.P., Clifton, L.A., Bogojevic, O., Leung, A., Fragneto, G., Knecht, W. (2022). New insights into the interaction of Class II dihydroorotate dehydrogenases with ubiquinone in lipid bilayers as a function of lipid composition. *International Journal of Molecular Sciences*, 23, 2437, DOI: 10.3390/ijms23052437.

In this paper, specular neutron reflectivity studies of the interaction between two dihydroorotate dehydrogenases – truncated human DHODH (*Hs*Δ29DHODH) and bacterial DHODH from *E. coli* (*Ec*DHODH) – with lipid bilayers of different composition and complexity were presented. These NR studies provided information regarding the structure and composition of the lipid bilayers, the amount of enzyme capable of binding the bilayer and the amount of enzyme that remains after rinsing.

The lipid bilayers were deposited from vesicles consisting of either synthetic lipid mixtures (POPC, TOCL, Q₁₀) or complex mixtures of lipids extracted from a eukaryotic organism (yeast). The QCM-D results obtained in **Paper I** indicated that the presence of TOCL in the bilayer was a prerequisite for the binding of both the human and bacterial enzyme. The TOCL content was kept at 10 mol% because higher contents did not allow for membrane deposition on a solid substrate.

A complex phospholipid mixture that was available was used. It was extracted from a eukaryotic organism, the yeast *Candida glabrata*. The phospholipid composition of this mixture consisted mostly of PC, PS, PE with smaller amounts of PI and CL. The fatty

acid composition consisted mostly of C18:1, C16:1 and C18:0 (Delhom, 2017). This complex lipid mixture was also supplemented with ubiquinone Q₁₀ at a concentration of 10 mol% relative to the phospholipids.

To mimic the cytoplasmic membrane of bacterial cells (such as *E. coli*), a mixture of 35 mol% POPE, 13 mol% POPG and 12 mol% TOCL was used. Even though POPC is not present in the membrane of *E. coli*, it had to be included at a concentration of 40 mol% to form a supported lipid bilayer.

The results can be summarized as follows. The bacterial enzyme displayed higher affinity towards bilayers consisting of POPC and TOCL compared to the truncated human enzyme as indicated by a more densely populated protein layer on the outer surface of the bilayer, validating the findings presented in **Paper I** of this report. The interaction of *Ec*DHODH and the synthetic lipid bilayer was also found to be more stable than that of *Hs*Δ29DHODH, as indicated by a lower amount of protein being removed by rinsing. The higher relative binding displayed by the bacterial enzyme may arise from the presence of an abundance of positively charged residues on the outer surface of the alpha helical microdomain of *Ec*DHODH (Arg7, Lys8, Arg17, Arg27, and Arg28), which are likely to be in direct contact with the lipid bilayer.

Another important finding is that the bilayer lipid composition had a major effect on protein affinity and retention, as bilayers prepared from yeast lipids were able to bind and retain *Hs*Δ29DHODH to a greater extent than bilayers consisting only of POPC and TOCL. Similarly, bilayers mimicking the composition of the bacterial plasma membrane and consisting of a mixture of POPC, POPE, POPG and TOCL displayed higher affinity and retention of *Ec*DHODH than those prepared with POPC and TOCL alone. Compared to the bilayers prepared with synthetic lipids, the yeast lipid mixture contains fewer neutral lipids (POPC) and more negatively charged lipids, such as PS and CL. In line with what has been suggested by other authors (Costeira-Paulo *et al.*, 2018), the electrostatic interactions between these negatively charged lipid headgroups and the cationic residues (mainly arginine and lysine) present in the amphipathic alpha helical microdomain of *Hs*Δ29DHODH are likely to be the main drivers for protein–membrane interaction.

Ubiquinone Q₁₀ was found to be located at the center of all the bilayers studied (between the lipid leaflets), including those prepared from synthetic lipids (POPC, TOCL) and those prepared from complex mixtures of lipids extracted from yeast membranes. This is consistent with previous experiments with neutron diffraction using multilamellar membranes of model lipids (Hauß *et al.*, 2005), showing that ubiquinone tends to localize at the center of lipid bilayers.

The most significant finding is that binding of both *Hs*Δ29DHODH and *Ec*DHODH to the surface of lipid bilayers results in the penetration of the enzymes into the outer lipid leaflet. No evidence for the migration of ubiquinone from the middle layer was found.

The penetration of the enzymes into the lipid bilayer could be relevant for all enzymes that bind membranes in a similar manner and use ubiquinones as electron acceptors (**Fig. 4.3**). Ubiquinones are found in all membranes, but Q₁₀ is the key node in the mitochondrial respiratory chain and the substrate for several enzymes located at the IMM.

In the case of synthetic lipid membranes, the presence of ubiquinone also resulted in an increased binding towards *Hs*Δ29DHODH. However, the incorporation of ubiquinone in bilayers prepared from yeast lipids did not result in a significant increase in affinity or retention of *Hs*Δ29DHODH.

The work in this paper was done with the soluble, truncated form of human DHODH instead of the full-length version to be able to perform protein-lipid affinity studies. The reconstitution of the full-length enzyme and investigation of the mechanism by which it interacts with ubiquinone and with the lipids of the inner mitochondrial membrane requires a completely different methodology and is covered in **Paper V** of this thesis.

In conclusion, the findings of **Paper IV** support a model in which the DHODH-ubiquinone interaction is mediated by protein penetration, rather than by ubiquinone migration.

Paper V

Orozco Rodriguez, J.M., Wacklin-Knecht, H.P., Clifton, L.A., Bogojevic, O., Leung, A., Micciulla, S., Fragneto, G., Knecht, W. (2022) Reconstitution of human dihydroorotate dehydrogenase into supported lipid bilayers using detergent-lipid micelles and liposomes: A neutron scattering study. *Manuscript*.

In this study, the reconstitution of *Hs*DHODH into supported lipid bilayers mimicking the inner mitochondrial membrane at the Si/SiO₂-water interface was investigated. The deposited membranes were analyzed by means of specular neutron reflection.

Three different reconstitution protocols were used. The first method consisted of the co-adsorption of detergent-lipid micelles containing the non-ionic detergent DDM and

synthetic lipids representative of the IMM (POPC, TOCL, and ubiquinone Q₁₀). In the second approach, the protein was reconstituted into proteoliposomes, which were later fused on the surface of the silicon crystal. Finally, a hybrid approach combining the adsorption of lipid-free DDM-protein micelles and the fusion of detergent-free lipid vesicles. Two version of this hybrid approach were attempted. The first one consisted of the adsorption of protein-DDM micelles followed by the addition of lipid vesicles to try to form a lipid bilayer around the protein molecules. The second hybrid approach consisted of first forming a supported lipid bilayer from lipid vesicles, followed by the addition of protein-DDM micelles, and by the addition of more lipid vesicles.

HsDHODH was recombinantly expressed in *E. coli* cells using the same methods described in **Paper I**. The protein was solubilized from bacterial cells using Triton X-100, which was later exchanged for DDM. Triton X-100 has been previously used to purify dihydroorotate dehydrogenases (Bader *et al.*, 1998; Knecht *et al.*, 1996) and is the detergent used in the standard buffer used to determine dihydroorotate dehydrogenase activity (Forman & Kennedy, 1977). DDM is suitable for neutron reflectivity studies, as it is uncharged and therefore does not interact with the solid substrate (SiO₂).

The reconstitution of *HsDHODH* by co-adsorption of detergent-lipid micelles resulted in membranes with low lipid and protein coverage. There was also a substantial amount of residual detergent in the membranes, suggesting that DDM interacts quite strongly with *HsDHODH*. Compared to previous results regarding the adsorption of DDM-lipid micelles (Vacklin, Tiberg, Fragneto, *et al.*, 2005; Vacklin, Tiberg & Thomas, 2005), the supported lipid bilayers (both in the presence and absence of protein) obtained contained significantly higher amounts of residual detergent as well as a lower surface coverage. It has been reported that removal of the detergent requires proper mixing and extensive rinsing (Vacklin, Tiberg & Thomas, 2005), which is difficult to achieve given the large area/volume ratio in the NR sample cell.

On the other hand, the reconstitution of *HsDHODH* from proteoliposomes resulted in well-defined lipid bilayers with high surface coverage, but the amount of protein incorporated was limited by the amount of protein added to the liposomes (0.5 mol% protein relative to the lipids). Unfortunately, the protein amount could not be increased arbitrarily, as this would have meant introducing more detergent into the sample, thus promoting the formation of a mixture of liposomes and micelles. This approach could be improved by attempting to remove the detergent using a hydrophobic adsorbent resin as was reported for the mitochondrial protein Bcl-2 (Mushtaq *et al.*, 2021). There was no evidence of protein denaturation on the SiO₂ surface or incorrect protein orientation.

Finally, the hybrid approaches resulted in a very high degree of protein coverage but also promoted the formation of an additional floating layer consisting of both lipid and residual detergent.

In conclusion, even though none of the techniques investigated created a well-defined single lipid bilayer with a high protein content, the results obtained provide useful and detailed information in terms of what surface coverage, protein incorporation and membrane composition can be achieved as a function of the reconstitution technique used. These studies can be used to guide and inform the reconstitution methods for other proteins structurally similar to *HsDHODH*.

SECTION III: CONCLUSIONS AND FUTURE PERSPECTIVES

Protein production methods and a thorough kinetic characterization of human DHODH as well as N-terminal truncated human DHODH and three variants associated with Miller syndrome (G19, E52G, R135C) with respect to DHO, as well as three ubiquinone analogues of varying chain length (Q_0 , Q_D and Q_{10}) have been performed, including the characterisation of the interactions of the enzymes with lipids in SLBs. The thermal stability and inhibition with respect to Brequinar and Teriflunomide of all these variants has also been determined. Additionally, protein production methods for *E. coli* DHODH were reported.

As part of this thesis, the interaction of a truncated form of human DHODH and a bacterial DHODH with the co-substrate, ubiquinone, in supported lipid bilayers prepared both from synthetic lipids and complex lipid mixtures derived from yeast by means of NR under non-crystalline, physiologically relevant conditions has been investigated.

In addition, the reconstitution of human DHODH using several approaches was attempted, including the co-adsorption of detergent-lipid micelles, proteoliposome fusion, as well as hybrid approaches consisting of a combination of both protein-detergent micelle adsorption and lipid vesicle fusion. Even though it was not possible to form well-defined lipid bilayers with high coverage and a high degree of protein incorporation, the results presented here provide useful information about what each of these alternative methods can achieve and can be used to guide efforts to reconstitute proteins that are structurally or functionally similar to DHODH into supported lipid bilayers.

To achieve better deposition of *Hs*DHODH, peptide nanodiscs could be tested in the future for the reconstitution of *Hs*DHODH. This method has proved successful for the reconstitution of integral membrane proteins consisting of a single transmembrane helix. Work regarding the reconstitution of *Hs*DHODH from lipid nanodiscs stabilized by peptides is currently ongoing. QCM-D experiments are planned to validate the best conditions for the formation of supported lipid bilayers from such peptide nanodiscs. The final goal would be to perform additional NR experiments to investigate the composition and structure of SLBs prepared from peptide nanodiscs with *Hs*DHODH and to compare these results to those obtained in **Paper IV**.

In the long term, the research derived from this thesis is expected to have the following impact in the field of membrane protein reconstitution and characterization:

- a) Provide new and complementary information regarding the structure and function of Class II DHODHs, particularly *Hs*DHODH and *Ec*DHODH, regarding the interaction between the enzyme, lipids, and ubiquinone, but also enzyme inhibitors, under non-crystalline conditions that mimic their natural environment.
- b) Improve the methods for the reconstitution of integral membrane proteins into supported lipid bilayers.
- c) Showcase and motivate the use of neutron scattering methods, in particular, NR, to provide information about the structure and function of integral membrane proteins.

Popular science summary

Membrane proteins are very important for human health because they are the target of many drugs. They are, however, very hard to study because they are not water soluble and they need to be kept in a fat-like environment. An example of this kind of proteins is dihydroorotate dehydrogenase, also called DHODH. DHODH is an enzyme that produces some of the building blocks used for making nucleic acids such as DNA and RNA and it also interacts with coenzyme Q₁₀, which is a fat-soluble antioxidant. In humans, DHODH is found inside cell organelles called mitochondria. However, bacteria such as *E. coli* also have their own form of DHODH. Human DHODH is very important in health because it fulfils more functions than helping to provide nucleic acid precursors and there are drugs that target DHODH that are used to treat arthritis and multiple sclerosis. In addition, mutations in the DHODH gene cause a rare genetic disease called Miller syndrome. People suffering from this disease have malformations in the head, face, and limbs. The objective is to study DHODH under conditions that mimic its natural environment to understand how DHODH interacts with the fat-soluble coenzyme Q₁₀. To accomplish this task, a method called neutron reflectometry which requires the use of large international infrastructures (in this case, in France and the UK) that can produce neutrons for research purposes was used. The method consists of bombarding the sample with subatomic particles called neutrons and measuring the neutrons reflected from the sample. These reflected neutrons contain information about our sample: including its structure and composition.

Populär sammanfattning

Membranproteiner är oerhört viktiga för människors hälsa, vilket gör dem ofta måltavlor för läkemedel. De är dock mycket svåra att studera eftersom de inte är vattenlösliga och de måste förvaras i en fettliknande (membran-lik) miljö för att bibehålla sin struktur och därmed funktion. Ett exempel på denna typ av proteiner är dihydroorotatdehydrogenas, även kallat DHODH. DHODH är ett enzym som producerar några av de byggstenar som används för att göra nukleinsyror som DNA och RNA och det interagerar också med koenzym Q₁₀, som är en fettlös antioxidant. Hos människor finns DHODH inuti cellorganeller som kallas mitokondrier, men också bakterier som *E. coli* har sin egen form av DHODH. Humant DHODH är mycket viktigt för vår hälsa eftersom det fyller fler funktioner än att hjälpa till att tillhandahålla nukleinsyraprekursorer och det finns läkemedel som riktar sig mot DHODH som används för att behandla artrit och multipel skleros. Dessutom orsakar mutationer i DHODH-genen en sällsynt genetisk sjukdom som kallas Millers syndrom. Människor som drabbas av denna sjukdom har missbildningar i huvudet, ansiktet och extremiteterna. Målet för denna avhandling är att studera DHODH under förhållanden som efterliknar dess naturliga miljö för att förstå hur DHODH interagerar med det fettlösliga koenzymet Q₁₀. Därför användes en metod som kallas neutronreflektometri, som just möjliggör att undersöka proteinet i en membran-lik miljö. Metoden går ut på att bombardera provet med subatomära partiklar som kallas neutroner och sedan mäta neutronerna som reflekteras från provet. Eftersom denna metod kräver neutroner kan den endast utföras på stora internationella (i detta fall Frankrike och Storbritannien) infrastrukturer som kan producera dessa subatomära partiklar för forskningsändamål. De från provet reflekterade neutronerna innehåller värdefull information, inklusive proteinets struktur och provets sammansättning.

Acknowledgements

I would like to thank my supervisor, Wolfgang Knecht, as well as my co-supervisors and advisors: Hanna Wacklin-Knecht, Zoë Fisher, Claes von Wachenfeldt, and Giovanna Fragneto. I also want to thank the departmental representative, Klas Flärdh, and my scientific mentor, Leif Bülow.

I am grateful for financial support from the Lindström Foundation and the Royal Physiographic Society of Lund. I would like to thank the Department of Biology at Lund University (LU), the Division of Physical Chemistry (LU), and the European Spallation Source (ESS) for supporting this PhD project.

I would like to thank our collaborators for technical support and materials. Special thanks to the staff (current and former) at the Lund Protein Production Platform (LP3): Ewa Krupinska, Maria Gourdon, Céleste Sele, Anna Rasmussen, Hassan Cicek, Heather Sullivan, Therese Lindström, and Annika Rogstam. Special thanks as well to the staff (both current and former) at the ESS Deuteration and Macromolecular Crystallography (DEMAX) platform: Anna Leung, Fatima Plieva, Oliver Bogojevic, and Jenny Andersson. Many thanks to Niklas Müller and Anne-Maria Ollech for their technical support.

I would also like to thank the Institut Laue-Langevin (ILL), Grenoble, France for access to the D17 beamline and for the use of the Partnership for Soft Condensed Matter laboratories, and the ISIS Neutron and Muon Source facility, Didcot, UK for access to the INTER beamline. Special thanks to the staff at both facilities: Luke Clifton and Samatha Micciulla.

Many thanks to the principal investigators, post-docs, administrative staff, and fellow PhD students at the Molecular Cell Biology Unit (Department of Biology, LU): Swati Aggarwal, Karla Aguilera, Fredric Carlsson, Beer Sen, Marita Cohn, Robin Delhom, Elisabeth Gauger Nilsson, Mats Hansson, Lars Hederstedt, Humberto Itriago, Carin Jarl-Sunesson, Katarina Koruza, Vinardas Kelpsas, Katie Laschankzy, Julia Lienard, Lena Magnusson, Judith Matavacas, Chatarina Matsson, Elin Mover, Esther Nobs, Abraham Ontiveros, Allan Rasmusson, Oscar Rollano, Courtney Stairs, David Stuart, Eva Svensson, Torbjörn Säll, Huy Cuong Tran, Olivier van Aken, Shakhira Zakhrebekova. I also wish to thank the former and current staff at the Division of Physical Chemistry (LU) that supported my work or provided feedback: Ulf Olsson, Maria Södergren, Maria Valldeperas, and Tommy Nylander.

Last but not least, I would like to thank my family and friends for their unconditional emotional support throughout my entire PhD. Special thanks to Mohammad Nesrini, Rebeka Kovacic, David Bozjak, Milad Abolhalaj, and Niloofar Nayeri.

Muchas gracias a mis padres, Juan Manuel y Rosy, y a mis hermanos, Daniel y Gaby, por su apoyo incondicional durante todos estos años. Gracias también a mis tíos y tías, abuelos, primos y primas por su afecto, cariño y apoyo.

References

- Abelès, F. (1950). Recherches sur la propagation des ondes électromagnétiques sinusoïdales dans les milieux stratifiés-Application aux couches minces. *Annales de physique*, 12(5), 596-640.
- Al Kaissi, A., Roetzer, K. M., Ulz, P., et al. (2011). Extra phenotypic features in a girl with Miller syndrome. *Clinical Dysmorphology*, 20(2), 66-72.
- Angermüller, S., & Löffler, M. (1995). Localization of dihydroorotate oxidase in myocardium and kidney cortex of the rat. *Histochemistry and Cell Biology*, 103(4), 287-292.
- Azzam, R. M. A., & Bashara, N. M. (1977). *Ellipsometry and Polarized Light*. North-Holland Publishing Company.
- Bader, B., Knecht, W., Fries, M., & Löffler, M. (1998). Expression, purification, and characterization of histidine-tagged rat and human flavoenzyme dihydroorotate dehydrogenase. *Protein Expression and Purification*, 13(3), 414-422.
- Baldwin, J., Farajallah, A. M., Malmquist, N. A., Rathod, P. K., & Phillips, M. A. (2002). Malarial Dihydroorotate Dehydrogenase: Substrate and Inhibitor Specificity. *Journal of Biological Chemistry*, 277(44), 41827-41834.
- Banerjee, R., Purhonen, J., & Kallijärvi, J. (2021). The mitochondrial coenzyme Q junction and complex III: biochemistry and pathophysiology. *The FEBS Journal*, 1-23.
- Bayburt, T. H., Grinkova, Y. V., & Sligar, S. G. (2002). Self-Assembly of Discoidal Phospholipid Bilayer Nanoparticles with Membrane Scaffold Proteins. *Nano Letters*, 2(8), 853-856.
- Bélar, S., & Ramharter, M. (2018). DSM265: a novel drug for single-dose cure of *Plasmodium falciparum* malaria. *The Lancet Infectious Diseases*, 18(8), 819-820.
- Benedetto, A., Heinrich, F., Gonzalez, M. A., et al. (2014). Structure and Stability of Phospholipid Bilayers Hydrated by a Room-Temperature Ionic Liquid/Water Solution: A Neutron Reflectometry Study. *The Journal of Physical Chemistry B*, 118(42), 12192-12206.
- Berman, H. M., Westbrook, J., Feng, Z., et al. (2000). The Protein Data Bank. *Nucleic Acids Research*, 28(1), 235-242.
- Björnberg, O., Grüner, A. C., Roepstorff, P., & Jensen, K. F. (1999). The activity of *Escherichia coli* dihydroorotate dehydrogenase is dependent on a conserved loop identified by sequence homology, mutagenesis, and limited proteolysis. *Biochemistry*, 38(10), 2899-2908.
- Björnberg, O., Rowland, P., Larsen, S., & Jensen, K. F. (1997). Active site of dihydroorotate dehydrogenase A from *Lactococcus lactis* investigated by chemical modification and mutagenesis. *Biochemistry*, 36(51), 16197-16205.
- Blom, H., & Widengren, J. (2017). Stimulated Emission Depletion Microscopy. *Chemical Reviews*, 117(11), 7377-7427.
- Boldog, T., Li, M., & Hazelbauer, G. L. (2007). Using Nanodiscs to Create Water-Soluble Transmembrane Chemoreceptors Inserted in Lipid Bilayers. In M. I.

- Simon, B. R. Crane, & A. Crane (Eds.), *Methods in Enzymology* (Vol. 423, pp. 317-335): Academic Press.
- Born, M., & Wolf, E. (2013). *Principles of optics: electromagnetic theory of propagation, interference and diffraction of light*: Elsevier.
- Boukalova, S., Hubackova, S., Milosevic, M., et al. (2020). Dihydroorotate dehydrogenase in oxidative phosphorylation and cancer. *Biochimica et Biophysica Acta*, 1866(5), 165759.
- Bouwknegt, J., Koster, C. C., Vos, A. M., et al. (2021). Class-II dihydroorotate dehydrogenases from three phylogenetically distant fungi support anaerobic pyrimidine biosynthesis. *Fungal Biology and Biotechnology*, 8(1), 10.
- Brouette, N., Fragneto, G., Cousin, F., et al. (2013). A neutron reflection study of adsorbed deuterated myoglobin layers on hydrophobic surfaces. *Journal of Colloid and Interface Science*, 390(1), 114-120.
- Bustamante, C. J., Chemla, Y. R., Liu, S., & Wang, M. D. (2021). Optical tweezers in single-molecule biophysics. *Nature Reviews Methods Primers*, 1(1), 1-29.
- Caballero, I., Lafuente, M. J., Gamo, F.-J., & Cid, C. (2016). A high-throughput fluorescence-based assay for Plasmodium dihydroorotate dehydrogenase inhibitor screening. *Analytical Biochemistry*, 506, 13-21.
- Cao, L., Weetall, M., Trotta, C., et al. (2019). Targeting of Hematologic Malignancies with PTC299, A Novel Potent Inhibitor of Dihydroorotate Dehydrogenase with Favorable Pharmaceutical Properties. *Molecular Cancer Therapeutics*, 18(1), 3-16.
- Cassera, M. B., Zhang, Y., Hazleton, K. Z., & Schramm, V. L. (2011). Purine and pyrimidine pathways as targets in Plasmodium falciparum. *Current Topics in Medicinal Chemistry*, 11(16), 2103-2115.
- Cavanagh, J., Fairbrother, W. J., Palmer, A. G., & Skelton, N. J. (1995). *Protein NMR spectroscopy: principles and practice*: Elsevier.
- Chapman, H. N., Barty, A., Bogan, M. J., et al. (2006). Femtosecond diffractive imaging with a soft-X-ray free-electron laser. *Nature Physics*, 2(12), 839-843.
- Chapman, H. N., Fromme, P., Barty, A., et al. (2011). Femtosecond X-ray protein nanocrystallography. *Nature*, 470(7332), 73-77.
- Christiansen, L. S., Munch-Petersen, B., & Knecht, W. (2015). Non-Viral Deoxyribonucleoside Kinases - Diversity and Practical Use. *Journal of Genetics and Genomics*, 42(5), 235-248.
- Clabbers, M. T. B., & Abrahams, J. P. (2018). Electron diffraction and three-dimensional crystallography for structural biology. *Crystallography Reviews*, 24(3), 176-204.
- Copeland, R. A. (2000). *Enzymes: a practical introduction to structure, mechanism, and data analysis*: John Wiley & Sons.
- Cornish-Bowden, A. (2013). *Fundamentals of enzyme kinetics*: John Wiley & Sons.
- Costeira-Paulo, J., Gault, J., Popova, G., et al. (2018). Lipids Shape the Electron Acceptor-Binding Site of the Peripheral Membrane Protein Dihydroorotate Dehydrogenase. *Cell Chemical Biology*, 25(3), 309-317.

- Couto, S. G., Nonato, M. C., & Costa-Filho, A. J. (2008). Defects in vesicle core induced by *Escherichia coli* dihydroorotate dehydrogenase. *Biophysical Journal*, 94(5), 1746-1753.
- Cubitt, R., & Fragneto, G. (2002). D17: the new reflectometer at the ILL. *Applied Physics A*, 74(1), 329-331.
- Cusack, S., Ruigrok, R. W. H., Krygsman, P. C. J., & Mellema, J. E. (1985). Structure and composition of influenza virus: A small-angle neutron scattering study. *Journal of Molecular Biology*, 186(3), 565-582.
- Daum, G. (1985). Lipids of Mitochondria. *Biochimica et Biophysica Acta*, 822(1), 1-42.
- Daum, G., & Vance, J. E. (1997). Import of lipids into mitochondria. *Progress in Lipid Research*, 36(2), 103-130.
- de Ghellinck, A., Fragneto, G., Laux, V., et al. (2015). Lipid polyunsaturation determines the extent of membrane structural changes induced by Amphotericin B in *Pichia pastoris* yeast. *Biochimica et Biophysica Acta - Biomembranes*, 1848(10), 2317-2325.
- Deems, R. A. (2000). Interfacial Enzyme Kinetics at the Phospholipid/ Water Interface: Practical Considerations. *Analytical Biochemistry*, 287(1), 1-16.
- delaFortelle, E., & Bricogne, G. (1997). Maximum-likelihood heavy-atom parameter refinement for multiple isomorphous replacement and multiwavelength anomalous diffraction methods. *Macromolecular Crystallography Part A*, 276, 472-494.
- Delhom, R. (2017). *Isolation and structural characterization of natural deuterated lipids and oils from microorganisms*. (PhD). Université Grenoble Alpes, Grenoble, France.
- Denis-Duphil, M. (1989). Pyrimidine biosynthesis in *Saccharomyces cerevisiae*: the *ura2* cluster gene, its multifunctional enzyme product, and other structural or regulatory genes involved in de novo UMP synthesis. *Biochemistry and Cell Biology*, 67(9), 612-631.
- Deutscher, M. P., & Burgess, R. R. (2009). *Guide to Protein Purification (Methods in enzymology, v. 463)*: Academic Press.
- Dileepan, K. N., & Kennedy, J. (1983). Rapid conversion of newly-synthesized orotate to uridine-5-monophosphate by rat liver cytosolic enzymes. *FEBS Letters*, 153(1), 1-5.
- Donnai, D., Hughes, H. E., & Winter, R. M. (1987). Postaxial acrofacial dysostosis (Miller) syndrome. *Journal of Medical Genetics*, 24(7), 422-425.
- Dubochet, J., Adrian, M., Chang, J. J., et al. (1988). Cryo-Electron Microscopy of Vitrified Specimens. *Quarterly Reviews of Biophysics*, 21(2), 129-228.
- Duley, J. A., Henman, M. G., Carpenter, K. H., et al. (2016). Elevated plasma dihydroorotate in Miller syndrome: Biochemical, diagnostic and clinical implications, and treatment with uridine. *Molecular Genetics and Metabolism*, 119(1-2), 83-90.
- Dunne, O., Weidenhaupt, M., Callow, P., et al. (2017). Matchout deuterium labelling of proteins for small-angle neutron scattering studies using prokaryotic and

- eukaryotic expression systems and high cell-density cultures. *European Biophysics Journal*, 46(5), 425-432.
- Eggeling, C., Ringemann, C., Medda, R., et al. (2009). Direct observation of the nanoscale dynamics of membrane lipids in a living cell. *Nature*, 457, 1159-1162.
- Evans, D. R., & Guy, H. I. (2004). Mammalian pyrimidine biosynthesis: fresh insights into an ancient pathway. *Journal of Biological Chemistry*, 279(32), 33035-33038.
- Fang, J. X., Uchiumi, T., Yagi, M., et al. (2012). Protein instability and functional defects caused by mutations of dihydro-otate dehydrogenase in Miller syndrome patients. *Bioscience Reports*, 32(6), 631-639.
- Fankuchen, I. (1945). X-ray diffraction and protein structure. *Advances in Protein Chemistry*, 2, 387-405.
- Feliciano, P. R., Cordeiro, A. T., Costa-Filho, A. J., & Nonato, M. C. (2006). Cloning, expression, purification, and characterization of Leishmania major dihydroorotate dehydrogenase. *Protein Expression and Purification*, 48(1), 98-103.
- Fernandez-Alonso, F., & Price, D. L. (2013). *Neutron Scattering: fundamentals*: San Diego : Academic Press, 2013.
- Fisher, Z., Jackson, A., Kovalevsky, A., Oksanen, E., & Wacklin, H. (2017). Chapter 1: Biological Structures. *Experimental Methods in the Physical Sciences*, 49, 1-75.
- Forman, H. J., & Kennedy, J. (1977). Purification of the Primary Dihydroorotate Dehydrogenase (Oxidase) from Rat Liver Mitochondria. *Preparative Biochemistry*, 7(5), 345-355.
- Fragneto-Cusani, G. (2001). Neutron reflectivity at the solid/liquid interface: examples of applications in biophysics. *Journal of Physics: Condensed Matter*, 13(21), 4973-4987.
- Fragneto, G., Charitat, T., Graner, F., et al. (2001). A fluid floating bilayer. *Europhysics Letters (EPL)*, 53(1), 100-106.
- Fujiyoshi, Y. (1998). The structural study of membrane proteins by electron crystallography. *Advances in Biophysics*, 35, 25-80.
- Gelb, M. H., Min, J.-H., & Jain, M. K. (2000). Do membrane-bound enzymes access their substrates from the membrane or aqueous phase: interfacial versus non-interfacial enzymes. *Biochimica et Biophysica Acta - Molecular and Cell Biology of Lipids*, 1488(1), 20-27.
- Genée, E. (1969). [An extensive form of mandibulo-facial dysostosis]. *Journal of Human Genetics*, 17(1), 45-52.
- Glassford, S. E., Byrne, B., & Kazarian, S. G. (2013). Recent applications of ATR FTIR spectroscopy and imaging to proteins. *Biochimica et Biophysica Acta - Proteins and Proteomics*, 1834(12), 2849-2858.
- Goncalves, R. L. S., Watson, M. A., Wong, H.-S., Orr, A. L., & Brand, M. D. (2020). The use of site-specific suppressors to measure the relative contributions of different mitochondrial sites to skeletal muscle superoxide and hydrogen peroxide production. *Redox Biology*, 28, 1-6.

- Hauß, T., Dante, S., Haines, T. H., & Dencher, N. A. (2005). Localization of coenzyme Q10 in the center of a deuterated lipid membrane by neutron diffraction. *Biochimica et Biophysica Acta - Bioenergetics*, 1710(1), 57-62.
- Haustein, E., & Schwille, P. (2007). Fluorescence correlation spectroscopy: Novel variations of an established technique. In *Annual Review of Biophysics and Biomolecular Structure* (Vol. 36, pp. 151-169). Palo Alto: Annual Reviews.
- Henderson, R. (2015). Overview and future of single particle electron cryomicroscopy. *Archives of Biochemistry and Biophysics*, 581, 19-24.
- Hendrickson, W. A. (1991). Determination of Macromolecular Structures from Anomalous Diffraction of Synchrotron Radiation. *Science*, 254(5028), 51-58.
- Hermansen, R. A., Mannakee, B. K., Knecht, W., Liberles, D. A., & Gutenkunst, R. N. (2015). Characterizing selective pressures on the pathway for de novo biosynthesis of pyrimidines in yeast. *BMC Evolutionary Biology*, 15, 1-13.
- Hines, V., Keys, L. D., & Johnston, M. (1986). Purification and properties of the bovine liver mitochondrial dihydroorotate dehydrogenase. *Journal of Biological Chemistry*, 261(24), 11386-11392.
- Hjorth-Jensen, S. J., Oksanen, E., Nissen, P., & Sørensen, T. L.-M. (2020). Chapter Three - Prospects for membrane protein crystals in NMX. In P. C. E. Moody (Ed.), *Methods in Enzymology* (Vol. 634, pp. 47-68): Academic Press.
- Horvath, S. E., & Daum, G. (2013). Lipids of mitochondria. *Progress in Lipid Research*, 52(4), 590-614.
- Hurt, D. E., Widom, J., & Clardy, J. (2006). Structure of Plasmodium falciparum dihydroorotate dehydrogenase with a bound inhibitor. *Acta Crystallographica Section D*, 62(3), 312-323.
- Jacques, D. A., & Trewella, J. (2010). Small-angle scattering for structural biology--expanding the frontier while avoiding the pitfalls. *Protein Science*, 19(4), 642-657.
- Johnson, K. A., & Goody, R. S. (2011). The Original Michaelis Constant: Translation of the 1913 Michaelis-Menten Paper. *Biochemistry*, 50(39), 8264-8269.
- Karibian, D. (1978). Dihydroorotate dehydrogenase (Escherichia coli). *Methods in Enzymology*, 51, 58-63.
- King, L. (2012). *The baculovirus expression system: a laboratory guide*: Springer Science & Business Media.
- Kinoshita, F., Kondoh, T., Komori, K., et al. (2011). Miller syndrome with novel dihydroorotate dehydrogenase gene mutations. *Pediatrics International*, 53(4), 587-591.
- Knecht, W., Altekruze, D., Rotgeri, A., Gonski, S., & Löffler, M. (1997). Rat Dihydroorotate Dehydrogenase: Isolation of the Recombinant Enzyme from Mitochondria of Insect Cells. *Protein Expression and Purification*, 10(1), 89-99.
- Knecht, W., Bergjohann, U., Gonski, S., Kirschbaum, B., & Löffler, M. (1996). Functional expression of a fragment of human dihydroorotate dehydrogenase by means of the baculovirus expression vector system, and kinetic investigation of the purified recombinant enzyme. *European Journal of Biochemistry*, 240(1), 292-301.

- Knecht, W., & Löffler, M. (1998). Species-related inhibition of human and rat dihydroorotate dehydrogenase by immunosuppressive isoxazol and cinchoninic acid derivatives. *Biochemical Pharmacology*, 56(9), 1259-1264.
- Komura, S., Toyoshima, Y., & Takeda, T. (1982). Neutron Small-Angle Scattering from Single-Walled Liposomes of Egg Phosphatidylcholine. *Japanese Journal of Applied Physics*, 21(Part 1, No. 9), 1370-1372.
- Krogh, A., Larsson, B., von Heijne, G., & Sonnhammer, E. L. L. (2001). Predicting transmembrane protein topology with a hidden markov model: application to complete genomes. *Journal of Molecular Biology*, 305(3), 567-580.
- Kučerka, N., Nagle, J. F., Sachs, J. N., et al. (2008). Lipid Bilayer Structure Determined by the Simultaneous Analysis of Neutron and X-Ray Scattering Data. *Biophysical Journal*, 95(5), 2356-2367.
- Lal, R., & John, S. A. (1994). Biological applications of atomic force microscopy. *American Journal of Physiology*, 266(1), 1-21.
- Larsen, J. N., & Jensen, K. F. (1985). Nucleotide sequence of the pyr D gene of Escherichia coli and characterization of the flavoprotein dihydroorotate dehydrogenase. *European Journal of Biochemistry*, 151(1), 59-65.
- Le Brun, A. P., Holt, S. A., Shah, D. S. H., Majkrzak, C. F., & Lakey, J. H. (2011). The structural orientation of antibody layers bound to engineered biosensor surfaces. *Biomaterials*, 32(12), 3303-3311.
- Lindon, J. C., Tranter, G. E., & Koppenaal, D. (2016). *Encyclopedia of spectroscopy and spectrometry*: Academic Press.
- Liu, S., Neidhardt, E. A., Grossman, T. H., Ocain, T., & Clardy, J. (2000). Structures of human dihydroorotate dehydrogenase in complex with antiproliferative agents. *Structure*, 8(1), 25-33.
- Luban, J., Sattler, R. A., Mühlberger, E., et al. (2021). The DHODH inhibitor PTC299 arrests SARS-CoV-2 replication and suppresses induction of inflammatory cytokines. *Virus Research*, 292, 1-12.
- Luchini, A., Tidemand, F. G., Johansen, N. T., et al. (2020). Peptide Disc Mediated Control of Membrane Protein Orientation in Supported Lipid Bilayers for Surface-Sensitive Investigations. *Analytical Chemistry*, 92(1), 1081-1088.
- Luckey, M. (2014). *Membrane structural biology: with biochemical and biophysical foundations*: Cambridge University Press.
- Lugtenberg, E. J. J., & Peters, R. (1976). Distribution of lipids in cytoplasmic and outer membranes of Escherichia coli K12. *Biochimica et Biophysica Acta - Lipids and Lipid Metabolism*, 441(1), 38-47.
- Löffler, M., Becker, C., Wegerle, E., & Schuster, G. (1996). Catalytic enzyme histochemistry and biochemical analysis of dihydroorotate dehydrogenase/oxidase and succinate dehydrogenase in mammalian tissues, cells and mitochondria. *Histochemistry and Cell Biology*, 105(2), 119-128.
- Löffler, M., Carrey, E. A., & Knecht, W. (2020). The pathway to pyrimidines: The essential focus on dihydroorotate dehydrogenase, the mitochondrial enzyme coupled to the respiratory chain. *Nucleosides, Nucleotides & Nucleic Acids*, 39(10-12), 1281-1305.

- Löffler, M., Fairbanks, L. D., Zameitat, E., Marinaki, A. M., & Simmonds, H. A. (2005). Pyrimidine pathways in health and disease. *Trends in Molecular Medicine*, 11(9), 430-437.
- Löffler, M., Jöckel, J., & Schuster, G. (1997). Dihydroorotat-ubiquinone oxidoreductase links mitochondria in the biosynthesis of pyrimidine nucleotides. *Molecular and Cellular Biochemistry*, 174(1), 125-129.
- Löffler, M., Knecht, W., Rawls, J., Ullrich, A., & Dietz, C. (2002). *Drosophila melanogaster* dihydroorotate dehydrogenase: the N-terminus is important for biological function in vivo but not for catalytic properties in vitro. *Insect Biochemistry and Molecular Biology*, 32(9), 1159-1169.
- Mahieu, E., & Gabel, F. (2018). Biological small-angle neutron scattering: recent results and development. *Acta Crystallographica Section D*, D74(2059-7983 (Electronic)), 715-726.
- Malmquist, N. A., Baldwin, J., & Phillips, M. A. (2007). Detergent-dependent kinetics of truncated *Plasmodium falciparum* dihydroorotate dehydrogenase. *Journal of Biological Chemistry*, 282(17), 12678-12686.
- Mao, C., Liu, X., Zhang, Y., et al. (2021). DHODH-mediated ferroptosis defence is a targetable vulnerability in cancer. *Nature*, 593(7860), 586-590.
- Marx, K. A. (2003). Quartz crystal microbalance: A useful tool for studying thin polymer films and complex biomolecular systems at the solution-surface interface. *Biomacromolecules*, 4(5), 1099-1120.
- McCoy, A. J. (2007). Solving structures of protein complexes by molecular replacement with Phaser. *Acta Crystallographica Section D - Structural Biology*, 63, 32-41.
- McKeage, K., & Scott, L. J. (2003). Atovaquone/Proguanil. *Drugs*, 63(6), 597-623.
- McLean, J. E., Neidhardt, E. A., Grossman, T. H., & Hedstrom, L. (2001). Multiple inhibitor analysis of the brequinar and leflunomide binding sites on human dihydroorotate dehydrogenase. *Biochemistry*, 40(7), 2194-2200.
- Michaelis, L., & Menten, M. L. (1913). Die Kinetik der Invertinwirkung. *Biochemische Zeitschrift*, 49, 333-369.
- Miller, M., Fineman, R., & Smith, D. W. (1979). Postaxial acrofacial dysostosis syndrome. *Journal of Pediatrics*, 95(6), 970-975.
- Miller, R. W., Kerr, C. T., & Curry, J. R. (1968). Mammalian dihydroorotate – ubiquinone reductase complex. *Canadian Journal of Biochemistry*, 46(9), 1099-1106.
- Munier-Lehmann, H., Vidalain, P. O., Tangy, F., & Janin, Y. L. (2013). On dihydroorotate dehydrogenases and their inhibitors and uses. *Journal of Medicinal Chemistry*, 56(8), 3148-3167.
- Murata, K., & Wolf, M. (2018). Cryo-electron microscopy for structural analysis of dynamic biological macromolecules. *Biochimica et Biophysica Acta*, 1862(2), 324-334.
- Mushtaq, A. U., Ådén, J., Clifton, L. A., et al. (2021). Neutron reflectometry and NMR spectroscopy of full-length Bcl-2 protein reveal its membrane localization and conformation. *Communications Biology*, 4(507), 1-10.

- Müller, H., Etzkorn, M., & Heise, H. (2013). Solid-State NMR Spectroscopy of Proteins. In H. Heise & S. Matthews (Eds.), *Modern NMR Methodology* (pp. 121-156). Berlin, Heidelberg: Springer Berlin Heidelberg.
- Nelson, A. (2006). Co-refinement of multiple-contrast neutron/X-ray reflectivity data using MOTOFIT. *Journal of Applied Crystallography*, 39, 273-276.
- Ng, S. B., Buckingham, K. J., Lee, C., et al. (2010). Exome sequencing identifies the cause of a mendelian disorder. *Nature Genetics*, 42(1), 30-35.
- Nguyen, H. H., Park, J., Kang, S., & Kim, M. (2015). Surface Plasmon Resonance: A Versatile Technique for Biosensor Applications. *Sensors*, 15(5), 10481-10510.
- Nitzschke, A., & Bettenbrock, K. (2018). All three quinone species play distinct roles in ensuring optimal growth under aerobic and fermentative conditions in *E. coli* K12. *PLOS ONE*, 13(4), 1-18.
- Nørager, S., Jensen, K. F., Björnberg, O., & Larsen, S. (2002). *E. coli* dihydroorotate dehydrogenase reveals structural and functional distinctions between different classes of dihydroorotate dehydrogenases. *Structure*, 10(9), 1211-1223.
- Orozco Rodriguez, J. M., Krupinska, E., Wacklin-Knecht, H., & Knecht, W. (2020). Preparation of human dihydroorotate dehydrogenase for interaction studies with lipid bilayers. *Nucleosides Nucleotides & Nucleic Acids*, 39(10-12), 1306-1319.
- Orozco Rodriguez, J. M., Krupinska, E., Wacklin-Knecht, H. P., & Knecht, W. (2022a). Protein production, kinetic and biophysical characterization of three human dihydroorotate dehydrogenase mutants associated with Miller syndrome. *Nucleosides, Nucleotides & Nucleic Acids*, Epub ahead of print, DOI: 10.1080/15257770.15252021.12023749.
- Orozco Rodriguez, J. M., Wacklin-Knecht, H., & Knecht, W. (2022b). Protein-lipid interactions of human dihydroorotate dehydrogenase and three mutants associated with Miller syndrome. *Nucleosides, Nucleotides & Nucleic Acids*, Epub ahead of print, DOI: 10.1080/15257770.15252022.12039393.
- Orozco Rodriguez, J. M., Wacklin-Knecht, H. P., Clifton, L. A., et al. (2022c). New Insights into the Interaction of Class II Dihydroorotate Dehydrogenases with Ubiquinone in Lipid Bilayers as a Function of Lipid Composition. *International Journal of Molecular Sciences*, 23(5), 2437.
- Osborne, H. B., Sardet, C., Michel-Villaz, M., & Chabre, M. (1978). Structural study of rhodopsin in detergent micelles by small-angle neutron scattering. *Journal of Molecular Biology*, 123(2), 177-206.
- Palatinus, L., Brázda, P., Boullay, P., et al. (2017). Hydrogen positions in single nanocrystals revealed by electron diffraction. *Science*, 355(6321), 166-169.
- Pandey, A., Shin, K., Patterson, R. E., Liu, X.-Q., & Rainey, J. K. (2016). Current strategies for protein production and purification enabling membrane protein structural biology. *Biochemistry and Cell Biology*, 94(6), 507-527.
- Paradies, H. H. (1980). Shape and size of a nonionic surfactant micelle. Triton X-100 in aqueous solution. *The Journal of Physical Chemistry*, 84(6), 599-607.
- Peeters, M. J. W., Aehnlich, P., Pizzella, A., et al. (2021). Mitochondrial-Linked De Novo Pyrimidine Biosynthesis Dictates Human T-Cell Proliferation but Not Expression of Effector Molecules. *Frontiers in Immunology*, 12, 1-10.

- Penfold, J., & Thomas, R. K. (1990). The application of the specular reflection of neutrons to the study of surfaces and interfaces. *Journal of Physics: Condensed Matter*, 2(6), 1369 - 1412.
- Phillips, M. A., Lotharius, J., Marsh, K., et al. (2015). A long-duration dihydroorotate dehydrogenase inhibitor (DSM265) for prevention and treatment of malaria. *Science Translational Medicine*, 7(296), 1-31.
- Postis, V., Rawson, S., Mitchell, J. K., et al. (2015). The use of SMALPs as a novel membrane protein scaffold for structure study by negative stain electron microscopy. *Biochimica et Biophysica Acta - Biomembranes*, 1848(2), 496-501.
- Rainger, J., Bengani, H., Campbell, L., et al. (2012). Miller (Genée-Wiedemann) syndrome represents a clinically and biochemically distinct subgroup of postaxial acrofacial dysostosis associated with partial deficiency of DHODH. *Human Molecular Genetics*, 21(18), 3969-3983.
- Rawls, J., Kirkpatrick, R., Yang, J., & Lacy, L. (1993). The dhod gene and deduced structure of mitochondrial dihydroorotate dehydrogenase in *Drosophila melanogaster*. *Gene*, 124(2), 191-197.
- Rawls, J., Knecht, W., Diekert, K., Lill, R., & Löffler, M. (2000). Requirements for the mitochondrial import and localization of dihydroorotate dehydrogenase. *European Journal of Biochemistry*, 267(7), 2079-2087.
- Rayleigh, L. (1903). On the Theory of Optical Images, with Special Reference to the Microscope. *Journal of the Royal Microscopical Society*, 23(4), 447-473.
- Reif, B., Ashbrook, S. E., Emsley, L., & Hong, M. (2021). Solid-state NMR spectroscopy. *Nature Reviews Methods Primers*, 1(2), 1-53.
- Reis, R. A. G., Calil, F. A., Feliciano, P. R., Pinheiro, M. P., & Nonato, M. C. (2017). The dihydroorotate dehydrogenases: Past and present. *Archives of Biochemistry and Biophysics*, 632, 175-191.
- Rigaud, J.-L., Pitard, B., & Levy, D. (1995). Reconstitution of membrane proteins into liposomes: application to energy-transducing membrane proteins. *Biochimica et Biophysica Acta - Bioenergetics*, 1231(3), 223-246.
- Robinson, A. D., Eich, M.-L., & Varambally, S. (2020). Dysregulation of de novo nucleotide biosynthetic pathway enzymes in cancer and targeting opportunities. *Cancer Letters*, 470, 134-140.
- Roskoski, R. (1983). Assays of protein kinase. In *Methods in Enzymology* (Vol. 99, pp. 3-6): Academic Press.
- Sackmann, E. (1996). Supported membranes: scientific and practical applications. *Science*, 271(5245), 43-48.
- Santos, N. C., & Castanho, M. A. R. B. (2004). An overview of the biophysical applications of atomic force microscopy. *Biophysical Chemistry*, 107(2), 133-149.
- Santos, R., Ursu, O., Gaulton, A., et al. (2017). A comprehensive map of molecular drug targets. *Nature Reviews Drug Discovery*, 16(1), 19-34.
- Schrader, B. (2008). *Infrared and Raman spectroscopy: methods and applications*: John Wiley & Sons.
- Sears, V. F. (1992). Neutron scattering lengths and cross sections. *Neutron News*, 3(3), 26-37.

- Seddon, A. M., Curnow, P., & Booth, P. J. (2004). Membrane proteins, lipids and detergents: not just a soap opera. *Biochimica et Biophysica Acta - Biomembranes*, 1666(1-2), 105-117.
- Sessa, G., & Weissmann, G. (1968). Phospholipid spherules (liposomes) as a model for biological membranes. *Journal of Lipid Research*, 9(3), 310-318.
- Singh, A., Maqbool, M., Mobashir, M., & Hoda, N. (2017). Dihydroorotate dehydrogenase: A drug target for the development of antimalarials. *European Journal of Medicinal Chemistry*, 125, 640-651.
- Sivia, D. S. (2011). *Elementary scattering theory: for X-ray and neutron users*. Oxford University Press.
- Skar-Gislunge, N., Simonsen, J. B., Mortensen, K., et al. (2010). Elliptical Structure of Phospholipid Bilayer Nanodiscs Encapsulated by Scaffold Proteins: Casting the Roles of the Lipids and the Protein. *Journal of the American Chemical Society*, 132(39), 13713-13722.
- Smith, H. L., Hickey, J., Jablin, M. S., et al. (2010). Mouse Fibroblast Cell Adhesion Studied by Neutron Reflectometry. *Biophysical Journal*, 98(5), 793-799.
- Smithers, G. W., Gero, A. M., & O'Sullivan, W. J. (1978). A simple radioassay for dihydroorotate dehydrogenase. *Analytical Biochemistry*, 88(1), 93-103.
- Sousa, F. M., Refojo, P. N., & Pereira, M. M. (2021). Investigating the amino acid sequences of membrane bound dihydroorotate:quinone oxidoreductases (DHOQOs): Structural and functional implications. *Biochimica et Biophysica Acta - Bioenergetics*, 1862(1), 1-13.
- Stubičar, N., Matejaš, J., Zipper, P., & Wilfing, R. (1989). Size, Shape and Internal Structure of Triton X-100 Micelles Determined by Light and Small-Angle X-Ray Scattering Techniques. In K. L. Mittal (Ed.), *Surfactants in Solution* (pp. 181-195). Boston, MA: Springer US.
- Stuhrmann, H. B. (2012). Contrast variation application in small-angle neutron scattering experiments. *Journal of Physics: Conference Series*, 351(1), 1-16.
- Sugiki, T., Kobayashi, N., & Fujiwara, T. (2017). Modern Technologies of Solution Nuclear Magnetic Resonance Spectroscopy for Three-dimensional Structure Determination of Proteins Open Avenues for Life Scientists. *Computational and Structural Biotechnology Journal*, 15, 328-339.
- Svergun, D. I., & Koch, M. H. J. (2003). Small-angle scattering studies of biological macromolecules in solution. *Reports on Progress in Physics*, 66(10), 1735-1782.
- Sykes, D. B., Kfoury, Y. S., Mercier, F. E., et al. (2016). Inhibition of Dihydroorotate Dehydrogenase Overcomes Differentiation Blockade in Acute Myeloid Leukemia. *Cell*, 167(1), 171-186.e115.
- Tanford, C., & Reynolds, J. A. (1976). Characterization of membrane proteins in detergent solutions. *Biochimica et Biophysica Acta - Reviews on Biomembranes*, 457(2), 133-170.
- Taylor, W. H., & Taylor, M. L. (1964). Enzymes of the pyrimidine pathway in *Escherichia coli*. *Journal of Bacteriology*, 88(1), 105-110.
- Trainor, P. A., & Andrews, B. T. (2013). Facial dysostoses: Etiology, pathogenesis and management. *American Journal of Medical Genetics Part C*, 163c(4), 283-294.

- Ullrich, A., Knecht, W., Fries, M., & Löffler, M. (2001). Recombinant expression of N-terminal truncated mutants of the membrane bound mouse, rat and human flavoenzyme dihydroorotate dehydrogenase. A versatile tool to rate inhibitor effects? *European Journal of Biochemistry*, 268(6), 1861-1868.
- Ullrich, A., Knecht, W., Piskur, J., & Löffler, M. (2002). Plant dihydroorotate dehydrogenase differs significantly in substrate specificity and inhibition from the animal enzymes. *FEBS Letters*, 529(2-3), 346-350.
- Wacklin, H. P. (2010). Neutron reflection from supported lipid membranes. *Current Opinion in Colloid and Interface Science*, 15(6), 445-454.
- Vacklin, H. P., Tiberg, F., Fragneto, G., & Thomas, R. K. (2005). Composition of supported model membranes determined by neutron reflection. *Langmuir*, 21(7), 2827-2837.
- Vacklin, H. P., Tiberg, F., & Thomas, R. K. (2005). Formation of supported phospholipid bilayers via co-adsorption with β -d-dodecyl maltoside. *Biochimica et Biophysica Acta - Biomembranes*, 1668(1), 17-24.
- Walse, B., Dufe, V. T., Svensson, B., et al. (2008). The Structures of Human Dihydroorotate Dehydrogenase with and without Inhibitor Reveal Conformational Flexibility in the Inhibitor and Substrate Binding Sites †. *Biochemistry*, 47(34), 8929-8936.
- van Kuilenburg, A. B. P., & Meinsma, R. (2016). The pivotal role of uridine-cytidine kinases in pyrimidine metabolism and activation of cytotoxic nucleoside analogues in neuroblastoma. *Biochimica et Biophysica Acta - Molecular Basis of Disease*, 1862(9), 1504-1512.
- Vanaken, T., Foxall-Vanaken, S., Castleman, S., & Ferguson-Miller, S. (1986). Alkyl glycoside detergents: Synthesis and applications to the study of membrane proteins. In *Methods in Enzymology* (Vol. 125, pp. 27-35): Academic Press.
- Wang, L. (2016). Mitochondrial purine and pyrimidine metabolism and beyond. *Nucleosides, Nucleotides & Nucleic Acids*, 35(10-12), 578-594.
- Wang, W., Cui, J., Ma, H., Lu, W., & Huang, J. (2021). Targeting Pyrimidine Metabolism in the Era of Precision Cancer Medicine. *Frontiers in Oncology*, 11, 1-17.
- Wang, Y., Bai, C., Ruan, Y., et al. (2019). Coordinative metabolism of glutamine carbon and nitrogen in proliferating cancer cells under hypoxia. *Nature Communications*, 10(1), 1-14.
- Webster, J., Holt, S., & Dalglish, R. (2006). INTER the chemical interfaces reflectometer on target station 2 at ISIS. *Physica B: Condensed Matter*, 385-386, 1164-1166.
- Vicente, E. F., Sahu, I. D., Costa-Filho, A. J., Cilli, E. M., & Lorigan, G. A. (2015). Conformational changes of the HsDHODH N-terminal Microdomain via DEER Spectroscopy. *Journal of Physical Chemistry B*, 119(28), 8693-8697.
- Vicente, E. F., Sahu, I. D., Crusca, E., et al. (2017). HsDHODH Microdomain-Membrane Interactions Influenced by the Lipid Composition. *Journal of Physical Chemistry B*, 121(49), 11085-11095.
- Wiedemann, H. R. (1973). [Malformation-retardation syndrome with bilateral absence of the 5th rays in both hands and feet, cleft palate, malformed ears

- and eyelids, radioulnar synostosis (author's transl)]. *Klinische Pädiatrie*, 185(3), 181-186.
- Wuthrich, K. (1990). Protein structure determination in solution by NMR spectroscopy. *Journal of Biological Chemistry*, 265(36), 22059-22062.
- Wyatt, P. J. (1997). Multiangle Light Scattering: The Basic Tool for Macromolecular Characterization. *Instrumentation Science & Technology*, 25(1), 1-18.
- Yin, S., Kabashima, T., Zhu, Q., Shibata, T., & Kai, M. (2017). Fluorescence assay of dihydroorotate dehydrogenase that may become a cancer biomarker. *Scientific Reports*, 7(40670), 1-7.
- Zadran, S., Standley, S., Wong, K., et al. (2012). Fluorescence resonance energy transfer (FRET)-based biosensors: visualizing cellular dynamics and bioenergetics. *Applied Microbiology and Biotechnology*, 96(4), 895-902.
- Zameitat, E., Gojković, Z., Knecht, W., Piskur, J., & Löffler, M. (2006). Biochemical characterization of recombinant dihydroorotate dehydrogenase from the opportunistic pathogenic yeast *Candida albicans*. *FEBS Journal*, 273(14), 3183-3191.
- Zhang, L., Zhang, J., Wang, J., et al. (2022). Recent advances of human dihydroorotate dehydrogenase inhibitors for cancer therapy: Current development and future perspectives. *European Journal of Medicinal Chemistry*, 232.
- Zhang, X., Ma, L., & Zhang, Y. (2013). High-resolution optical tweezers for single-molecule manipulation. *The Yale Journal of Biology and Medicine*, 86(3), 367-383.
- Zhao, X. (2011). Protein structure determination by solid-state NMR. In *NMR of Proteins and Small Biomolecules* (pp. 187-213): Springer.
- Zhao, X. J., & Xie, D. H. (2012). Anionic Wormlike Micelles. *Progress in Chemistry* 24(4), 456-462.

Papers I-V

Reconstitution of Membrane-Bound Enzymes for Neutron Scattering Studies

JUAN MANUEL OROZCO RODRIGUEZ started his PhD at the Department of Biology, Lund University (LU) in 2017. He previously completed a Master's degree in Biotechnology (LU) and a Bachelor's degree in Bioprocess Engineering (Tecnológico de Monterrey, Mexico). His doctoral research is presented in this thesis.



The aim of this doctoral thesis was to investigate the mechanism of action and inhibition of membrane-bound enzymes that interact with lipids and lipophilic substrates under non-crystalline, physiologically relevant conditions using neutron scattering methods. Neutron scattering techniques are suitable for the study of biological systems. Neutrons have no net charge and can penetrate deeply into matter. It is also possible to distinguish between isotopes of the same element, as is the case with the isotopes of hydrogen (protium and deuterium). Selective deuteration can be used to determine the structure and location of biological molecules in complex systems. Neutron reflectometry (NR) is a surface scattering technique capable of determining the structure and composition of thin films in the direction perpendicular to the surface and is therefore suitable for the study of membrane proteins and lipid bilayers.

A relevant example of this type of membrane proteins is human dihydroorotate dehydrogenase (*HsDHODH*). *HsDHODH* is an integral protein found in the inner mitochondrial membrane (IMM), where it catalyzes the oxidation of dihydroorotate to orotate with the concomitant reduction of ubiquinone Q_{10} . *HsDHODH* is the target of anti-inflammatory drugs and anti-proliferative compounds, and mutations in the *HsDHODH* gene have been identified as the cause of Miller syndrome, a rare genetic disorder.

A full biochemical characterization of *HsDHODH* and truncated *HsDHODH* as well as three variants associated with Miller syndrome (G19E, E52G, R135C) was performed. A particular focus was placed on their interaction with lipids including quartz crystal microbalance with dissipation (QCM-D) measurements of their binding to supported lipid bilayers (SLB). As part of this thesis, the interactions between SLBs consisting of either synthetic lipids or a complex lipid mixture extracted from yeast with or without Q_{10} and a soluble truncated form of *HsDHODH*, as well as the soluble bacterial analog from *E. coli* (*EcDHODH*), were investigated by NR.

The reconstitution of *HsDHODH* into supported lipid bilayers was attempted using three different methodologies: adsorption of lipid-detergent micelles prepared with dodecyl D-maltoside (DDM), fusion of proteoliposomes, and hybrid approaches combining the adsorption of DDM-protein micelles and lipid vesicle fusion and characterized by NR.